RSC Advances

REVIEW

View Article Online
View Journal | View Issue

Cite this: *RSC Adv.*, 2021, **11**, 2804

Green synthesis of silver nanoparticles using plant extracts and their antimicrobial activities: a review of recent literature

Chhangte Vanlalveni,[a] Samuel Lallianrawna,[b] Ayushi Biswas,[c] Manickam Selvaraj,[d] Bishwajit Changmai*[c] and Samuel Lalthazuala Rokhum *[ce]

Synthesis of metal nanoparticles using plant extracts is one of the most simple, convenient, economical, and environmentally friendly methods that mitigate the involvement of toxic chemicals. Hence, in recent years, several eco-friendly processes for the rapid synthesis of silver nanoparticles have been reported using aqueous extracts of plant parts such as the leaf, bark, roots, *etc.* This review summarizes and elaborates the new findings in this research domain of the green synthesis of silver nanoparticles (AgNPs) using different plant extracts and their potential applications as antimicrobial agents covering the literature since 2015. While highlighting the recently used different plants for the synthesis of highly efficient antimicrobial green AgNPs, we aim to provide a systematic in-depth discussion on the possible influence of the phytochemicals and their concentrations in the plants extracts, extraction solvent, and extraction temperature, as well as reaction temperature, pH, reaction time, and concentration of precursor on the size, shape and stability of the produced AgNPs. Exhaustive details of the plausible mechanism of the interaction of AgNPs with the cell wall of microbes, leading to cell death, and high antimicrobial activities have also been elaborated. The shape and size-dependent antimicrobial activities of the biogenic AgNPs and the enhanced antimicrobial activities by synergetic interaction of AgNPs with known commercial antibiotic drugs have also been comprehensively detailed.

Received 23rd November 2020
Accepted 30th December 2020

DOI: 10.1039/d0ra09941d

rsc.li/rsc-advances

1. Introduction

Nanotechnology is gaining enormous attention as a new area of research dealing with the development of nanomaterials and nanoparticles (NPs) for their utilization in diverse fields such as catalysis, electrochemistry, biomedicines, pharmaceuticals, sensors, food technology, cosmetics, *etc.*[1–3] Nanoparticles (NPs) are nanometer-sized (<100 nm) atomic or molecular scale solid particles having some excellent physical properties compared to the bulk molecules depending on their size and morphology.[4,5] Among all types of NPs, metal and metal oxide nanoparticles have been thoroughly examined using science and technology due to their excellent properties such as high surface to volume ratio, high dispersion in solution, *etc.*[6,7] Owing to these, metal and metal oxide nanoparticles display enhanced antimicrobial properties.[8,9]

Currently, modified or fabricated of NPs is widely utilized in industrially manufactured items *e.g.*, cosmetics, electronics, and textiles. Furthermore, the rapid increased in the number of microbes resistant to existing antibiotic drugs that has led to the requirement of novel medicines in the form of bare NPs or in conjunction with existing antibiotics to exert a favourable synergistic effect resulted in the wide spread use of NPs in several medical fields.[10,11] Nowadays, NPs have been utilized for molecular imaging to achieve profoundly resolved pictures for diagnosis. In addition, contrast agents are impregnated onto NPs for the tumour and atherosclerosis diagnosis.[12–14] Furthermore, nanotherapeutic has been promoted everywhere throughout the world after the first FDA affirmed nanotherapeutic in 1990, to build up different nano-based drugs.[15]

At the beginning of 20th century, various physical and chemical methodologies such as chemical reduction, milling *etc.*, have been utilized for the synthesis of NPs synthesis as well as to enhance its efficiency.[16] However, these conventional techniques involve costly and toxic chemicals and cannot be considered an environmentally benign process.[17] Taking into account, nowadays researchers showed great interest on the synthesis of metal and metal oxides NPs employing bio-genic route, that utilized aqueous plant extract and microbes, as

[a]*Department of Botany, Mizoram University, Tanhril, Aizawl, Mizoram, 796001, India*
[b]*Department of Chemistry, Govt. Zirtiri Residential Science College, Aizawl, 796001, Mizoram, India*
[c]*Department of Chemistry, National Institute of Technology Silchar, Silchar, 788010, India. E-mail: rokhum@che.nits.ac.in; lr512@cam.ac.uk; bishwajit_rs@che.nits.ac.in*
[d]*Department of Chemistry, Faculty of Science, King Khalid University, Abha 61413, Saudi Arabia*
[e]*Department of Chemistry, University of Cambridge, Lensfield Road, Cambridge CB2 1EW, UK*

they are environment-friendly, stable, clinically adaptable, biocompatible and cost-effective.[16,18] Therefore, bio-inspired technology for NPs synthesis became a significant branch in the field of nanoscience and nanotechnology.[19,20] Till now, numerous metal and metal oxide NPs have been synthesized using plant extract and microbes *etc.*[21,22] Owing to their wide availability, renewability and environment-friendly nature, in addition to their vast applications in the synthesis of NPs, plant biomass are also largely targeted by our group and others as a catalyst for chemical synthesis[23,24] and biodiesel productions.[25,26]

Among metal NPs, silver NPs is gaining enormous interest in the research community due to their wide scope of application in microbiology, chemistry, food technology, cell biology, pharmacology and parasitology.[27,28] The morphology of the silver NPs is the deciding factor of their physical and chemical properties.[28] Basically, several techniques such as sol–gel method, hydrothermal method, chemical vapour deposition, thermal decomposition, microwave-assisted combustion method *etc.*, have been utilized for the synthesis of silver NPs.[29–31] Recently, bio-genic synthesis of silver NPs (AgNPs) using biomaterials such as plant extract and microbes as reducing agent and their antimicrobial activity is widely investigated.[32,33] AgNPs are produced by oxidation of Ag^{+} to Ag^{0} by different biomolecules such as flavonoids, ketones, aldehydes, tannins, carboxylic acids, phenolic and the protein of the plant extracts.

UV-visible spectroscopy is a simple and widely used analytical technique to monitor the formation of AgNPs. Upon interaction with an electromagnetic field, the conducting electrons present in the outermost orbital of metal NPs collectively oscillate in resonance with certain wavelengths to exhibit a phenomenon called surface plasmon resonance (SPR). The excitation of SPR is responsible for the formation of color and absorbance in a colloidal solution of AgNPs. The SPR peaks at around 435 nm are usually taken to confirm the reduction of silver nitrate into AgNPs.[34] In general, spherical NPs exhibit only a single SPR band in the absorbance spectra, whereas two or more SPR bands were observed for anisotropic particles depending on the shape.[35] The absence of peak in the region 335 and 560 nm in UV-Vis spectra are sometime used as an indication of the absence of aggregation in NPs.[32,36]

Statistical data analysis in Fig. 1 depicted the increasing trend of published research papers in the field of biogenic synthesis of AgNPs. These data were collected in September 2020 from "SciFinder Database" using the keyword "Green synthesis of silver nanoparticles". From a meagre 259 publications in the year 2001, it has exponentially increased to 3374 publications in 2019. Thus, in this review, an attempt has been made to inspire the researchers to explore the natural resources to synthesize silver nanoparticles by diverse plants and their organs to interconnect nanotechnology with biotechnology into one, termed as nanobiotechnology. This review will also unlock ideas to utilize different paths for the production of silver nanoparticles, which can help human beings. We have comprehensively discussed the bio-genic synthesis and silver nanoparticles using various plants and their application in antimicrobial activity. We also discussed the effect of the synthesized silver nanoparticles' size and shape in antimicrobial activity towards various pathogenic bacteria. In an attempt to synthesize metals NPs one has to bear in mind that the success of NPs depends not only on the size and shape but also on stability of NPs as they have the tendency to form large aggregates that lead to precipitation, thereby reducing their efficacy.

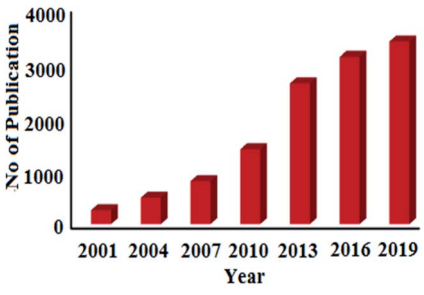

Fig. 1 Publications per year for green synthesis of AgNPs during the period 2001 to 2019 (data collected from SciFinder Database).

2. Protocols for the biosynthesis of AgNPs

Biogenic synthesis of AgNPs is an easy single-step protocol without generating harsh and toxic chemicals; hence, they are save, economical and eco-friendly. In recent years, both plant and microbes are extensively investigated for the biosynthesis of AgNPs of varying size, shape, stability, and antimicrobial efficacy.

2.1 From plant extract

Various parts of plant such as leaves, roots, flowers, fruits, rhizomes *etc.*, have been successfully utilized for the synthesis of AgNPs.[37–39] Different parts of plant are collected from various sources, washed properly with ordinary water followed by distilled water to exclude debris and any other unwanted materials. After that, the portions are dried and ground to make powder or utilized as fresh to make the extract. To prepare the extract, the chopped pieces or the ground powder of the parts of the plant are put in deionized water or alcohol and usually heated below 60 °C for few hours as high-temperature heating long time may leads to the decomposition of phytochemicals in the biomass extract. Plant extract of different pH is added to the solutions having a different concentration of Ag salt as metal precursor followed by heating at different temperature led to the synthesis of AgNPs.[40–42] This synthesis process avoids the use of chemical stabilizer as biomaterials present in the extract act as a reducing agent as well as a stabilizing agent for the synthesis of AgNPs.[43,44] The progress of the formation of AgNPs can be monitored by visual color changes or using UV-Vis. Spectroscopy, where a sharp peak due to surface plasmon resonance (SPR) of AgNPs at around 430–450 nm is clearly observed.[34] After successful synthesis of the AgNPs, the mixture is centrifuged at high rpm to separate the NPs followed by

proper washing using solvents and dried in an oven at low temperature.[45,46] The different plant parts extracts that have been successfully utilized in the green synthesis of AgNPs are given in Fig. 2.

2.2 From microbes

Nowadays, the use of microbial cell for the synthesis of metal NPs has come out as a great approach. Microbial cells turn to be excellent biofactories for the synthesis of AgNPs.[47,48] At first, the cultures are allowed to develop as culture suspension in disinfected distilled water having the culture medium. Then, different concentration of precursor of AgNPs is added into the cultured microbial followed by continuous mechanical stirring under dark conditions. The progress of the reaction is monitored by UV-Vis spectrophotometer. Finally, the resultant AgNPs is separated from the mixture *via* centrifugation at around 3000 rpm for 10–15 min.[49]

3. Plant-mediated biogenic synthesis of AgNPs and their antimicrobial activity

Owing to the environmental issue, biogenic synthesis of metal and metal oxide NPs is gaining immense attention from the past decades. Reported literature revealed that various plant parts such as leaf, roots, seed, fruits and stem *etc.*, have been utilized for the biosynthesis of NPs. The synthesis of NPs is fully dependent on the biomaterials/phytochemicals present in the extract. This section aims to discuss the various plant parts extract mediated synthesis of AgNPs and their application as antimicrobial.

3.1 From leaf

To date, a numerous number of leaves extract have been utilized for the biosynthesis of AgNPs as shown in Table 1. *Skimmia laureola* was reported for the synthesis of spherical AgNPs with size 38 ± 0.27 nm and tested against *E. coli*, *K. pneumoniae*, *P. aeruginosa*, *P. vulgaris*, *S. aureus*.[50] Miri *et al.*[51] have utilized *Prosopis farcta* extract for the biosynthesis of AgNPs with an average size of 10.8 nm at room temperature (RT). The antimicrobial activity of synthesized AgNPs was tested using disc diffusion method against the Gram-positive (*Staphylococcus aureus* (PTCC 1431), *Bacillus subtilis* (PTCC 1420)) and Gram-negative bacteria (*Escherichia coli* (PTCC 1399), *Pseudomonas aeruginosa* (PTCC 1074)) and compared with the control. The results showed that the inhibition diameter is increased for every tested pathogen (Fig. 3), indicates that synthesized AgNPs induces cellular damage to the bacteria's, hence can be used as nanoantibiotics. *Aloe vera*,[52] *Eclipta alba*,[53] *Momordica charantia*,[54] *Leptadenia reticulata*[55] are also used for the production of spherical biogenic AgNPs. In another study, AgNPs were synthesized by using tea leaf extract. Bactericidal activity of the synthesized NPs was tested against *S. aureus* and *E. coli* showed that inhibition action is more effective in case of *S. aureus* (89% inhibition rate) compared to *E. coli* (75% inhibition rate). In addition, treatment of the NPs against the bacteria leads to impairment of bacterial cell–cell adhesion.[56] *Mukia maderaspatana* leave extract was utilized for the biosynthesis of AgNPs with the size range of 58–458 nm. The synthesized nanoparticle was conjugated to the antibiotic ceftriaxone to investigate the antimicrobial activity towards the human pathogens such as *B. subtilis*, *K. pneumonia*, *S. typhi*, *S. aureus* and compared with the pathogen inhibition efficiency of the free nanoparticle and the antibiotic. The result obtained revealed that the AgNPs conjugated with ceftriaxone showed highest inhibition activity compared to the others.[57]

Clitoria ternatea and *Solanum nigrum*[58] were also reported to synthesize very small-size AgNPs and evaluated against *B. subtilis*, *S. aureus*, *S. pyogenes*, *E. coli*, *P. aeruginosa*, *K. aerogenes*. Interestingly, among the two leaf *Clitoria ternatea* extract gave smaller nanoparticles, which indicated the important role of extract constituents on the size of the produced nanoparticles. In addition, AgNPs of *Clitoria ternatea* showed higher activity than the AgNPs of *Solanum nigrum* against nosocomial pathogens due to its small size. It has been well-documented in literature that smaller size NPs showed higher antimicrobial activities due to larger surface area.[56] *Grewia flaviscences*,[59] *Prunus yedoensis*,[60] *Justicia adhatoda* L,[61] *Withania somnifera*[62] produced AgNPs in the range 8–100 nm which mainly are spherical. Numerous microbes such as skin bacteria are responsible for skin infection and body odor, as well as odor in feet, shoes, and/or socks mediated through the breakdown of amino acids present in sweat. Hence proper medication is required for human's wellbeing. Velmurugan *et al.*[60] applied the synthesized AgNPs from *Prunus yedoensis* to treat *P. acnes*, *S. epidermidis*, a well-known skin bacteria, and found that the synthesized NPs are more effective against skin bacteria than commercial AgNPs. The biogenic AgNPs showed 18 mm ZOI (zone of inhibition) in 30 μg scale against *P. acnes*, whereas commercial AgNPs displayed a lower ZOI of only 12 in the same concentration.

Pistacia atlantica,[63] *Tectona grandis* Linn,[64] *Ficus virens*[65] also reported for the synthesis of AgNPs and are evaluated against

Fig. 2 Different parts of plants used for biosynthesis of antimicrobial silver nanoparticles.

Table 1 Various leaf extract used for the green synthesis of AgNPs and their antimicrobial activity

No.	Plants	Size and shape	Test microorganisms	Ref.
1	*Skimmia laureola*	Spherical; 38 ± 0.27 nm	*E. coli*, *K. pneumoniae*, *P. aeruginosa*, *P. vulgaris*, *S. aureus*	50
2	*Prosopis farcta*	Spherical; 8–11 nm	*S. aureus*, *B. subtilis*, *E. coli*, *P. aeruginosa*	51
3	*Aloe vera*	Spherical; 70 nm	*Aspergillus* sp., *Rhizopus* sp.	52
4	*Eclipta alba*	310 to 400 nm	*E. coli*, *S. aureus*, *P. aeruginosa*	53
5	*Momordica charantia*	Spherical; 11–16 nm	*B.* spp., *S.* spp., *P.* spp., *E. coli*, *A. niger* subsp., *A. flavus* subsp., *P.* spp.	54
6	*Leptadenia reticulata*	Spherical; 50–70 nm	*S. pneumonia*, *K. pneumonia*	55
7	*Tea leaf*	Spherical; 20 nm	*S. aureus*, *E. coli*	56
8	*Raphanus sativus*	Spherical; 6–38 nm	*A. fumigatus*, *C. specifier*, *F. solani*	40
9	*Mukia maderaspatana*	Spherical; 58–458 nm	*B. subtilis*, *K. pneumonia*, *S. typhi*, *S. aureus*	57
11	*Clitoria ternatea*	Spherical; 20 nm	*B. subtilis*, *S. aureus*, *S. pyogenes*, *E. coli*, *P. aeruginosa*, *K. aerogenes*	58
12	*Solanum nigrum*	Spherical; 28 nm	*B. subtilis*, *S. aureus*, *S. pyogenes*, *E. coli*, *P. aeruginosa*, *K. aerogenes*	58
13	*Croton sparsiflorus morong*	Spherical; 22–52 nm	*S. aureus*, *E. coli*, *B. subtilis*	46
14	*Grewia flaviscences*	Spherical; 60 nm	*Bacillus*, *P. aeruginosa*	59
15	*Terminalia arjuna*	Spherical; 8–16 nm	*S. aureus*, *E. coli*	21
16	*Prunus yedoensis*	Spherical, oval; 18–20 nm	*P. acnes*, *S. epidermidis* (skin bacteria)	60
17	*Justicia adhatoda* L.	Spherical; 5–50 nm	*P. aeruginosa*	61
18	*Withania somnifera*	70–110 nm; spherical	*S. aureus*, *P. aeruginosa*, *C. albicans*, *P. vulgaris*, *E. coli*, *A. tumefaciens*	62
19	*Pistacia atlantica*	Spherical; 10–50 nm	*S. aureus*	63
20	*Tectona grandis* Linn	Spherical; 26–28 nm	*E. coli* and *S. aureus*	64
21	*Ficus virens*	Spherical; 4.98–29 nm	*B. subtilis*, *S. epidermidis*, *E. faecalis*, *K. pneumoniae*, *V. cholerae*, *V. vulnificus*	65
22	*Azadirachta indica*	Spherical; 250–700 nm	*E. coli*	66
23	*Artocarpus altilis*	Spherical; 20–50 nm	*E. coli*, *P. aeruginosa*, *S. aureus*, *A. versicolor*	67
24	*Crotalaria retusa*	Spherical; 80 nm	*E. coli* and *S. aureus*	68
25	*Cardiospermum halicacabum*	Spherical; 74 nm	*P. vulgaris*, *P. aeruginosa*, *S. aureus*, *B. subtilis*, *S. paratyphi*, *A. solani*, *F. oxysporum*	69
26	*Psidium guajava*	Spherical; 10–90 nm	*P. aeruginosa*	70
27	*Cassia fistula*	Spherical; 39.5 nm	*B. subtilis*, *S. aureus*, *E. coli*, *P. aeruginosa*, *C. albicans*, *C. kruseii*, *C. viswanathii*, *T. mentagrophytes*	71
28	*Terminalia chebula*	Spherical; 10–30 nm	*E. coli*, *B. subtilis*	72
29	*Pedalium murex*	Spherical; 20–50 nm	*E. coli*, *K. pneumonia*, *M. flavus*, *P. aeruginosa*, *B. subtilis*, *B. pumilus* and *S. aureus*	73
30	*Azadirachta indica*	Spherical; 34 nm	*E. coli*, *S. aureus*	74
31	*Croton bonplandianum*	Spherical; 15–40 nm	*P. aeruginosa*, *E. coli*, *S. aureus*	75
32	*Tamarix gallica*	Spherical; 5–40 nm	*E. coli*	76
33	*Urtica dioica*	Spherical; 20–30 nm	*B. cereus*, *B. subtilis*, *S. aureus* and *S. epidermidis*, *E. coli*, *K. pneumoniae*, *S. marcescens*, *S. typhimurium*	77

Table 1 (*Contd.*)

No.	Plants	Size and shape	Test microorganisms	Ref.
34	*Ziziphus oenoplia*	Spherical; 10 nm	*P. aeruginosa*, *K. pneumoniae*, *E. coli*, *S. typhi*	78
35	*Lawsonia inermis*	Spherical; 25 nm	*E. coli*, *Pseudomonas* spp., *Bacillus* spp., *Staphylococcus* spp., *A. niger*, *A. flavus*, *Penicillium* spp.	79
36	*Lantana camara*	Spherical; 20–200 nm	*S. aureus*, *E. coli*, *P. aeruginosa*, *K. pneumonia*	81
37	*Jatropha curcas*	Spherical; 20–50 nm	*E. coli*, *P. aeruginosa*, *B. cereus*, *S. enterica*, *L. monocytogenes*, *S. aureus*	82
38	*Salvinia molesta*	Spherical; 10 nm	*S. aureus*, *E. coli*	83
39	*Sesbania grandiflora*	Spherical; 20 nm	*E. coli*, *Pseudomonas* spp., *Bacillus* spp., *Staphylococcus* spp., *A. niger* subsp., *A. flavus* subsp., *Penicillium* spp.	84
40	*Indoneesiella echioides*	Spherical; 29 nm	*R. rhodochrous*, *A. hydrophila*, *S. aureus*, *Pseudomonas aeruginosa*, *C. albicans*	85
41	*Phlomis*	Spherical; 25 nm	*S. aureus*, *B. cereus*, *S. typhimurium*, *E. coli*	86
42	*Hydrocotyle rotundifolia*	Spherical; 7.39 nm	*E. coli*	87
43	*Maclura pomifera*	Spherical; 6–16 nm	*S. aureus*, *Bacillus cereus*, *E. coli*, *P. aeruginosa*, *A. niger*, *C. albicans*	88
44	*Paederia foetida* Linn.	Spherical; 5–25 nm	*B. cereus*, *S. aureus*, *E. coli*, *A. niger*	89
45	*Atalantia monophylla*	Spherical; 35 nm	*B. subtilis*, *B. cereus*, *S. aureus*, *E. coli*, *P. aeruginosa*, *K. pneumoniae*, *C. albicans*, *A. niger*	90
46	*Talinum triangulare*	Spherical; 13.86 nm	*E. coli*, *S. typhi*, *B. subtilis*, *S. aureus*, *C. albicans*	91
47	*Ricinus communis*	Spherical; 8.96 nm	*S. aureus*, *P. aeruginosa*	92
48	*Erythrina suberosa*	Spherical; 15–34 nm	*S. aureus*, *P. aeruginosa*, *C. kruseii*, *T. mentagrophytes*	93
49	*Lippia citriodora*	Spherical; 10–45 nm	*S. aureus*, *B. subtilis*, *S. typhi*, *E. coli*, *C. albicans*	94
50	*Brassica oleracea* L.	Spherical; 30–100 nm	*S. aureus*, *E. coli*, *C. albicans*	95
51	*Catharanthus roseus*	Spherical; 10–88 nm	*E. coli*, *C. koseri*, *K. pneumonia*, *P. aeruginosa*, and *S. aureus*	96
52	*Lavandula x intermedia*	Spherical; 11–47 nm	*E. coli*, *P. aeruginosa*, *P. mirabilis*, *B. cereus*, *K. oxytoca*, *S. typhi*, *S. aureus*, *C. albicans*, *A. niger*, *F. oxysporum*	98
53	*Canna edulis*	Spherical; less than 40 nm	*B. cereus*, *S. aureus*, *E. coli*, *S. typhimurium*, *E faecalis*, *C. tropicalis*, *C. kruseii*, *C. lusitaniae*, *C. guilliemondii*, *P. chrysogenum*	99
54	*Artemisia vulgaris*	Spherical; 27–53 nm	*E. coli*, *S. aurous*, *P. aeruginosa*, *K. pneumoniae*, *H. influenza*	100
55	*Psidium guajava*	Spherical; 25 nm	*B. aryabhattai*, *B. megaterium*, *B. subtilis*, *A. creatinolyticus*, *E. coli*, *Alcaligenes faecalis*, *S. cerevisiae*, *A. niger*, *R. oryzae*	102
56	*Taraxacum officinale*	Spherical; 5–30 nm	*X. axonopodis*, *P. syringae*	104
57	*Petiveria alliacea* L.	Spherical; 16.7–33.74 nm	*E. coli*, *K. pneumoniae*, *S. aureus*	105

Table 1 (*Contd.*)

No.	Plants	Size and shape	Test microorganisms	Ref.
58	*Nervalia zeylanica*	Spherical; 34.2 nm	*S. aureus*, *L. brevis*, *P. putida*, *Pseudomonas* sp., *P. chrysogenum*, *P. citrinum*	106
59	*Ficus ingens*	Spherical; 81.37 nm	*E. coli*, *S. typhi*, *B. cereus*	107
60	*Thymbra spicata*	Spherical; 70.2 nm	*B. cereus*, *S. aureus*, *E. coli*, *S. typhimurium*	108
61	*Indigofera tinctoria*	Spherical; 9–26 nm	*B. pumilis*, *S. aureus*, *Pseudomonas* sp., *E. coli*, *A. fumigatus*, *A. niger*	110
62	*Tecoma stans*	Spherical; 2–40 nm	*B. subtilis*, *S. aureus*, *K. pneumoniae*	114
63	*Salvia leriifolia*	Spherical; 27 nm	*P. aeruginosa*, *E. coli*, *S. coagulase*, *C. frurdii*, *E. aerogenes*, *A. baumannii*, *S. marcescens*, *K. pneumonia*, *S. pneumoniae*	115
64	*Leucaena leucocephala* L.	Spherical; 25–50 nm	*P. aeruginosa*, *S. pyogenes*, *S. aureus*, *E. coli*, *S. typhi*, *B. subtilis*	116
65	*Selaginella bryopteris*	Spherical; 5–10 nm	*S. aureus*, *E. coli*, *A. niger*	117
66	*Galega officinalis*	Spherical; 27.12 nm	*E. coli*, *P. syringae*, *S. aureus*	118
67	*Camellia sinensis*	Spherical; 30 nm	*S. aureus*, *K. pneumoniae*	119
68	*Justicia spicigera*	Spherical; 86–100 nm	*B. cereus*, *K. pneumoniae*, and *E. aerogenes*, *M. phaseolina*, *A. alternate*, *Colletotrichum* sp., *F. solani*	120
69	*Kleinia grandiflora*	Spherical; 20–50 nm	*P. aeruginosa*, *C. albicans*	121
70	*Eucalyptus citriodora*	Spherical; 17.51 nm	*C. albicans*, *A. baumannii*, *E. coli*, *K. pneumoniae*, *P. aeruginosa*	122
71	*Juniperus procera*	Spherical and cubic; 30–90 nm	*M. luteus*, *B. subtilis*, *P. mirabilis*, *K. pneumoniae*, *C. albicans*	123
72	*Capparis zeylanica*	Spherical; 23 nm	*S. epidermis*, *E. faecalis*, *S. paratyphi*, *S. dysenteriae*, *C. albicans*, *A. niger*	124
73	*Caesalpinia pulcherrima*	Spherical; 9 nm	*B. cereus*, *B. subtilis*, *S. aureus*, *C. rubrum*, *E. coli*, *P. aeruginosa*, *S. typhimurium*, *K. pneumoniae*, *C. albicans*, *C. glabrata*, *C. neoformans*	126
74	*Ligustrum lucidum*	Spherical; 13 nm	*S. turcica*	127
75	*Aesculus hippocastanum*	Spherical; 50 ± 5 nm	*S. aureus*, *S. epidermidis*, *L. monocytogenes*, *C. renale*, *M. luteus*, *B. subtilis*, *B. cereus*, *E. faecalis*, *P. aeruginosa*, *P. fluorescens*, *E. coli*, *E. aerogenes*, *K. pneumonia*, *P. mirabilis*, *C. albicans*, *C. tropicalis*, *C. krusei*	128
76	*Melaleuca alternifolia*	Spherical; 11.56 nm	*S. aureus*, methicillin-resistant *Staphylococcus aureus*, *S. epidermidis*, *S. pyogenes*, *K. pneumoniae*, *P. aeruginosa*, *T. mentagrophytes*, *C. albicans*	129
77	*Carya illinoinensis*	Spherical; 12–30 nm	*E. coli*, *P. aeruginosa*, *S. aureus*, *L. monocytogenes*	130
78	*Murraya koenigii*	Spherical;; 35–80 nm	*E. coli*, *P. aeruginosa*, *E. faecalis*, *C. albicans*	131
79	*Clerodendrum inerme*	Spherical; 5.54 nm	*B. subtilis*, *S. aureus*, *Klebsiella*, *E. coli*, *A. niger*, *T. harzianum*, *A. flavus*	132

Table 1 (*Contd.*)

No.	Plants	Size and shape	Test microorganisms	Ref.
80	*Aspilia pluriseta*	Spherical; 1–20 nm	*B. subtilis*, *S. aureus*, *E. coli*, *P. aeruginosa*, *C. albicans*	133
81	*Melia azedarach*	Spherical; 18 to 30 nm	*V. dahliae*	134
82	*Scoparia dulcis*	Spherical; 3–18 nm	*P. aeruginosa*, *E. coli*, *B. subtilis*, *S. aureus*, *A. niger*, *C. albicans*	135
83	*Lantana trifolia*	Spherical; 5 and 70 nm	*E. coli*, *P. aeruginosa*, *C. albicans*, *S. aureus*, *B. subtilis*	136
84	*Mikania micrantha*	Spherical; 10–20 nm	*B. subtilis*, *E. coli*, *P. aeruginosa*, *S. pneumonia*	137
85	*Solanum nigrum*	Spherical; 3.46 nm	*E. coli*	138
86	*Curcuma longa* L.	Spherical; 15–40 nm	*S. aureus*, *P. aeruginosa*, *S. pyogenes*, *E. coli*, *C. albicans*	139
87	*Syzygium cumini*	Spherical; 11–19 nm	*S. aureus*, *A. flavus*, *A. parasiticus*	140
88	*Cleistanthus collinus*	Spherical however not mentioned in manuscript; 30 to 50 nm	*S. sonnei*, *P. aeruginosa*, *S. aureus*, *B. subtilis*, *S. dysenteriae*, *V. cholerae*, *P. mirabilis*	142
89	*Cestrum nocturnum*	Spherical; 20 nm	*Citrobacter*, *E. faecalis*, *S. typhi*, *E. coli*, *P. vulgaris* and *V. cholerae*	143
90	*Rice*	Spherical; 16.5 nm	*R. solani*	144
91	*Mentha aquatica*	Spherical; 8 nm	*P. aeruginosa*, *E. coli*, *B. cereus*, and *S. aureus*	146
92	*Rosmarinus officinalis*	Sphere; 29 nm	*S. aureus*, *B. subtilis*, *E. coli*, *P. aeruginosa*	147
93	*Ceropegia thwaitesii*	Sphere; 100 nm	*S. typhi*, *B. subtilis*, *S. aureus*, *S. epidermis*, *V. cholerae*, *S. epidermidis*, *K. pneumonia*, *M. luteus*, *P. mirabilis*, *P. aeruginosa*, *S. flexneri*	148
94	*Ziziphus jujuba*	Irregular; 20–30 nm	*E. coli*	149
95	*Ocimum tenuiflorum*, *Solanum trilobatum*, *Syzygium cumini*, *Centella asiatica* and *Citrus sinensis*	Irregular; 28 nm, 26.5 nm, 65 nm, 22.3 nm and 28.4 nm	*S. aureus*, *P. aeruginosa*, *E. coli*, *K. pneumoniae*	154
96	*Amaranthus gangeticus* Linn	Globular-shaped; 11–15 nm	*S. flexneri*, *B. subtilis*, *Sclerotinia* sp.	155
97	*Andrographis paniculata*	Cubic; 40 and 60 nm	*P. aeruginosa*, *E. coli*, *V. cholerae*, *S. flexneri*, *B. subtilis*, *S. aureus*, *M. luteus*	156
98	*Andrographis echioides*	Cubic, pentagonal, hexagonal; 68.06–91.28 nm;	*E. coli*, *S. aureus*, *S. typhimurium*, *M. luteus*, *P. aeruginosa*	158
99	*Azadirachta indica* (neem)	Polydispersed; less than 40 nm	*P. nitroreducens*, *A. unguis*	159
100	*Phyllanthus amarus*	Flower-liked; 30 nm to 42 nm	*E. coli*, *P.* spp., *B.* spp., *S.* spp., *A. niger*, *A. flavus*, *P.* spp.	160

several microbes. Verma *et al.*[66] reported *Azadirachta indica* (neem) leaf inspired synthesis of AgNPs and evaluated the effects of pH of the solution on the formation of nanoparticles as change in pH affects the shape and size of the particles by altering the charge of biomolecules, which might affect their capping as well as stabilizing abilities. They have observed that as the pH increases from 9 to 13, the absorption maximum shifts from 383 to 415 nm in the UV-spectrum and detects an increase in absorption intensity with increasing pH. This showed that pH 13 is the most favourable pH for the synthesis of AgNPs leaf extract. The shift in the peak wavelength indicates that the size of the particles increases with increasing pH of the solution. As the particles' diameter gets larger, the energy required for excitation of surface plasmon electrons decreases, as a result the absorption maximum shifted towards the longer wavelength region. Moreover, it was observed that at acidic pH

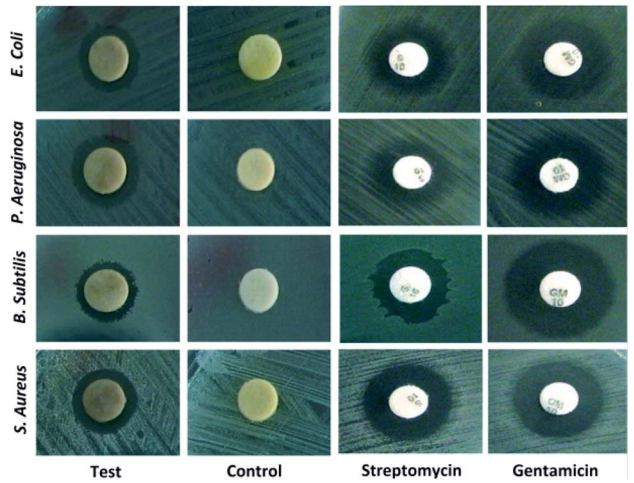

Fig. 3 Bactericidal activity of *Prosopis farcta* extract mediated Ag-NPs against human pathogens. This figure has been reproduced from ref. [51] with permission from Elsevier, copyright 2015.

i.e. pH < 7, the formation of nanoparticles is suppressed. At high pH, the bioavailability of functional groups in *Azadirachta indica* leaf extract promoted the synthesis of nanoparticles. However, at very high pH *i.e.* pH ~13, the particles became unstable and agglomerated, when kept for overnight.

AgNPs were also recently synthesized using several leaf extract of plants such as *Artocarpus altilis*,[67] *Crotalaria retusa*,[68] *Cardiospermum halicacabum*,[69] *Psidium guajava*,[70] *Cassia fistula*[71] and *Terminalia chebula*.[72] In 2016, Anandalakshmi *et al.*[73] reported *Pedalium murex* leaf extract mediated AgNPs. The produced NPs were tested against several microbes and displayed highest ZOI of 10.5 mm (in 15 μL mL^{-1} scale) against *E. coli* and *P. aeruginosa* and least activity against *Klebsiella pneumoniae* (8.5 mm). The shape and size of the resultant AgNPs were elucidated with the help of TEM. The TEM micrographs showed that the sizes of the particles were around 50 nm and were predominantly spherical in shape. The PXRD pattern showed fcc crystal structure. *Azadirachta indica* promoted synthesis of AgNPs was reported by Ahmed *et al.*[74] The produced NPs displayed equal efficacy (9 mm ZOI) against *E. coli*, *S. aureus* whereas the plant extract show no antimicrobial activity.

Croton bonplandianum mediated AgNPs were also found to be highy active against microbes.[75] The minimum inhibitory concentrations of synthesized AgNPs were found to be 50, 45, 75 g mL^{-1} in case of *E. coli*, *P. aeruginosa*, and *S. aureus* respectively. It was concluded that Gram-negative strains of bacteria with thin cell wall such as *E. coli* and *P. aeruginosa* are more susceptible to cell wall damage compared to Gram-positive strain bacteria with a thick cell wall (*S. aureus*). In another work, *Tamarix gallica* leaf extract was used for synthesis of AgNPs. To test its activity against *E. coli*, three sterile filter paper discs (5 mm diameter) were impregnated with 6 μL of AgNPs produced with 5 mL of *Tamarix gallica* extract and 10 mL of 5 mM $AgNO_3$ solution, López-Miranda *et al.* studied the green synthesis of AgNPs using and evaluated the effect of extract and $AgNO_3$ concentration on the synthesis.[76] They have observed an increase in the intensity of surface plasmon resonance (SPR) with the increase in extract concentration, which is attributed to an increasing number of AgNPs formed. Also, as the $AgNO_3$ concentration increases, many silver ions are increasingly reduced to AgNPs. However, they have seen that the SPR band intensities are nearly independent for 5, 7, and 9 mM $AgNO_3$, which reflected that the reaction is close to an equilibrium system because the reducing compounds and stabilizers from the extract are completely consumed, hence it is impossible to reduce a larger amount of silver ions. Henceforth, from the UV-vis analysis they concluded that the best results were obtained for the sample 0.15 g mL^{-1} extract with 5 mM $AgNO_3$. The produced showed 9 mm ZOI against *E. coli*. Similarly, leaf extract of *Urtica dioica*,[77] *Ziziphus oenoplia*[78] and *Lawsonia inermis*[79] are reported for the production of AgNPs with high antimicrobial activities. In 2016, a remarkable work on the synthesis of AgNPs using *Urtica dioica* leaf extract that showed excellent synergistic effect with known antimicrobial drugs was reported by Jyoti *et al.*[77] Interestingly, the synthesized AgNPs apart from showing high antimicrobial activities against several microbes, showed excellent synergistic effect in combination with antibiotics and displayed higher antibacterial effect as compared with AgNPs alone. A high 17.8 fold increase in ZOI was observed for amoxicillin with AgNPs against *S. marcescens* proving the synergistic role of AgNPs.[77] This work provides helpful insight into the development of new antibacterial agents to fight against several new stain of microbes resistant to existing antibiotic drugs. Fig. 4 displayed the synergistic effect of AgNPs and common antimicrobial drugs. The synergistic interaction between AgNPs and antibiotic drugs has been clearly identified using UV-Vis and Raman spectrometer by McShan *et al.*[80] The authors claimed that this synergistic interaction speed up the ejection of Ag^+ from AgNPs which inturn boost its antimicrobial activities.

Recently, Manjamadha *et al.*[81] have reported ultrasonic-assisted biosynthesis of spherical AgNPs using *Lantana camara* L. leaf extract. Biosynthesis of AgNPs using ultrasonication improves the reaction conditions such as reducing reaction time and enhancing the reaction rate. Bactericidal activity of the synthesized AgNPs revealed that it shows excellent antibacterial activity against Gram-positive and Gram-negative bacteria. Leaves of *Jatropha curcas* collected from Micro model complex, Indian Institute of Technology Delhi campus was used for the production of AgNPs.[82] The transmission electron microscopy (TEM) analysis showed variation in particle shape and size (20–50 nm), whereas the diameter of NPs was found to be in range of 50–100 nm by scanning electron microscopy (SEM). Complete destruction of the microbial cell was visible using TEM examination. The synthesized NPs were tested for their antimicrobial activities and based on ZOI data, the pattern of sensitivity was observed in the order as *E. coli* > *P. aeruginosa* > *B. cereus* > *S. enterica* = *L. monocytogenes* > *S. aureus*.

Salvinia molesta,[83] *Sesbania grandiflora*,[84] *Indoneesiella echioides*[85] and *Phlomis*[86] leaf extract were also useful for the bioreduction of $AgNO_3$ to AgNPs. An ultra-small AgNPs with an average diameter of 7.39 nm were prepared using *Hydrocotyle rotundifolia*.[87] The synthesized AgNPs were tested for its

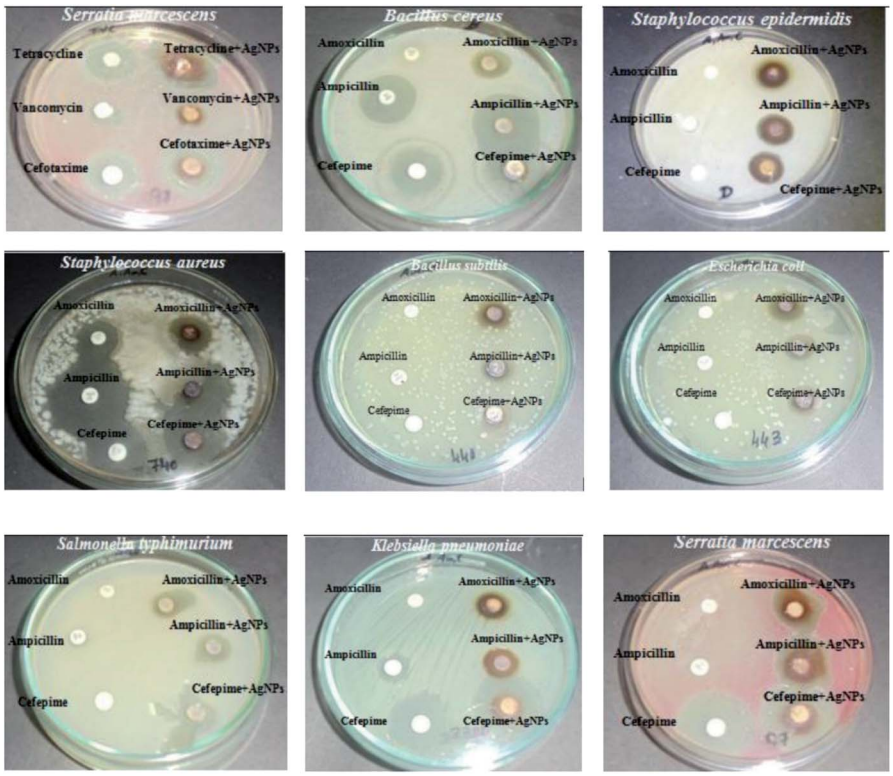

Fig. 4 Synergistic effect of *Urtica dioica* mediated AgNPs with several antibiotics. This figure has been reproduced from ref. [77] with permission from Elsevier, copyright 2016.

antimicrobial property against *E. coli* (DH5α). The MIC value was recorded as 5 μg mL^{-1} and demonstrated significant growth inhibition on agar plate. Formation of spherical AgNPs using *Maclura pomifera* was achieved in 2017 by Azizian-Shermeh *et al.*[88] The produced NPs (0.1 mg mL^{-1} concentration) displayed a very high ZOI of 23.4 ± 0.1 mm against *E. coli*, which is higher than Ampicillin, a well-known antibiotic drug. In the same year, Bhuyan and coworkers at National Institute of Technology Silchar reported *Paederia foetida* Linn. inspired AgNPs synthesis.[89] The order of activities of the AgNPs against tested microbes is *B. cereus* > *E. coli*, *S. aureus* > *A. niger*. The author claimed that the AgNPs owing to their small size range (5–25 nm) could have easily penetrated the cell membrane, disturbing the metabolism, cause irretrievable damage finally leading to the microbial cell death. Au NPs has also been synthesized but has not shown any antimicrobial activity which testament the higher activity of AgNPs than that of Au NPs. Biosynthesized AgNPs from leaf extract of *Atalantia monophylla*,[90] *Talinum triangulare*,[91] *Ricinus communis*,[92] *Erythrina suberosa*,[93] *Lippia citriodora*,[94] and *Brassica oleracea* L.[95] are also successfully used as an outstanding antimicrobial drug.

In 2017 Al-Shmgani *et al.* prepared AgNPs using *Catharanthus roseus*.[96] They have used identification by color change, UV-vis spectrum, XRD, FTIR, and AFM techniques to confirm the biosynthesis of AgNPs. The leaf extract color changes from yellowish to reddish-brown after adding 2 mM $AgNO_3$ and exposing to heat at 70 °C for 3 min indicating the formation of the NPs. AFM displays the crystalline NPs with grains sized 10–88 nm in diameter with mean size of about 49 nm. The authors claimed that synthesized AgNPs enter the cell of microbes that resulted in a disruption of adenosine triphosphate (ATP) production and DNA replication, generation of ROS and damage the cell structures as earlier observed by Sahayaraj and Rajesh.[97]

Spherical shape AgNPs with diameter in the range 11–47 nm (by TEM analysis) were produced using *Lavandula x intermedia*.[98] The AgNPs were found to be most effective against *E. coli* among all the tested microorganisms shown in Table 1, entry 51. Interestingly, the author also observed that biogenic AgNPs showed ZOI 23 ± 0.0 mm against *E. coli* whereas streptomycin displayed only 20 ± 0.0 mm under the same concentration. This reflected the high antibacterial efficacy of AgNPs than that of common antimicrobial drug like streptomycin, which could promote its wide use in the future. In another work, a highly crystalline AgNPs were reported to be synthesized from *Canna edulis*.[99] The NPs showed highest antimicrobial activity against *S. typhimurium* which is closely related to the finding by Sumitha *et al.*[38]

In 2017 *Artemisia vulgaris* mediated AgNPs were reported by Rasheed *et al.*[100] Antimicrobial test revealed that the AgNPs exhibited significant inhibition activities against tested pathogens with the highest value being recorded against *S. aureus* (18 ± 0.27 mm inhibition zone). Similar to this, earlier in 2016, Thatoi *et al.*[101] reported high activity of AgNPs against *S. aureus* using AgNPs synthesized from *Sonneratia apetala* plant extract.

Psidium guajava was applied for the production of spherical AgNPs with average dimension of 25 nm.[102] The authors observed that for 100 μg mL^{-1} *Psidium guajava* mediated AgNPs, the ZOI were 18.13 ± 0.02 mm and 16.92 ± 0.18 mm against *A. faecalis* and *E. coli*, respectively, whereas ZOI of 13.24–14.41 mm were recorded at the same concentration against tested Gram-positive bacteria shown in Table 1, entry 54. This finding clearly testament the higher activity of the synthesized AgNPs towards Gram-negative bacteria than the Gram-positive ones. Similar to this finding, earlier in 2013, Geethalakshmi *et al.* also reported the higher susceptibility of Gram-negative bacteria to silver nanoparticles compared with Gram-positive bacteria.[103] Ironically, *Psidium guajava* mediated AgNPs is however consistently less sensitive towards tested fungi such as *S. cerevisiae*, *A. niger* and *R. oryzae* as compared to both Gram-positive and Gram-negative bacteria.

Taraxacum officinale leaf extract mediated AgNPs were proved to exhibit an excellent synergistic antibacterial activity with standard antibiotics (such as oxy-tetracycline, tetracycline, ampicillin, and streptomycin) and showed strong positive response against both *X. axonopodis*, *P. syringae*, a plant pathogens.[104] The combined effect of tetracycline with AgNPs significantly inhibited the growth of selected phytopathogens by increasing ZOI about 40% compared to only antibiotics. The authors are of the opinion that NPs-antibiotic combination and their synergistic action would result in higher penetration in the bacterial cell membrane thereby leads to destruction of various cell organelles and death of bacteria, although the mechanism is not yet fully understood till now.

Lateef *et al.*[105] reported that *Petiveria alliacea* L. mediated AgNPs showed 100% inhibition against *E. coli*, *K. pneumoniae*, *S. aureus*, *A. fumigatus* and *A. flavus*. But only 66.67% inhibition in *A. niger*. In another work, microwave-assisted synthesis of AgNPs using leaf extract of *Nervalia zeylanica* was reported.[106] The authors observed no formation of NPs (monitored using UV-spectroscopy) even after 5 h under RT stirring of the extract and $AgNO_3$. However, the nanoparticle formation takes place suddenly after 60 s of microwave irradiation. *Ficus ingens* mediated AgNPs recorded MIC value of 10 μg mL^{-1} on *E. coli* and 20 μg mL^{-1} on both *S. typhi* and *B. cereus*[107] which is in close agreement with the earlier report of 10 μg mL^{-1} for *E. coli*. The AgNPs showed highest inhibition against *E. coli* and least with *S. cereus*. Commercial antibiotic Ciprofloxacin showed better activities than the synthesized NPs.

In general, the reduction in the size of the metallic nanoparticles is expected to increase the antibacterial activity due to significantly large surface area of the smaller nanoparticles. However, the results obtained by Erci *et al.*[108] using *Thymbra spicata* leaf extract is worth discussing. In their study higher antibacterial activity of, say, AgNPs2 (average diameter 70.2 nm) in comparison to AgNPs1 (average diameter 25.1 nm) was recorded. They reasoned that this could be due to the shape of AgNPs2, which have triangles, hexagons, spheres and irregular shapes, whereas AgNPs1 exhibit mostly spherical formation. This interesting finding confirmed the shape-dependent bacterial activity of AgNPs, and support earlier reported protocol.[109] The MIC of 50 μg mL^{-1} was recorded for *S. cereus* whereas, it was 100 μg mL^{-1} for *E. coli*. This finding is in sharp contrast to the work of Kavaz *et al.*[107] mentioned earlier where Gram-negative bacteria has lower MIC than Gram-positive bacteria. However, Erci *et al.*[108] defended their finding of the more pronounced effect of AgNPs against Gram-positive bacteria than Gram-negative bacteria based on the structural difference in cell wall composition of Gram-positive and Gram-negative bacteria. Gram-negative cell wall was covered with an outer lipid membrane (lipopolysaccharide), which is more negatively charged than Gram-positive. As is evident from the zeta value, the biogenic silver nanoparticles were also negatively charged and the electrostatic repulsion between the nanoparticles and Gram-negative bacteria hinders particle attachment and penetration into the cell[37] However, this postulate is not yet fully understood. Again, as against the finding of Erci *et al.*[108] the Gram-positive bacteria are less affected by AgNPs (produced from *Indigofera tinctoria*) than Gram-negative bacteria as reported by Vijayan *et al.*[110] The authors credited the presence of large number of peptidoglycan layers on the walls of Gram-positive bacteria than Gram-negative bacteria that have to some extent prevent the nanoparticles entry to cytoplasmic membrane than Gram-negative bacteria. Hence, the true role of chemicals in the cell wall of bacteria needed to be properly investigated to understand the underlying mechanism of the cell death due to NPs.

Another interesting work on the shape-dependent activity of biogenic AgNPs was reported using *Trichoderma viride* extract where the authors reported a higher antimicrobial activity of penta- and hexagonal NPs than spherical NPs when the size are of similar range.[111] The different shape AgNPs such as pentagonal, hexagonal and spherical were synthesized by manipulating physical parameters, temperature, pH, and reaction time. At neutral pH (7), spherical NPs were observed under all reaction conditions. Delightfully, at pH 5.0 and 9.0, rectangular and penta-/hexagonal NPs were obtained at 40 °C after 72 h of incubation. In general, longer is the reaction, bigger is the size of NPs whereas higher temperature always affords a smaller NP. It was also found that triangular shape AgNPs showed better antimicrobial activity compared to that of spherical and rod shaped as it has high percentage of facet (1 1 1) that possess a high atomic density which increases binding efficiency of Ag to sulfur containing components, whereas spherical and rod shaped particles have a high percentage of (1 0 0) facets.[112,113]

Recently, *Tecoma stans*,[114] *Salvia leriifolia*,[115] *Leucaena leucocephala* L.[116] and *Selaginella bryopteris*[117] were also reported to produced AgNPs which are mainly spherical in nature. *Galega officinalis* leaf extract mediated AgNPs with size-dependent activities were reported by Manosalva *et al.*[118] AgNPs with 23 nm and 220 nm recorded MIC of 5 μL mL^{-1} and 30 μL mL^{-1} respectively against *E. coli* showing the higher activity of the smaller NPs. Interestingly MIC of *S. aureus* (a Gram-positive bacteria) is higher (50 μL mL^{-1}) than *E. coli* (a Gram-negative bacteria) using 23 nm size AgNPs which implies the higher activity of AgNPs against Gram-negative bacteria.

In the year 2019, antimicrobial fabric tests on the dyed cloths were conducted using AgNPs derived from *Camellia sinensis* (tea leaf) extract where bleached cotton cloths were dyed using the

NPs colloidal solutions. The attachment of AgNPs on the cloths was confirmed by SEM. SEM images of AgNPs with green tea extract also showed the generation of AgNPs. The AgNPs showed excellent antimicrobial activities against *S. aureus*, *K. pneumoniae* in the cotton fabric which potentially endorse the suitability of using AgNPs as an effective antimicrobial in cloths.[119] Bernardo-Mazariegos *et al.* used DLS to measure the average hydrodynamic size and zeta potential of the AgNPs synthesized from *Justicia spicigera*.[120] The sample with a mixture of AgNPs of different sizes gave two broad peaks and was weighted toward the larger particles (*z*-average size of 4.04 μm and 192 nm). The authors are of the opinion that DLS measurement may not be accurate for polydisperse samples due to its nature to respond toward larger particles. Additionally, the zeta potential was of the NPs was found to be 0.2 mV that indicated the less stability and hence, a tendency to agglomerate to form large particles.

In recent times, highly antimicrobial AgNPs were synthesized using *Kleinia grandiflora*,[121] *Eucalyptus citriodora*,[122] *Juniperus procera*[123] and *Capparis zeylanica*.[124] Two different shapes structure in the form of sphere and cubic are observed in SEM analysis of the AgNPs generated from *Juniperus procera* leaf extract. The produced NPs recorded the highest ZOI against *P. mirabilis* measured at 29 ± 1.3 mm. The author suggested that the high antimicrobial activity of the NPs is due to the inherent activity of the NPs coupled with the plant particulates attached to the NPs, as the plant which contain high flavonoids and polyphenols are a well-known antimicrobial by themselves.[125] Small size AgNPs (9 nm) synthesized using *Caesalpinia pulcherrima* leaf extract were found to exhibited an MIC as low as 0.078 mg mL^{-1} and 0.156 mg mL^{-1} for *K. pneumoniae* and *E. coli* respectively. Accordingly, the AgNPs possessed maximum antimicrobial activity against *K. pneumoniae* and *E. coli* whereas only moderate effects were shown against *C. xerosis*, *S. mutans*, *S. aureus*, *S. viridians*, *S. pyrogenes*, *S. viridians* and *C. diphtheriae* that have higher MICs.[126]

Synergistic antimicrobial activity of *Ligustrum lucidum* mediated AgNPs and Epoxiconazole under different conjugation ratio was studied against *S. turcica*, a common maize pathogen.[127] The antifungal activity of AgNPs was evaluated alone, and the synergistic inhibition effect was also measured at various conjugation ratios of AgNPs and epoxiconazole, where a prominent synergistic antifungal effect was observed at 8 : 2 and 9 : 1 (AgNPs/epoxiconazole) and the inhibition toxicity ratio reached as high as 1.22 and 1.24, respectively.

Aesculus hippocastanum (horse chestnut) mediated special AgNPs with size 50 ± 5 nm was reported to have highest antimicrobial activity (ZOI 20.0 ± 0.00 mm) against a Gram-negative bacteria *P. aeruginosa* among all the tested microorganisms listed in Table 1, entry 74.[128] Interestingly, although the AgNPs have profound effects on all the tested bacteria, it have no effect against fungal strains such as *C. albicans* ATCC 10231, *C. tropicalis* ATCC 13803 and *C. krusei* ATCC 1424. The MIC and MBC of AgNPs for the tested microorganisms were in the range from 0.19–12.5 μg mL^{-1} and 1.56–25 μg mL^{-1}.

Ramadan *et al.*[129] studied the antiviral activity of green synthesized AgNPs and found that AgNPs greatly enhanced the antiviral activity of *M. alternifolia* leaf extract, which on its own has no effect on the tested viruses such as herpes simplex virus type 1 (HSV-1), and herpes simplex virus type 2 (HSV-2). In addition, the NPs showed excellent activities against several persistent skin bacteria including *S. epidermis* and methicillin-resistant *Staphylococcus aureus* (MRSA). Interestingly, tea tree oil of *M. alternifolia* itself showed even higher activity than the AgNPs against some tested microbes which is hardly the case in literature. In another work, *Carya illinoinensis* mediated AgNPs were found to be more efficient against Gram-negative (*E. coli*) than Gram-positive bacteria (*S. aureus*)[130] in a similar trend reported earlier.[118]

Although literature revealed that bacterial cell are generally more sensitive to AgNPs, biogenic AgNPs derived from *Murraya koenigii* leaf extract interestingly shown highly equal activity against Gram-negative bacteria *P. aeruginosa* (ZOI of 18 mm) and a fungus *C. albicans* (18 mm ZOI).[131] In 2020, several leaf extracts of plant such as *Clerodendrum inerme*,[132] *Aspilia pluriseta*,[133] *Melia azedarach*,[134] *Scoparia dulcis*,[135] and *Lantana trifolia*.[136] All these AgNPs are shown to exhibit an excellent antimicrobial activity against numerous common pathogenic microbes. *Mikania micrantha* leaf extract mediated AgNPs were also reported to show a high ZOI of 26.17 mm and 26.05 mm against *B. subtilis* and *E. coli* respectively.[137]

More recently, AgNPs of average size 3.46 nm were produced using *Solanum nigrum* plant leaf extract.[138] This is one of the smallest biogenic AgNPs reported so far and NPs as small as 1.74 nm were observed. SPR bands band at 442 nm in UV-visible spectroscopy confirmed the formation of AgNPs. Interestingly, the authors observed a much prominent antimicrobial activity exerted by AgNPs compared to AuNPs and PdNPs potentially due to the more effective capping of AgNPs nanoparticles than either Au or PdNPs which results in well-dispersed small AgNPs without much agglomeration as detected by HRTEM. The authors are of the opinion that polyphenols present in *Solanum nigrum* extract forms a negative environment around the particles and hence create a repulsive force which overcomes the *van der Waals* force of attraction and prevent AgNPs agglomeration. The AgNPs showed 22 mm ZOI, while 20 mm and 19 mm ZOI are observed in Au and Pd NPs respectively against *E. coli* at 10 μL mL^{-1} concentration. However, although the authors credit the effective capping of AgNPs as a reason for its higher antimicrobial activity, it may also be due to the smaller size of the AgNPs (3.46 nm) as compared to Au (9.39 nm) and Pd NPs (21.55 nm).

Maghimaa *et al.*[139] reported biosynthesis of AgNPs using *Curcuma longa* leaf extract and investigate their antimicrobial activity in AgNP coated cotton fabric. The loading of AgNPs on the cotton fabric was confirmed by SEM analysis, which was further assisted by the EDX analysis. The authors have reported that the cotton fabric loaded with AgNPs showed great resistance to the growth of pathogenic microorganisms and hence they claimed that the cotton fabric loaded with AgNPs synthesized from *Curcuma longa* can be used for the diverse application in the medical patient as well as in medical workers to resist microbial infection.

In 2020, green synthesis of spherical AgNPs, CuNPs and FeNPs with size 11–19, 28–35 and 40–52 nm, respectively using *Syzygium cumini* leaf extract was reported.[140] The order of antibacterial property against methicillin- and vancomycin-resistance *S. aureus*, *A. flavus* and *A. parasiticus* microbes was found to be Ag- > Cu- > Fe NPs, which linearly relates with the size of the NPs, thereby reinforcing the size-dependent activity of NPs.[141] In addition, the bioproduction of aflatoxins (a family of toxins produced by certain fungi that are found on agricultural crops such as maize (corn), peanuts, cottonseed, and tree nuts) in *A. flavus* and *A. parasiticus* was also significantly inhibited by AgNPs when compared with the Fe and Cu NPs. Interestingly, the pH of the plants extract reduced after the formation of NPs in all the cases. *Cleistanthus collinus*[142] and *Cestrum nocturnum*[143] are also known to have produced AgNPs.

In another work, rice leaf extract was utilized for the biosynthesis of AgNPs with size 16.5 nm.[144] Antifungal activity of the synthesized NPs was tested against mycelium and sclerotia of *R. solani*, a fungus that causes sheath blight disease in rice and found that it inhibits the growth of fungus and the growth inhibition is dependent on the concentration of the AgNPs. The MIC values of AgNPs were in the range of 5–10 and 15–20 μg mL^{-1} towards fungal mycelium and sclerotia, respectively. Results revealed that growth inhibition at 10 μg mL^{-1} AgNPs is 81.7–96.7% for mycelium and 20 μg mL^{-1} treatment completely inhibited disease cause by *R. solani*. In a previous investigation, 43.3–73.6% growth inhibition of *R. solani* was observed at a higher concentration of 2 mg mL^{-1} with larger AgNPs with 40–60 nm.[145]

Recently, an ultra sound-assisted AgNPs of size 8 mm were synthesized using *Mentha aquatica* leaf extract as reducing and capping agent.[146] To the best of our knowledge, this is the smallest biogenic AgNPs reported so far. The production of NPs could occur at RT, but ultrasound greatly reduced the reaction time to 10 min whereas RT took 1 h. The authors highlighted that the phenolic compounds in the *Mentha aquatica* leaf extract get oxidized to Quinone in an alkaline condition which provides free electrons for reduction of the Ag^+ ion to Ag^0 to form the desired AgNPs. Largely due to its ultra-small size, the AgNPs displayed a very low MIC of 2.2 μg mL^{-1} for *P. aeruginosa*, which showed its high efficacy against the tested microbe.

Rosemary (*Rosmarinus officinalis* Linn.)[147] and *Ceropegia thwaitesii*[148] leaf extract mediated AgNPs which showed consistent higher activities against Gram-negative bacteria were also reported. Interestingly, *S. flexneri*, *S. typhi*, *B. subtilis*, *M. luteus*, and *P. mirabilis* are more susceptible to AgNPs than *E. coli*[148] which is not very common in literature.

In the year 2015, Gavade *et al.* prepared AgNPs using the leaf extract of *Ziziphus jujuba* under RT.[149] The AgNPs have different shapes with 20–30 nm size as revealed by TEM images. The authors investigated the effect of pH on the size and stability of the NPs, and observed form UV-Visible spectroscopic graphs that absorbance value linearly increases with increasing pH increases from 4 to 9, which indicates the rate of formation of AgNPs increases from acidic to basic medium. In addition, at acidic pH, bands were wider and display red shift which is an indication of increase in particle size. However, in basic condition, bands were narrow and display blue shift due to decrease in particle size. The rapid formation of AgNPs in neutral and basic pH this may be due to the ionization of the phenolic groups present in the leaf extract.[150] The slow rate of formation and aggregation of AgNPs in acidic pH could be related to electrostatic repulsion of anions present in the solution.[151,152] Ironically, at basic pH there is a possibility of AgOH precipitation which need to be avoided.[150] Hence, the authors concluded that the optimum condition for the preparation of AgNPs with desired size and stability was neutral medium. The NPs have a zeta potential of −26.4 mV which is an indication of its excellent stability in colloidal state as a zeta potential higher than 30 mV or lesser than −30 mV is indicative of a stable system.[153] The AgNPs showed high efficacy against *E. coli* and found to be stable for more than 6 months probably due an excellent capping of NPs (indicated by FR-IR) and low zeta potential.

Irregular shape AgNPs of average size 28 nm, 26.5 nm, 65 nm, 22.3 nm and 28.4 nm were prepared from *O. tenuiflorum*, *S. cumini*, *C. sinensis*, *S. trilobatum* and *C. asiatica*, respectively.[154] Among several tested microbes the highest antimicrobial activity of AgNPs synthesized by *S. trilobatum* and *O. tenuiflorum* extracts was found against Gram-positive bacteria *S. aureus* (30 mm ZOI) and Gram-negative bacteria *E. coli* (30 mm) respectively. Interestingly, *C. sinensis*, *S. trilobatum* and *C. asiatica* derived AgNPs consistently showed higher susceptibility towards a Gram-positive bacteria *S. aureus* and Gram-negative bacteria *E. coli* and *K. pneumoniae*. These findings clearly shown that some AgNPs are more sensitive towards a Gram-positive bacteria whereas some towards a Gram-negative bacteria, hence the question of selective sensitivity of biogenic AgNPs toward Gram-positive or negative bacteria still remains unsolved. Is the selectivity depending on the biomaterial capping agents attached to NPs or the size of NPs? Hence, one may need to consider the biomolecules present in the plant extract or the size of AgNPs to truly understand the selectivity.

A globular shape AgNPs were prepared using *Amaranthus gangeticus* Linn leaf extract in 2015 which exhibited an inhibitory activity towards Gram-positive, Gram-negative bacteria as well as fungus.[155] In another work *Andrographis paniculata* leaf extract produced a rarely reported cubic shape AgNPs.[156] Study on different shape of AgNPs is of great interest due to the shape-dependent activities of AgNPs towards microbes as noted earlier.[109] The AgNPs showed a high ZOI of 21.3 ± 0.4 mm for Gram-negative bacteria *P. aeruginosa* with very low MIC of 3.125 μL mL^{-1} which testament its high antimicrobial activity. Yao *et al.*[157] noted that the thickness of the peptidoglycan layer of other Gram-negative bacteria such as *E. coli* is somewhat more than *P. aeruginosa*, hence the author, in good agreement with Yao's work, observed a lower ZOI (16.6 ± 0.3 mm) in case of *E. coli*.

Elangovan *et al.*[158] reported the biosynthesis of AgNPs having cubic, pentagonal and hexagonal shape with size range of 68.06–91.28 nm using *Andrographis echioides* leaf extract and investigate its bactericidal activity against several microbes. The result revealed a high ZOI in the case of *E. coli* (28 mm) and *S. aureus* (23 mm) in 100 μg mL^{-1} concentration of AgNPs.

Azadirachta indica (neem) leaf extract was also reported for the green synthesis of polydisperse AgNPs at RT and evaluated as a potent antimicrobial agent against *P. nitroreducens*, a biofilm-forming bacterium and fungus *A. unguis*.[159]

While most biogenic AgNPs are spherical, a flower-like structure was reported by Ajitha *et al.* in 2017.[160] The AgNPs showed very high activity towards bacterial culture *Pseudomonas* spp. (ZOI of 11 mm) even at very low AgNPs concentration (8 μL mL^{-1}). It is worth note that the AgNPs also consistently displayed a better activity in fungal strain, *Penicillium* spp. than bacteria such as *E. coli* and *Staphylococcus* spp. which is hardly a case in any literature as bacteria are usually considered more sensitive to AgNPs than fungi.

3.2 From seeds

Plant seed extract also well established for the biosynthesis of nanoparticles. Till date, various seeds extract has been utilized for the biosynthesis AgNPs (Table 2, entries 1–27). *Sinapis arvensis* seeds mediated AgNPs was reported for more than 83% inhibition of mycelium growth of fungus *N. parvum*. Inductively coupled plasma spectrometry (ICP) analysis revealed complete reduction of Ag^{+} to Ag^{0} in more than 95% conversion within 50 days of reaction.[161] In another work, grape seed extract was utilized for the biosynthesis of spherical and polygonal AgNPs with size ranging from 25–35 nm. Bactericidal activity of the synthesized NPs was tested against eight different ocean pathogenic bacteria; however, it showed great inhibition activity only against four bacteria such as *V. alginolyticus*, *V. anguillarum*, *V. parahaemolyticus* and *A. punctate*.[162] Sumitha *et al.*[38] reported bio-reduction of $AgNO_3$ to AgNPs using *Durio zibethinus* seed extract. It is reported that saccharides present in the extract induces the bio-reduction and the amino acids present in the extract stabilized the synthesized AgNPs. Bactericidal activity was tested against different pathogenic bacteria and found that the NPs showed greater activity against *S. typhimurium*, *S. haemolyticus* and *S. aureus* over *B. subtilis*, *E. coli* and *S. typhi*. However, the synthesized NPs showed lesser inhibition compared to the drug Gentamicin against all the mentioned pathogenic bacteria even at a lower dose of Gentamicin.

Pimpinella anisum,[163] *Synsepalum dulcificum*,[164] *Vigna radiate*,[165] *Dracocephalum moldavica*[166] leaf extracts were also successfully applied for the green synthesis of AgNPs. *Vigna radiata* mediated AgNPs, was found to be more susceptible towards Gram-negative bacteria *E. coli* (ZOI 20 mm) than Gram-positive *S. aureus* (ZOI 16 mm) due to the higher thickness of the peptidoglycan layer (approx. 80 nm thick) of the cell wall of Gram positive bacteria which is 10 times thicker than the peptidoglycan Gram-negative bacteria, hence is less susceptible to be destroyed by AgNPs.[165]

Several reported literatures revealed that the efficiency of AgNPs as antimicrobial agent is extensively dependent on the shape of the nanoparticles. The comparison of spherical, disc like and triangular shaped AgNPs as antimicrobial agent revealed the activity trend follows as spherical AgNPs > disc-like AgNPs > triangular AgNPs.[65,136]The highest inhibition effect of 94.1% and 84% were observed at 40 ppm concentration of AgNPs against *R. solani* and *N. parvum* respectively, using AgNPs derived from *Trifolium resupinatum* seeds extract.[167] In a closely related study, Khatami *et al.* reported more than 86% inhibition of mycelium growth of *R. solani* at a concentration 25 μg mL^{-1} (or 25 ppm) of the biogenic AgNPs.[168] Several plant seeds such as *Nigella arvensis*,[169] *Linseed*,[170] *Embelia ribes*,[171] *Melissa officinalis*[172] are applied for the generation of spherical shape AgNPs. While biogenic AgNPs are reported to be more efficient antimicrobial than any other metal NPs in most of the case, it is worth mentioned that the *Embelia ribes* derived AgNPs is less susceptible to *E. coli* at showing ZOI of 20 mm against 28 mm ZOI for AuNPs at 250 μL mL^{-1} concentration.[171] Although having small size of NPs (6–25 nm), *Leucaena leucocephala* mediated AgNPs displayed very low toxicity against both *E. coli* and *S. aureus* with ZOI of 18 mm and 22 mm (approx.) respectively at 1000 ppm AgNPs concentration.[173] *Alpinia katsumadai* seeds extract mediated AgNPs showed excellent activities against *E. coli* and *S. aureus* than that of *P. aeruginosa*,[174] whereas those derived from *Myristica fragrans* are found to be highly sensitive to multidrug-resistant (MDR) *Salmonella enterica serovar typhi* (*S. typhi*) where a highest ZOI of 16.4 ± 0.45 was observed at 100 μg μL^{-1} concentration of AgNPs.[175]

Common skin bacteria such as *P. acnes* and *S. epidermidis* are found to be highly inhibited by AgNPs synthesized using *Phoenix sylvestris* L. The authors also proved that AgNPs is more susceptible to the tested shin bacteria than the seeds extract as well as $AgNO_3$ solution as can be seen from the ZOI.[176] The high toxicity of *Phoenix dactylifera* derived AgNPs against Methicillin-resistant *S. aureus* is clearly seen in SEM images (Fig. 5a–d) and HRTEM images (Fig. 5e and f). Cells treated with AgNPs undergo deformities and irregular cell surface (red arrow). Attachment and penetration of NPs and deformities of the outer most layers of cell wall and cytoplasmic membrane are also clearly visible in HRTEM.[177]

The seeds extracts of plants such as *Tectona grandis*,[178] *Persea americana*,[179] *Salvia hispanica* L[180] and *Trigonella foenum-graecum*[181] produced AgNPs with high antimicrobial activities. Interestingly the size of AgNPs depends on the concentration of *Persea americana* extract where a small NPs was recorded at low concentration of aqueous extract, whereas high concentration results in the formation of larger NPs.[179] Ironically, the AgNPs from *Salvia hispanica* L showed lower susceptibility towards antibiotic Ampicillin against *E. coli* and *S. aureus* although its high ZOI against *E. coli* (18.5 mm) and *S. aureus* (14.9 mm) at 7.7 μL mL^{-1} concentration.[180]

The increase in lactate dehydrogenase (LDH) and alkaline phosphatase (ALP) enzyme concentration were used as a means to visualize the change in physiology and inhibition caused to microbes such as *S. aureus* (263 U L^{-1}) and *S. aureus* (263 U L^{-1}) by *Trigonella foenum-graecum* mediated AgNPs.[181] This increase in enzyme reflected that bacteria are under stress conditions due to unfavorable environment on treatment with AgNPs.[182] Synergistic behavior of ampicillin with *Hibiscus cannabinus* seeds produced AgNPs against *S. aureus*, *B. cereus*, *E. coli* was investigated by Adnan *et al.* in 2020.[183] Biogenic AgNPs that possessed high inhibitory effect on biofilms formation in *P. aeruginosa*, *C. violaceum* and *S. marcescens* was reported.[184] The

Table 2 Various seeds, flower, root extract used for the green synthesis of AgNPs and their antimicrobial activity

No.	Plants	Plant parts	Shape and size	Test microorganisms	Ref.
1	*Sinapis arvensis*	Seeds	Spherical; 1–35 nm	*N. parvum*	161
2	*Grape*	Seeds	Spherical and polygonal; 25–35 nm	*V. alginolyticus*, *V. anguillarum*, *V. parahaemolyticus*, *A. punctata*, *E. coli*, *S. dysenteriae*, *P. Aeruginosa*, *S. aureus*	162
3	*Coffea arabica*	Seeds	Spherical and ellipsoidal; 20–30 nm	*E. coli* and *S. aureus*	41
4	*Durio zibethinus*	Seeds	Spherical and rod shaped, 20–75 nm	*S. typhi*, *S. typhimurium*, *E. coli*, *S. aureus*, *S. haemolyticus*, *B. subtilis*	38
5	*Pimpinella anisum*	Seeds	Spherical; 3.2–16 nm	*S. pyogenes*, *A. baumannii*, *K. pneumoniae*, *S. typhi*, *P. aeruginosa*	163
6	*Synsepalum dulcificum*	Seeds	Spherical; 4–26 nm	*P. aeruginosa* and *K. granulomatis*, *A. flavus*, *A. fumigatus*, *A. niger*	164
7	*Vigna radiata*	Seeds	Spherical; 18 nm	*Escherichia coli* and *Staphylococcus aureus*	165
8	*Dracocephalum moldavica*	Seeds	Spherical; 5–50 nm	*E. coli*, *P. aeruginosa*, *S. aureus*, *S. marcescens*, *S. epidermidis*, *B. subtilis*	166
9	*Trifolium resupinatum*	Seeds	Spherical; 17 nm	*R. solani*, *N. parvum*	167
10	*Descurainia sophia*	Seeds	Spherical; 1–35 nm	*A. rhizogenes*, *A. tumefaciens*, *R. solani*	168
11	*Nigella arvensis*	Seeds	Spherical; 2–15 nm	*S. pyogenes*, *B. subtilis*, *S. aureus*, *E. coli*, *P. mirabilis*, *S. typhimurium*	169
12	*Linseed*	Seeds	Spherical; 10–35 nm	*S. mutans*, *S. epidermidis*, *P. aeruginosa*, *E. coli*, *S. aureus*, *B. subtilis*, *A. odontolyticus*, *A. niger*	170
13	*Embelia ribes*	Seeds	Spherical; 5–35 nm	*E. coli*, *S. aureus*	171
14	*Melissa officinalis*	Seeds	Spherical; 34.64 nm	*E. coli*, *B. subtilis*, *B. vallismortis*	172
15	*Leucaena leucocephala*	Seeds	Spherical; 6–25 nm	*P. gigantea*, *E. taxodii*, *E. coli*, *S. aureus*	173
16	*Alpinia katsumadai*	Seeds	Spherical; 12.6 nm	*S. aureus*, *P. aeruginosa*, *E. coli*	174
17	*Myristica fragrans*	Seeds	Spherical; 25 nm	Multidrug-resistant (MDR) *Salmonella enterica serovar typhi* (*S. typhi*)	175
18	*Durio zibethinus*	Seeds	Spherical; 20–75 nm	*S. aureus*, *S. typhimurium*, *E. coli*, *B. subtilis*, *S. typhi*, *S. haemolyticus*, *S. aureus*	38
19	*Phoenix sylvestris* L.	Seeds	Spherical; 40–50 nm	*P. acnes*, *S. epidermidis*	176
20	*Phoenix dactylifera*	Seeds	Spherical; 14–30 nm	Methicillin-resistant *S. aureus*	177
21	*Tectona grandis*	Seeds	Spherical; 10–30 nm	*B. cereus*, *S. aureus*, *E. coli*	178
22	*Persea americana*	Seeds	Spherical; 50 nm	*E. coli*	179
23	*Salvia hispanica*	Seeds	Spherical; 1–27 nm	*E. coli*, *S. aureus*	180
24	*Trigonella foenum-graecum*	Seeds	Spherical; 33.93 nm	*E. coli*, *K. pneumoniae*, *S. aureus*, *S. typhi*, *P. aeruginosa*, *A. flavus*, *C. albicans*, *T. rubrum*, *P. notatum*, *T. viridiae*	181
25	Sesame (*Sesamum indicum*, L.)	Seeds	Spherical; 6.6–14.80 nm	*P. aeruginosa*, *K. pneumoniae*, *B. subtilis*, *S. aureus*	214
26	*Hibiscus cannabinus*	Seeds	Spherical; 7–11 nm	*S. aureus*, *B. cereus*, *E. coli*	183
27	*Carum copticum*	Seeds	Spherical; 21.48 nm	*P. aeruginosa*, *S. marcescens*, *C. violaceum*	184
28	*Coffea arabica*	Seeds	Spherical and ellipsoidal; 20–30 nm	*E. coli*, *S. aureus*	41
29	*Pimpinella anisum*	Seeds	Irregular; 16–48 nm	*E. coli*, *S. aureus*, *A. flavus*, *C. albicans*	185
30	Marigold (*Tagetes erecta*)	Flower	Spherical; 46.11 nm	*S. aureus*, *B. cereus*, *S. coli*, *P. aeruginosa*, *C. glabrata*, *C. albicans*, *C. neoformans*	188
31	*Nyctanthes arbortristis*	Flower	Spherical and oval; 5–20 nm	*E. coli*	189
32	*Caesalpinia pulcherrima*	Flower	Spherical; 12 nm	*S. aureus*, *C. glabrata*, *B. cereus*, *E. coli*, *S. typhimurium*, *C. albicans*, *C. neoformans* *B. subtilis*, *C. rubrum*, *Pseudomonas aeruginosa*, *K. pneumoniae*	190
33	*Alcea rosea*	Flower	Spherical; 7.2 nm	*E. coli*, *S. aureus*	191
34	*Argemone mexicana*	Flower	Spherical; 29.34 nm	*S. aureus*, *P. aeruginosa*, *E. coli*, *K. aerogenes*	192
35	*Turnera ulmifolia*	Flower	Spherical; 32.42 nm	*S. aureus*, *P. aeruginosa*, *E. coli*, *K. aerogenes*	192
36	*Tecoma stans*	Flower	Spherical; 50–60 nm	*E. coli*, *S. aureus*	193
37	*Moringa oleifera*	Flower	Spherical; 8 nm	*K. pneumonia*, *S. aureus*	194
38	*Syzygium aromaticum*	Flower	Polydisperse; 23 nm	*Staphylococcus* spp. *E. coli*, *Pseudomonas* spp., *Bacillus* spp., *A. flavus*, *A. niger*, *Penicillium* spp.	195
39	*Potentilla fulgens*	Root	Spherical; 10–15 nm	*E. coli*, *B. subtilis*	196
40	*Alpinia calcarata* (ginger)	Root	Spherical; 5–15 nm	*P. mirabilis*, *E. coli*, *B. cereus*, *S. aureus*	197
41	*Erythrina indica* Lam	Root	Spherical; 20–118 nm		198

Table 2 (*Contd.*)

No.	Plants	Plant parts	Shape and size	Test microorganisms	Ref.
				S. aureus, *M. luteus*, *Escherichia coli*, *B. subtilis*, *S. typhi*, *S. paratyphi*	
42	*Diospyros paniculata*	Root	Spherical; 14–28 nm	*P. notatum*, *A. flavus*, *A. niger*, *C. albicans*, *S. cerevisiae*	199
43	*Diospyros sylvatica*	Root	Spherical; 8 nm	*B. pumilis*, *P. aeruginosa*, *B. subtilis*, *S. aureus*, *K. pneumoniae*, *E. coli*, *S. pyogenes*, *P. vulgaris*, *A. niger*, *P. notatum*, *A. flavus*, *S. cerevisiae*, *C. albicans*	200
44	*Annona muricata*	Root	Spherical; 15.08–33.11 nm	*K. pneumonia*, *S. aureus*	201
45	*Cibotium barometz*	Root	Spherical; 23 nm	*Escherichia*, *S. aureus*, *S. enterica*, *P. aeruginosa*	202
46	*Diospyros assimilis*	Root	Spherical; 14–28 nm	*B. pumilis*, *B. subtilis*, *S. aureus*, *S. pyogenes*, *K. pneumoniae*, *E. coli*, *P. aeruginosa*, *P. vulgaris*, *A. niger*, *A. flavus*, *C. albicans*, *P. notatum*, *S. cerevisiae*	203
47	*Pelargonium endlicherianum* Fenzl.	Root	Spherical; 25–80 nm	*P. aeruginosa*, *E. coli*, *S. epidermidis*	204
48	*Rheum palmatum*	Root	Spherical; 121 ± 2 nm	*S. aureus*, *P. aeruginosa*	205
49	*Lepidium draba*	Root	Spherical; 20–80 nm	*S. aureus*, *B. cereus*, *S. typhimurium*, *E. coli*	207
50	*Angelica pubescens* Maxim	Root	Quasi-spherical; 12.48 nm	*E. coli*, *S. aureus*, *P. aeruginosa*, and *S. enterica*	208
51	*Phoenix dactylifera*	Root	Spherical; 15–40 nm	*E. coli*, *C. albicans*	209
53	*Arctium lappa*	Root	Spherical; 21.3 nm	*E. coli*, *A. tumefaciens*, *L. acidophilus*, *S. aureus*	210
53	*Asparagus racemosus*	Root	Spherical; 10–17 nm	*E. coli*, *S. aureus*, *B. subtilis*, *K. pneumonia*, *P. fluorescence*, *A. hydrophila*, *E. tarda*, *F. branchiophilum*, *Y. ruckeri*	211
54	*Lysiloma acapulcensis*	Root	Spherical; 1.2 to 62 nm	*E. coli*, *P. aeruginosa*, *S. aureus*, *C. albicans*	212
55	*Raphanus sativus*	Root	Irregular; 3.2–6.0 nm	*S. aureus*, *E. coli*, *C. albicans*, *C. glabrata*, *C. tropicalis*	213

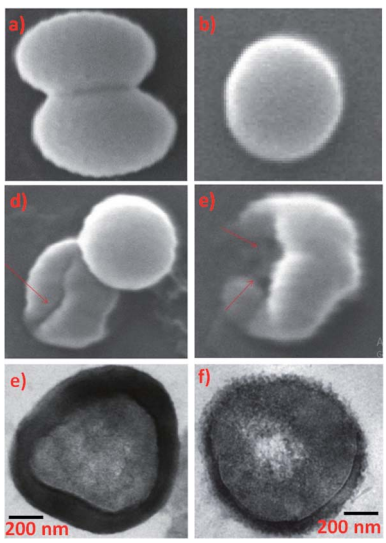

Fig. 5 (a and b) Untreated control cells, (c and d) cells treated with 25 and 50 μg mL^{-1} of AgNPs respectively, SEM images; (e) untreated control cell and (f) treated with 50 μg mL^{-1} AgNPs TEM images. This figure has been adapted from ref. [177] with permission from Hindawi, copyright 2018.

biofilms of *P. aeruginosa* was inhibited by 10.6, 18.8, 36.1, 62.0, and 77.6% in presence of 1, 2, 5, 10, and 15 μg mL^{-1} of *Carum copticum* mediated AgNPs respectively.

In their effort to synthesize AgNPs from *Pimpinella anisum* seeds extract, Zayed *et al.* systematically studied to influence of different parameters such as extraction solvent used, extraction temperature, solvent/plant ratio and extraction time which are crucial for the successful synthesis of AgNPs.[185] Hexane, methylene chloride, 70% methanol and water were evaluated as an extraction solvent and 70% methanol was chosen as a best solvent for the fast synthesis of NPs indicated by color change of the reaction solution, whereas this color change is very slow or not visible in other solvent extracts. The high reactivity of 70% aqueous methanol extract towards the reduction of Ag^{+} to Ag^{0} NPs is due to an excellent solubility of polyphenols in the plant seeds which is efficiently washed down during the extraction process. The SPR peak intensities of both AgNPs and AuNPs increased as the extraction temperature is raised from 25 to 60 °C. This may be due to increasing the solvent's diffusion rate into plant tissues by destroying the cell structures with raising the temperature.[31] They also observed increasing SPR by increasing the extraction temperature 25–60 °C but extraction at 60 to 85 °C resulted in decreasing SPR probably due to decomposition of bioreductant at high temperature. The solvent/plant ratio of 10 mL g^{-1} was optimized for the AgNPs

synthesis. Increasing the ratio from 3–10 mL g^{-1} inceased the SPR due to increasing solubility of biomolecule, however above 10, SPR went down due to high dilution of the extract. The band intensity reached its maximum value with extracts prepared at 60 min, further increase in contact time caused a decrease in the band intensity. It was observed that as extraction time increases the mass transfer coefficient between the solute and solvent increases that potentially increase the amount of the extracted biomolecule from plants which enhance the formation of the NPs.[186] However, prolonged extraction time resulted in the thermal decomposition and oxidation of reactive biomolecules due to prolong heating.[187]

Similarly, the dried and roasted coffee (*Coffea arabica*) seed was employed as a reducing and stabilizing agent for the biosynthesis of AgNPs. TEM micrographs of synthesized AgNPs (Fig. 6) were revealed that the nanoparticles are spherical and ellipsoidal in structure with size ranging from (a) 10–40 nm for 0.1 M, (b) 10–50 nm for 0.05 M and (c) 20–150 nm for 0.02 M. The biomolecules that act as a capping agent around the NPs are visible in TEM images. The SAED patterns indicated that the nanoparticles are crystalline in nature with a certain d-spacing corresponds to fcc structure. The authors investigated its bactericidal activity against *E. coli* and *S. aureus*. The results revealed that AgNPs solution of 0.05 M and 0.1 M showed a high ZOI in both cases. However, ZOI is higher against *E. coli*.[41]

3.3 From flowers

Recently, flower extracts have been immensely utilized for the biosynthesis of NPs. There are various literatures available for the bio-reduction of $AgNO_3$ to AgNPs (Table 2, entries 28–37). Padalia *et al.*[188] reported the utilization of flower extract of *Tagetes erecta* for the bio-reduction of $AgNO_3$ to synthesized AgNPs and investigate their bactericidal activity against both Gram-positive and Gram-negative bacteria such as *S. aureus*, *B. cereus*, *S. coli*, *P. aeruginosa*, *C. glabrata*, *C. albicans*, *C. neoformans*. The result obtained revealed that the bactericidal activity is greater for *E. coli* and *P. aeruginosa* compared to other pathogenic bacteria. Apart from that, the authors reported that the antifungal activity of the AgNPs along with antibiotic against the fungal strain and Gram-

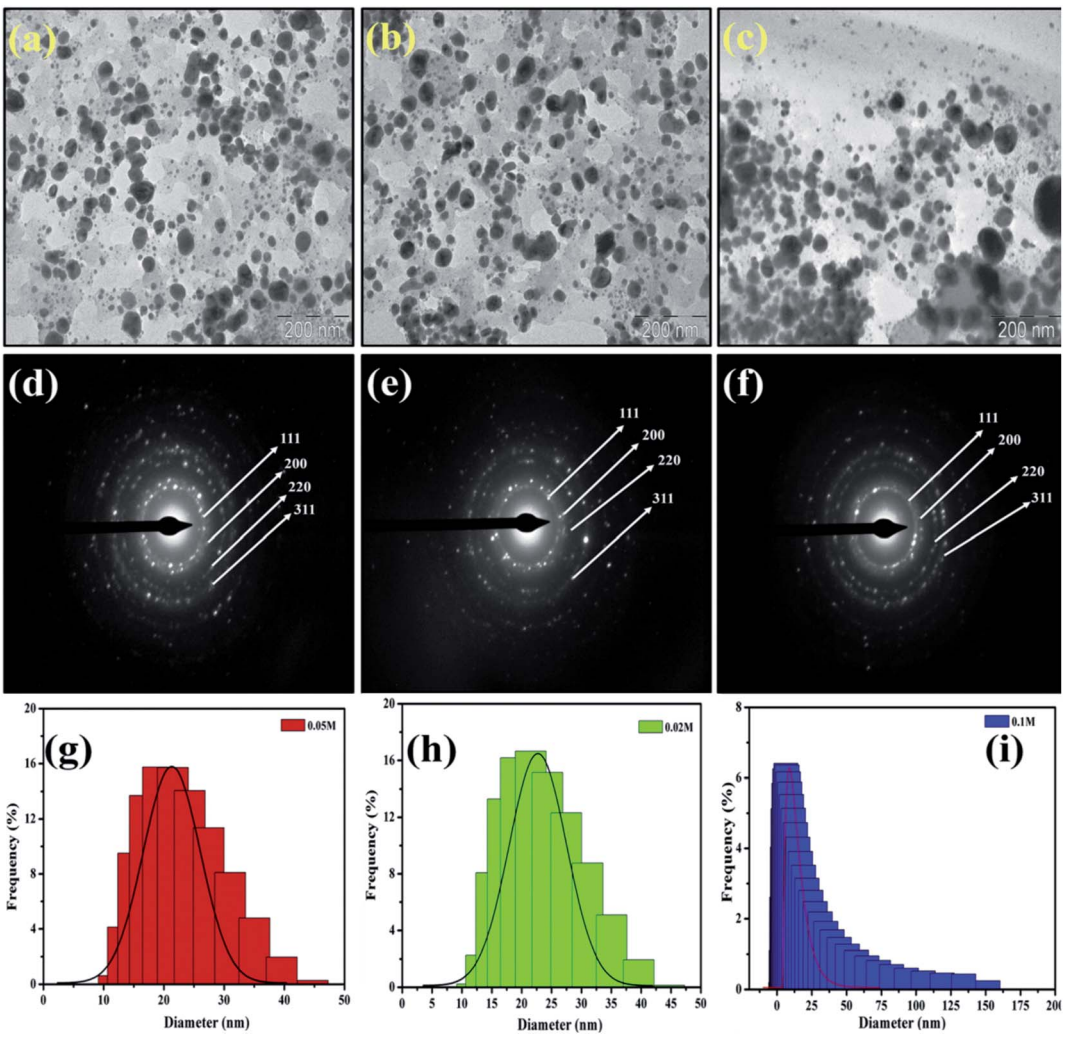

Fig. 6 TEM micrographs and SAED pattern of AgNPs with concentration 0.1 M (a and d), 0.05 M (b and e) and 0.02 (c and f) respectively. This figure has been reproduced from ref. [41] with permission from Elsevier, copyright 2016.

negative bacteria showed great activity compared to antibiotic alone. Flower extract of plants such as *Nyctanthes arbortristis*,[189] *Caesalpinia pulcherrima*,[190] *Alcea rosea*[191] and *Argemone mexicana*[192] were also reported from the synthesis of biogenic AgNPs. *Tecoma stans* flower extract was employed for the biosynthesis of spherical AgNPs with size ranging from 50–60 nm. Antimicrobial activity was tested against *S. aureus* and *E. coli* and found that ZOI is higher for *S. aureus* (24 mm) over *E. coli* (16 mm).[193] *Moringa oleifera* generated ultra-small AgNPs that showed a high ZOI of 29 mm against *S. aureus*.[194] This is one of the highest ZOI observed at this concentration so far using biogenic AgNPs, probably due to its small size. Another exciting finding in this work is the higher antimicrobial activity of the AgNPs in Gram-positive bacteria (*S. aureus*) than the Gram-negative one (*K. pneumonia*), which is a rare case. In another work, Ajitha *et al.* reported the biosynthesis of polydisperse AgNPs using *Syzygium aromaticum* flower extract as bio-reducing as well as a capping agent. Antimicrobial activity of the synthesized NPs was explored against several microbes and found that the NPs induces cell disruption of the bacterial strain and it is maximum in case of *Pseudomonas* spp.[195]

3.4 From roots

Green synthesis of AgNPs and their application as antimicrobial using plants root extract have gained immense attention nowadays (Table 4, entries 38–54). The root extract of *Potentilla fulgens* was reported as a potent antimicrobial agents against *E. coli*, *B. subtilis* showing a ZOI of 9.5 ± 0.2 and 9.7 ± 0.6 respectively.[196] Recently, *Alpinia calcarata* root extract was utilized as a bio-reducing as well as a stabilizing agent for the green synthesis of spherical AgNPs. Antimicrobial activity was tested against *P. mirabilis*, *E. coli*, *B. cereus*, *S. aureus* and the results showed that *Alpinia calcarata* root extract assisted synthesized AgNPs have great potential to induce cell disruption of the bacterial strain. Apart from that, the synthesized AgNPs is stable for up to six months.[197] AgNPs with microbial activities were also reported to be produced from the root extract of *Erythrina indica* L.[198] *Diospyros paniculate*[199] and *Diospyros sylvatica*.[200]

Ezealisiji *et al.* have reported the green synthesis of AgNPs using root bark extract of *Annona muricata* Linn and investigate their application as an antimicrobial agent against pathogenic bacteria such as *B. subtilis*, *S. aureus*, and *K. pneumonia*, *E. coli*, and *Pseudomonas aeruginosa*. The zone of inhibition (ZOI) in diameters were 10.00, 15.00 mm and 12.50, 17.50, 20.00 mm for the five pathogens respectively at AgNPs concentration of 5 μg mL^{-1}. The ZOI is increased to 12.50, 14.50 mm and 14.00, 18.50, and 26.00 mm respectively at AgNPs dose of 10 μg mL^{-1}. Taking into account, the authors have reported that the bactericidal activity of AgNPs is concentration-dependent.[201]

Cibotium barometz,[202] *Diospyros assimilis*,[203] *Pelargonium endlicherianum* Fenzl.[204] roots derived AgNPs were also highly sensitive towards tested microorganisms. *Diospyros assimilis* derived AgNPs showed high ZOI (18 mm approx. at 100 μL mL^{-1} AgNPs concentration) against *E. coli* and *S. aureus*; however, they showed lower activity than antibiotic chloramphenicol.[203]

Interestingly the AgNPs derived from *Pelargonium endlicherianum* Fenzl. seed extract (using 11% ethanol extract contain gallic acid and apocynin as major phytochemicals) are monodisperse, whereas those prepared from 70% methanol extract containing gallic acid, apocynin, and quercetin as major components afforded polydisperse NPs as shown in Fig. 7. These indicated the effect of extract solvent on the composition of the extract and nature of the synthesized AgNPs, which have further bearing on the antimicrobial activities of the NPs.[204]

Protein leakage and SEM studies were used as means to study the bactericidal activities of the AgNPs using *Rheum palmatum* seeds extract.[205] SEM images showed abnormality in the cell wall of the tested bacteria, whereas protein was found to leak in high amount due to disruption of membrane in the bacteria when treated with AgNPs which showed the damage caused by AgNPs, which is supported by previous literature.[206] The AgNPs showed higher susceptibility towards *P. aeruginosa* (14.35 ± 0.24 mm ZOI) than *S. aureus* (10.12 ± 1.81 mm). The antimicrobial activities of AgNPs from seeds extract of *Lepidium draba*,[207] *Angelica pubescens* Maxim,[208] and *Phoenix dactylifera*[209] were also proven. Interestingly, *Angelica pubescens* mediated AgNPs showed excellent activities whereas AuNPs and root extract do not possess antimicrobial activity against the tested Gram-negative and Gram-positive bacterial strain.[208] Green synthesized AgNPs and AuNPs using *Arctium lappa* as potent antimicrobial agents are of great interest considering the shape and size of the NPs produced. While AgNPs are mainly spherical with average size 21.3 nm, AuNPS are with different shapes such as spherical, hexagonal and triangular geometry with average size of 24.7 nm were seen in TEM. The authors believed these differences in shape and size of AgNPs and AuNPs are due to the difference in reduction potential as well as the capping agents specific to each NPs.[210] In another work, the ZOI of *Asparagus racemosus* mediated AgNPs were 17.0 ± 0.89 and 16.0 ± 0 for *S. aureus*, *B. subtilis* respectively. However, the AgNPs showed low ZOI (12.33 ± 0.51 mm) *E. coli*.[211]

Lysiloma acapulcensis extract was utilized for the green synthesis of AgNPs with size ranging from 3.2–6.0 nm.[212] It is reported that *Lysiloma acapulcensis* plant is widely used as a traditional medicine in Mexico for the treatment of microbial contamination. Thus, the authors reported that *Lysiloma*

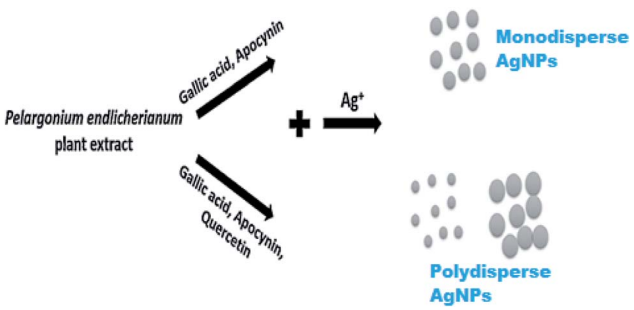

Fig. 7 AgNPs formation when Ag + ions were separately mixed with (gallic acid + apocynin) and (gallic acid + apocynin + quercetin). This figure has been adapted from ref. [204] with permission from Elsevier, copyright 2017.

acapulcensis root extract mediated AgNPs have higher antimicrobial activity. Antimicrobial activity was tested against the different microorganisms such as *E. coli*, *P. aeruginosa*, *S. aureus*, *C. albicans* and found that the inhibition potency is in the order *E. coli* ≥ *S. aureus* ≥ *P. aeruginosa* > *C. albicans.*

Irregular, triangular nanoplates with nanorods, and spherical with average size 6–20 nm, 50–450 nm, 5–30 nm respectively recorded for seed extract, starch, and CTAB-capped AgNPs from *Raphanus sativus*, which reflected the crucial influence of capping agents on the size and shape of final NPs. In this study, the average NPs size were measured by dynamic light scattering (DLS) technique. The magnitude of the change in the hydrodynamic radius of CTAB-capped AgNPs lower than both extract and starch-capped ones in DLS measurement; hence, the authors proved CTAB is the best shape-directing agent.[213]

3.5 From fruit

The plant fruit extract is widely investigated in the field of green synthesis of nanoparticles.[214] There are numerous literature available on the green synthesis of AgNPs employing fruit extracts (Table 3, entries 1–36). *Emblica officinalis*,[215] guava,[216] carambola,[217] *Helicteres isora*[218] and *Solanum trilobatum*[219] fruit extract were utilized successfully for the bio-genic synthesis of spherical AgNPs to investigate its various microbial pathogens such as *S. aureus*, *B. subtilis*, *E. coli*, *K. pneumonia*, *S. mutans*, *B. cereus* and *S. typhi*. It is reported that, with increase in the concentration of the fruit extract, size of the AgNPs decreases and subsequently antibacterial activity increases.[218] *Emblica officinalis* showed excellent antibacterial activity against Gram-negative bacteria compared to Gram-positive bacteria.[215] Due to the very small size of *Emblica officinals*, guava and *Helicteres isora* mediated AgNPs, they showed great ZOI against the mentioned pathogens.[215,216,218] Apart from that, *Lemon*,[220] *Syzygium alternifolium* Walp[221] and *Nothapodytes nimmoniana*[222] fruit extract were also utilized for the green synthesis of AgNPs. Shape directive CTAB was utilized with lemon extract to control the shape of the AgNPs, which was utilized directly to the various bacterial strains and showed excellent activity against the bacterial strains.[220] In contrary, both *Syzygium alternifolium* Walp[221] and *Nothapodytes nimmoniana*[222] fruit extract act as a shape directive and bio-reducing agent for the biosynthesis of AgNPs. In another work, *Lemon* extract was utilized as a bio-reducing agent for the green synthesis of AgNPs and investigate its antimicrobial activity against four pathogenic bacteria such as *P. aeruginosa*, *E. coli* and *S. aureus* and compared with controls amikacin and lemon extract. The results showed that the synthesized NPs have excellent potency to induce cell disruption of the bacterial strain and ZOI is almost similar to the medicinal antibiotic drug, amikacin.[223] Similarly, spherical AgNPs were also prepared using various fruit extract such as apple extract,[224] *Adansonia digitata* L.[225] and *Momordica charantia*[226] extract and examined their bactericidal activity against Gram-positive and Gram-negative bacteria. It is reported that, combined extract-AgNPs exert more bacterial cell damage compared to AgNPs and extract alone due to the synergistic effect produced by the phytochemicals capped on the surface of the AgNPs.[226] Jayaprakash *et al.*[227] reported microwave-assisted synthesis of spherical AgNPs using Tamarind fruit extract. The produced AgNPs by this method is very stable without the formation of oxide and displayed excellent bactericidal activity. Moreover, this process for AgNPs synthesis is economic, time efficient and straight forward. *Phoenix dactylifera*,[228] strawberry,[229] Ginseng-berry,[230] *Kigelia africana*[231] and *Chaenomeles sinensis*[232] fruit extract were also successfully utilized for the green synthesis of spherical AgNPs with high antimicrobial activity. Ginseng-berry fruit extract derived AgNPs showed greater ZOI against *S. aureus* (12.3 mm) compared to *E. coli* (11 mm).[230] A high bactericidal activity against the Gram-positive bacteria was observed by using AgNPs derived from *Phoenix dactylifera* extract.[228]

Biogenic synthesis of AgNPs are achieved by using various fruit extract such as *Soymida febrifuga*,[233] *Ribes nigrum*,[234] *Garcinia indica*,[235] *Carissa caranda* berries[236] and *Diospyros lotus*[237] and investigate their bactericidal activity against various bacterial pathogens. It is reported that biogenic synthesis of AgNPs depends on the various factors such as $AgNO_3$ concentration, extract to $AgNO_3$ ratio, pH, incubation temperature and time.[235] The optimal conditions for green synthesis of AgNPs using *Garcinia indica* are 1.5 mM $AgNO_3$, 1 : 1 $AgNO_3$/Kokum fruit extract, pH 10, incubation temperature of 37 °C and 24 h time.[235] *Carandas* berry mediated AgNPs displayed great ZOI against various Gram-negative bacteria. However, to inhibit the growth of bacteria *S. aureus*, a comparatively high concentration of AgNPs is required.[236] There are several reports where different fruit extract such as *Terminalia bellirica*,[238] clammy cherry,[239] *Phyllanthus emblica*,[240] *Forsythia suspense*,[241] *Rosa canina*[242] and *Manilkara zapota* (Sapota)[243] have been productively utilized for the green synthesis of AgNPs and evaluate their bactericidal activity against various bacterial pathogens. The results revealed that, AgNPs generated from each fruit extract displayed great antimicrobial activity against both Gram-negative and Gram-positive bacteria. It is reported that microwave-assisted synthesis of AgNPs using cherry extract is a time efficient and cost-effective process. The synthesized NPs are very small with size 7. 13 nm, thus displayed easy cell disruption of various human pathogens.[239]

Besides, antimicrobial activity of various fruit extract such as *Abelmoschus esculentus*,[244] *Phyllanthus emblica*,[245] *Aegle marmelos*,[246] *Nauclea latifolia*,[247] *Myristica fragrans*,[248] *Capsicum frutescens*[249] and *Areca catechu*[250] mediated AgNPs was also tested and found that the synthesized AgNPs displayed great cell disruption of bacterial strains. The effect of solvent extract of *Aegle marmelos* on antimicrobial activity was tested by making fruit extract in various solvents such as petroleum, ether, methanol, acetone and chloroform and found that methanol extract of *Aegle marmelos* displayed highest cell disruption against *B. cereus* and lowest for *E. coli*.[246]

3.6 From gum

Gum extracts of various plants have been widely utilized as a bio-reducing as well as a stabilizing agent for the green synthesis of AgNPs (Table 3, entries 37–45). Velusamy *et al.*[251]

Table 3 Various fruit extract used for the green synthesis of AgNPs and their antimicrobial activity

No.	Plants	Plant part	Shape and size	Test microorganisms	Ref.
1	*Emblica officinalis*	Fruit	Spherical; 15 nm	*S. aureus*, *B. subtilis*, *E. coli*, *K. pneumonia*	215
2	*Psidium guajava*	Fruit	Spherical; 2–10 nm	*S. mutans*, *B. cereus*, *E. coli*, *S. aureus*, and *S. typhi*	216
3	*Carambola*	Fruit	Spherical; 10–40 nm	*E. coli*, *P. aeruginos*	217
4	*Helicteres isora*	Fruit	Spherical; 8–20 nm	*P. aeruginosa*	218
5	*Solanum trilobatum*	Fruit	Spherical; 12.50–41.90 nm	*S. mutans*, *E. faecalis*, *E coli*, *K. pneumoniae*	219
6	*Lemon*	Fruit	Spherical and polyhedral; 15–30 nm	*S. aureus*, *E. coli*, *Candida albicans*, *Candida glabrata* and *Candida tropicalis*	220
7	*Syzygium alternifolium*	Fruit	Spherical; 5–68 nm	*B. subtilis*, *S. aureus*, *E. coli*, *K. pneumoniae*, *P. vulgaris*, *P. aeruginosa*, *S. typhimurium*, *A. solani*, *A. flavus*, *A. niger*, *P. chrysogenum*, *T. harzianum*	221
8	*Nothapodytes nimmoniana*	Fruit	Spherical; 44–64 nm	*B. subtilis*, *E. coli*, *S. aureus*, *S. paratyphi*, *P. vulgaris*, *A. hydrophillus*, *K. pneumoniae*	222
9	*Citrus lemon*	Fruit	Spherical; 2–10 nm	*P. aeruginosa*, *E. coli*, *S. aureus*	223
10	*Apple*	Fruit	Spherical; 30.25 ± 5.26 nm	*E. coli*, *S. aureus*	224
11	*Adansonia digitata* L.	Fruit	Spherical; 3–57 nm	*P. vulgaris*, *K. pneumoniae*, *P. aeruginosa*, *S. typhimurium*, *E. coli*, *B. subtilis*, *S. aureus. T. harzianum*, *A. niger*, *A. flavus*, *P. chrysogenum*, *A. solani*	225
12	*Momordica charantia*	Fruit	Spherical; 78.5–220 nm	*E. coli*, *S. typhi*, *S. aureus*, *P. aeruginosa*	226
13	*Tamarindus indica* (Tamarind)	Fruit	Spherical; 6–8 nm	*B. cereus*, *S. aureus*, *M. luteus*, *B. subtilis*, *Enterococcus* sp., *P. aeruginosa*, *S. typhi*, *E. coli*, *K. pneumonia*	227
14	*Phoenix dactylifera*	Fruit	Spherical; 25–60 nm	*E. coli*, *K. pneumonia*, *S. epidermidis*, (d) *B. cereus*, *S. aureus*	228
15	*Strawberry*	Fruit	Spherical; 7–65 nm	*P. aeruginosa*, *B. licheniformis*	229
16	*P. ginseng* Meyer	Fruit	Spherical; 10–20 nm	*E. coli*, *S. aureus*	230
17	*Kigelia africana*	Fruit	Spherical; 10 nm	*K. pneumoniae*, *P. aeruginosa*, *C. albicans*	231
18	*Chaenomeles sinensi*	Fruit	Spherical; 20 nm	*S. aureus*, *E. coli*	232
19	*Soymida febrifuga*	Fruit	Spherical; 14.27 nm	*B. subtilis*, *E. coli*, *S. aureus*, *P. putrida*	233
20	*Ribes nigrum*	Fruit	Spherical; 5–10 nm	*S. aureus*, *P. aeruginosa*, *E. coli*, *C. albicans*, *Trichophyton rubrum*, *A. niger*	234
21	*Garcinia indica*	Fruit	Spherical, hexagonal; 5–30 nm	*E. coli*, *B. subtilis*, *S. aureus*, *P. aeruginosa*, *Salmonella enterica typhi*, *P. vulgaris*, *S. marcescens*	235
22	*Carissa carandas*	Fruit	Spherical; 10–60 nm	*A. hydrophila*, *Acinetobacter* sp., *S. aureus*	236
23	*Diospyros lotus*	Fruit	Spherical; 19 nm	*E. coli*, *S. aureus*	237
24	*Terminalia bellirica*	Fruit	Spherical; 10 nm	*P. aeruginosa*, *K. pneumoniae*	238
25	*Cordia obliqua* Willd	Fruit	Spherical; 7.13 nm	*B. circulans*, *E. coli*, *P. aeruginosa*, *S. aureus*	239
26	*Phyllanthus emblica*	Fruit	Spherical; 19.8–92.8 nm	*A. oryzae*	240
27	*Forsythia suspensa*	Fruit	Spherical; 47.3 ± 2.6 nm	*V. parahaemolyticus*, *S. aureus*	241
28	*Rosa canina*	Fruit	Spherical; 13–21 nm	*B. cereus*, *E. hirae*, *S. aureus*, *E. coli*, *L. pneumophila*, *Candida albicans*, *P. aeruginosa*	242
29	*Manilkara zapota* (Sapota)	Fruit	Spherical; 8–16 nm	*E. coli*, *P. aeruginosa*, *K. pneumoniae*, *Bacillus subtilis* subsp. *Spizizenii*, *S. aureus*	243
30	*Abelmoschus esculentus*	Fruit	Spherical; 3–11 nm	*B. subtilis*	244
31	*Phyllanthus emblica*	Fruit	Spherical; 19 nm to 45 nm	*K. pneumoniae*, *S. aureus*	245
32	*Aegle marmelos*	Fruit	Spherical; 10–200 nm	*B. cereus*, *S. aureus*, *E. coli*, *P. aeruginosa*, *S. typhi*, *S. dysenteriae Y. pestis*	246
33	*Nauclea latifolia*	Fruit	Irregular, 12 nm	*E. coli*, *C. albicans*, *Rhizopus* sp., *A. niger*, *C. fruendii*, *S. aureus*, *Staphylococcus* sp. *Klebsiella* sp.	247
34	*Myristica fragrans*	Fruit	Irregular; 31.31 nm	*E. coli*, *P. aeruginosa*, *S. aureus*, *B. subtilis*	248
35	*Capsicum frutescens*	Fruit	Monodispersed; 20–25 nm	*E. coli*, *B. subtilis*	249
36	*Areca catechu*	Fruit	Polydispersed; 12 nm	*E. coli*, *P. aeruginosa*, *K. aerogenes*, *S. aureus*	250
37	*Azadirachta indica* L.	Gum	Spherical; 12.09–29.65 nm	*S. enteritidis*, *B. cereus*	251
38	*Salmalia malabarica*	Gum	Spherical; 7 nm	*S. aureus* and *E. coli*	252

Table 3 (*Contd.*)

No.	Plants	Plant part	Shape and size	Test microorganisms	Ref.
39	*Styrax benzoin*	Gum	Spherical; 12–38 nm	*P. aeruginosa*, *S. aureus*, *E. coli*, *C. tropicalis*	253
40	*Anacardium occidentale* L.	Gum	Spherical; 51.9 nm	*S. aureus*, *E. coli*	254
41	*Araucaria heterophylla*	Gum	Spherical; less than 50 nm	*E. coli*, *Streptococcus* sp	255
42	*Azadirachta indica*	Gum	Spherical; less than 50 nm	*E. coli*, *Streptococcus* sp	255
43	*Prosopis chilensis*	Gum	Spherical; less than 50 nm	*E. coli*, *Streptococcus* sp	255
44	*Buchanania lanzan*	Gum	Spherical; 14.74–19.86 nm	*E. coli*, *A. avium*, *S. intermedius*, *P. macerans*, *S. rubidaea*, *E. mallatovora*, *E. faecalis*, *S. haemolyticus*, *P. mirabilis*, *S. epidermidis S. chromogenes*, *E. agglomerans*, *Staphylococcus capitis* ssp. *capitis*, *Staphylococcus capitis* ssp. *urealyticus*	256
45	*Mimosa pudica*	Gum	Irregular; no report	*E. coli*, *S. commune*	257
46	*Moringa oleifera*	Stem	Spherical; 3–70 nm	*E. coli*, *K. cloacae*, *S. epidermidis*	258
47	Waste grass	Stem	Spherical-oblate; 4–34 nm	*P. aeruginosa*, *A. baumannii*, *F. solani R. solani*	259
48	*Swertia paniculate*	Stem	Spherical; 31–44 nm	*P. aeruginosa*, *K. pneumoniae*, *S. aureus*	260
49	*Caesalpinia pulcherrima*	Stem	Spherical; 8 nm	*B. cereus*, *S. aureus*, *C. rubrum*, *B. subtilis*, *E. coli*, *K. pneumonia*, *P. aeruginosa*, *S. typhimurium*, *C. albicans*, *C. glabrata*, *C. neoformans*	261
50	*Garcinia mangostana*	Stem	Spherical; 30 nm	*K. planticola*, *E. coli*, *B. subtilis*	262
51	*Dorema ammoniacum* D.	Stem	Spherical; 28.4 nm	*E. coli*, *S. typhimurium*, *S. aureus*, *B. cereus*	263
52	*Fumariae herba*	Stem	Spherical; 25 nm	*S. aureus*, *B. cereus*, *B. luteus*, *B. subtilis*, *L. monocytogenes*, *E. coli*, *P. aeruginosa*, *K. pneumoniae*, *P. vulgaris*, *C. albicans*	264
53	*Anthemis atropatana*	Stem	Spherical; 38.89 nm	*S. aureus*, *S. pyogenes*, *P. aeruginosa*, *E. coli*	265
54	*Afzelia quanzensis*	Bark	Spherical; 10–80 nm	*E. coli*, *S. aureus*	266
55	*Syzygium alternifolium*	Bark	Spherical; 4–48 nm	*B. subtilis*, *S. aureus*, *E. coli*, *K. pneumoniae*, *P. vulgaris*, *P. aeruginosa*, *S. typhimurium*, *A. solani*, *A. flavus*, *A. niger*, *P. chrysogenum*, *T. harzianum*	267
56	*Cochlospermum religiosum*	Bark	Spherical; 20–35 nm	*Bacillus*, *E. coli*, *Proteus*, *Pseudomonas*, *Staphylococcus*, *A. flavus*, *Fusarium*, *C. lunata*, *Rhizopus*, *A. niger*	268
57	*Ficus benghalensis*	Bark	Spherical; 85.95 nm	*E. coli*, *P. aeruginosa*, *B. subtilis*	269
58	*Azadirachta indica*	Bark	Spherical; 90.13 nm	*E. coli*, *P. aeruginosa*, *B. subtilis*	269
59	*Plumbago zeylanica*	Bark	Spherical; 28.47 nm	*B. subtilis*, *P. aeruginosa*, *S. aureus*, *C. tropicalis*, *E. coli*, *A. flavus*	270
60	*Helicteres isora*	Bark	Spherical; 16–95 nm	*E. coli*, *V. cholera*, *S. typhi*, *P. aeruginosa*, *B. subtilis* and *M. luteus*	271
61	*Terminalia arjuna*	Bark	Spherical; 65 nm	*E. coli*	272
62	*Butea monosperma*	Bark	Spherical; 18–50 nm	*B. subtilis*, *E. coli*	273
63	*Prosopis juliflora*	Bark	Spherical; 10–50 nm	*E. coli*, *P. aeruginosa*	274
64	*Garcinia mangostana*	Bark	Spherical; 65 nm	*E. coli*, *B. subtilis*, *S. aureus*, *B. cereus*, *K. pneumoniae*	275
65	*Solanum trilobatum*	Bark	Spherical; 25 nm	*A. niger*, *E. coli*, *Bacillus* sp.	276
66	*Butea monosperma* (Lam.) Taub.	Bark	Spherical; 81 nm	*E. coli*, *S. aureus*, *A. niger*	277
67	*Syzygium cumini*	Bark	Spherical; 15 nm	*E. coli*, *B. subtilis*	278
68	*Diospyros montana*	Bark	Spherical; 5–40 nm	*K. aerogenes*, *E. coli*, *B. subtilis*, *S. aureus*	279
69	*Handroanthus impetiginosus*	Bark	Spherical; 13.4 nm	*S. aureus*, *E. coli*	280

have reported the autoclave-assisted green synthesis of AgNPs using gum extract of *Azadirachta indica* L. AFM analysis of the synthesized AgNPs displayed that the nanoparticles are spherical in shape without any aggregation. Furthermore, the line profile analysis revealed that the average particle size is 23.44 nm. Bactericidal activity test revealed that the synthesized AgNPs can effectively disrupt the cell membranes of *S. enteritidis* and *B. cereus*, hence can be exploited in biomedical applications. Similarly, the bactericidal activity of AgNPs generated from various gum extract such as *Salmalia malabarica*,[252] *Styrax benzoin*[253] and *Anacardium occidentale* L.[254] displayed prominent cell damage against both Gram-positive and

Gram-negative bacteria. In a comparison study, three different gum extract such as *Azadirachta indica*, *Araucaria heterophylla* and *Prosopis chilensis* have been utilized for the synthesis of AgNPs and compare their antimicrobial activity against both Gram-negative and Gram-positive bacteria. The results revealed that, *Azadirachta indica* and *Prosopis chilensis* mediated AgNPs are effective for cell disruption of both Gram-positive and Gram-negative bacterial strains. On contrary, *Araucaria heterophylla* mediated AgNPs is effective for Gram-negative bacterial strains (*E. coli*) only.[255] In another study, *Buchanania lanzan* gum extract was utilized for the green synthesis of AgNPs with size ranging from 14.74–19.86 nm. Antimicrobial activity was tested against 14 Gram-negative and 3 Gram-positive bacteria and found that the synthesized AgNPs was more prominent against Gram-negative bacteria over Gram-positive bacteria. Besides, MIC for two Gram-negative bacteria such as *E. coli* and *A. avium* was found to be 0.52 μg mL^{-1} and 0.53 μg mL^{-1} respectively.[256] Beside, *Mimosa pudica* gum extract was utilized for the green synthesis of AgNPs and investigate its antimicrobial activity against *Escherichia coli* and *Schizophyllum commune*, observed that the ZOI for *E. coli* is higher than the *S. commune.*[257]

3.7 From stem

Plants stem extract was widely utilized as a reducing agent for the green synthesis of AgNPs (Table 3, entries 46–53). Aqueous extract of *Moringa oleifera*,[258] waste grass[259] and *Swertia paniculate*[260] have been utilized for the bio-synthesis of AgNPs to investigate its antimicrobial activity against various bacterial strains. It is reported that the waste grass mediated AgNPs are smaller in size (15 nm) compared to *Moringa oleifera* and *Swertia paniculate* mediated AgNPs, hence AgNPs obtained from waste grass extract shows greater antimicrobial activity as it can easily disrupt the bacterial cell wall.[259] Similarly, green synthesis of AgNPs by using *C. pulcherrima* stem extract was reported by Moteriya *et al.*[261] and examine their antimicrobial activity against various pathogenic microorganisms. The results showed that the MIC value for the bacteria is ranging from 0.312 to 2.5 mg mL^{-1} and for fungi is 2.5 mg mL^{-1} using AgNPs only. Interestingly, AgNPs together with two antibiotics such as chloramphenicol and amphotericin B recorded a lower MIC value against both bacteria and fungi compared to the bare AgNPs. The combination of AgNPs and chloramphenicol displayed synergistic effect against *B. cereus*, *B. subtilis*, *S. aureus*, *C. rubrum* and *S. typhimurium*, while displayed partial synergistic effect against *E. coli*, *P. aeruginosa*, *K. pneumonia*. In addition, green synthesis of AgNPs by using different stem extract of *Garcinia mangostana*,[262] *Dorema ammoniacum* D.[263] and *Fumariae herba*[264] is also reported. The synthesized AgNPs were applied against various bacterial strains of Gram-positive and Gram-negative bacteria and found that the NPs is very active for the cell disruption of Gram-negative bacteria as the Gram-negative bacteria possesses weak cell wall due to the less content of peptidoglycan in the cell wall. In another work, *Anthemis atropatana* extract was utilized for the biosynthesis of AgNPs and investigated the antimicrobial activity of the produced NPs against various pathogenic bacteria such as *S. aureus (ATCC 6538)*, *S. pyogenes (ATCC 19615)*, *P. aeruginosa (ATCC 15442)* and *E. coli*. The result obtained revealed that the highest and lowest MIC value is for *P. aeruginosa* and *S. aureus*, respectively.[265]

3.8 From bark

In recent years, bark extract has been widely exploited as a reducing agent as well as a stabilizing agent for the green synthesis of AgNPs (Table 3, entries 54–69). Green synthesis of AgNPs for antimicrobial activity was obtained by using various plant bark extract *Afzelia quanzensis*,[266] *Syzygium alternifolium*[267] and *Cochlospermum religiosum*.[268] Nayak *et al.*[269] have reported the green synthesis of AgNPs with the size of 90.13 nm using bark extract of *Ficus benghalensis* and *Azadirachta indica.* Bactericidal activity of the synthesized AgNPs was tested against Gram-positive and Gram-negative bacteria such as *E. coli*, *P. aeruginosa*, *V. cholera* and *B. subtilis*, observed great inhibition potential of the synthesized AgNPs against the bacterial pathogens. The authors reported that the phytochemicals present around the synthesized AgNPs provide unique surface characteristic and thus, can damage various cell membranes. Apart from that, different plant bark extract such as *Plumbago zeylanica*,[270] *Helicteres isora*,[271] *Terminalia arjuna*,[272] *Butea monosperma*,[273] *Prosopis juliflora*,[274] *Garcinia mangostana*[275] and *Solanum trilobatum*[276] were also utilized for the green synthesis of AgNPs and investigate its antimicrobial activity against various bacterial strains. It is reported that the *Butea monosperma* bark extract is inefficient for any ZOI, however, the extract mediated AgNPs displayed great ZOI at very low concentration. The ZOI induced by $AgNO_3$ solution is more compared to AgNPs, but required high concentration of $AgNO_3$, which is harmful for the consumer. On contrary, a very small concentration of AgNPs showed good ZOI against the bacterial strains and hence can be used as therapeutic agent.[273]

Recently, *Butea monosperma*,[277] *Syzygium cumini*[278] and *Diospyros montana*[279] bark extract were utilized for the green synthesis of AgNPs and investigate its antimicrobial activity. The resultant AgNPs are displayed prominent cell damage to the various bacterial strains. *Syzygium cumini* mediated AgNPs displayed greater ZOI against the Gram-negative bacteria compared to Gram-positive bacteria as the cell wall of Gram-negative bacteria is more susceptible for the synthesized AgNPs. The study also revealed that the bactericidal activity of *Syzygium cumini* mediated AgNPs is more compared to the *Syzygium cumini* extract and $AgNO_3$ solution, which can attributed to the small size of the AgNPs.[278] To increase the rate of the biosynthesis process for AgNPs, the microwave technique was used by Tormena *et al.*[280] where they have used *Handroanthus impetiginosus* bark extract as a reducing as well as capping agent. Bactericidal activity of the synthesized NPs was tested against two pathogenic bacteria such as *S. aureus* and *E. coli* and found good inhibition potential to both bacterial strains with MIC value 3.1×10^2 μg mL^{-1} and 6.7×10^4 μg mL^{-1} respectively. However, the pure extract displayed a low MIC value of 2.7×10^3 μg mL^{-1} and 1.2×10^3 μg mL^{-1} for *S. aureus* and *E. coli*, respectively. Interestingly, the bactericidal activity of AgNPs is higher for *S. aureus* compared to *E. coli* (Fig. 8). This is contrary

to the generally accepted assumption that AgNPs are more susceptible to Gram-negative bacteria due to their thin cell-wall. However, the authors defended their claim by considering the synergetic effects of biomolecules capping agents and AgNPs.

3.9 From rhizome

Rhizome extract is also utilized in the green synthesis of size-selective AgNPs (Table 4, entries 1–8). Bio-synthesis of spherical AgNPs was obtained by using various rhizome extract such as *Bergenia ciliate*[281] and *Dryopteris crassirhizoma.*[282] The synthesized AgNPs was utilized against different bacterial strains to investigate its antimicrobial activity and found that the NPs displayed excellent cell disruption of the bacterial strains. A wide variety of LED light source such as green, red and blue light have been utilized for the synthesis of AgNPs and examined its bactericidal activity. The authors reported that the ZOI against *B. cereus* is maximum when the green light mediated AgNPs is used followed by red and blue light mediated AgNPs.[282] Rhizome extract of *Coptis chinensis* was exploited for the green synthesis of AgNPs with size 15 nm. The surface of the synthesized AgNPs was further modified with chitosan. Bactericidal activity of both free AgNPs and chitosan modified AgNPs was tested against *E. coli* and *B. subtilis.* The results revealed that the chitosan modified AgNPs showed greater inhibition efficiency compared to free AgNPs against the bacterial strains.[37] Recently, rhizome extract of *Coptidis*,[283] *Curcuma longa* (turmeric),[284] *Canna indica* L.[285] and *Ferula foetida* (asafoetida gum)[286] were utilized for the green synthesis of spherical AgNPs with size in the nanometer range. The resultant AgNPs was tested against various bacterial strains to investigate its bactericidal activity and found that the NPs is effective for the bacterial cell damage. It is observed that the *Canna indica* L. mediated AgNPs displayed greater bactericidal activity against *E. coli* compared to the other bacteria such as *S. aureus* and *K. pneumoniae*. However, on comparison of the bactericidal activity of *Canna indica* L. mediated AgNPs with conventionally antibiotic drug *Gentamicin* revealed that the NP is less active compared to *Gentamicin*.[285] In another work, *Ginger* rhizome extract and sodium citrate were utilized for biosynthesis of B-AgNPs and C-AgNPs respectively followed by investigated their antibacterial activity against six aquatic pathogens such as *V. anguillarum*, *V. alginolyticus*, *A. punctate*, *V. parahaemolyticus*, *V. splendidus*, *V. harveyi.* The results revealed that the chemically synthesized AgNPs showed slightly greater ZOI against the six pathogens compared to Oxford cup indicates that both have very weak bactericidal activity. In contrast, ginger rhizome extract mediated AgNPs (B-AgNPs) showed greater ZOI against the 6 aquatic pathogens, which confirmed that B-AgNPs displayed greater bactericidal activity compared to the chemically synthesized AgNPs.[287]

3.10 From peels

Recently, utilization of peel extract as a reducing agent for the green synthesis of nanoparticles with selective size gaining immense attention. To date, various peel extract was used for the biosynthesis of AgNPs (Table 4, entries 9–17). Peel extract of *Cavendish banana*,[45] banana (*Musa paradisiaca*).[288] *Carica papaya*[289] and *Citrus sinensis*[290] were utilized for the green synthesis of AgNPs. The synthesized AgNPs were tested against various bacterial strains to investigate its bactericidal activity and found that the AgNPs obtained from various peel extract displayed great cell disruption. The influence of various factors on the bio-reduction of $AgNO_3$ was investigated and found that 1.75 mM $AgNO_3$, 20.4 mg dry banana peel 4.5 pH and 72 h

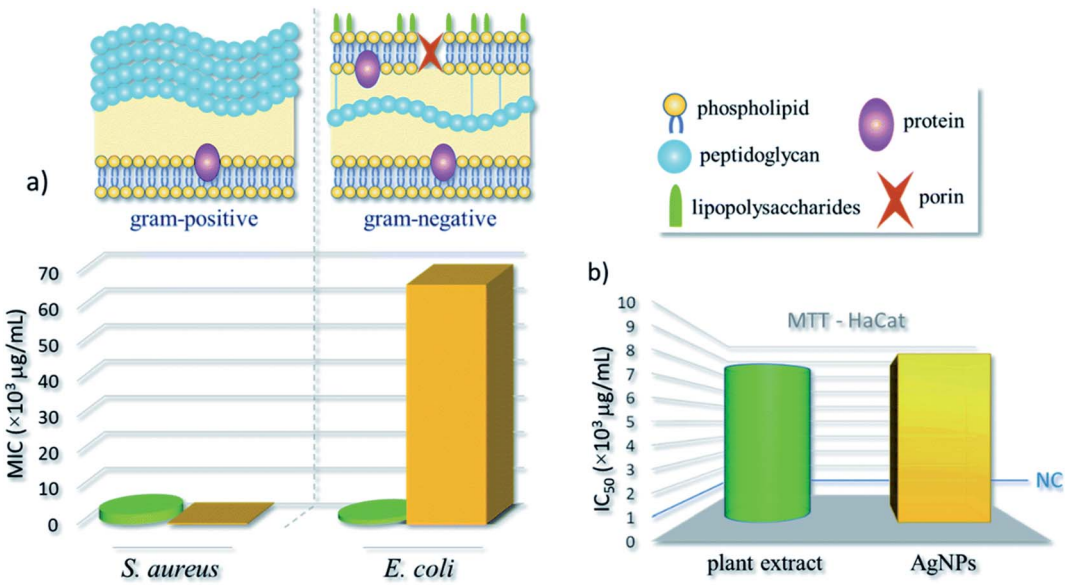

Fig. 8 Infographic with (a) minimal inhibitory concentration of AgNPs against Gram-positive (*S. aureus*) and Gram-negative (*E. coli*) bacteria models and (b) half maximal inhibitory concentration (IC_{50}) using MTT assay – the blue line indicates the cytotoxicity criteria for preliminary tests of new compounds, as established by the United States' National Cancer Institute (NCI). Green cylinders and yellow bars represent the plant extract and AgNPs results, respectively. This figure has been reproduced from ref. [280] with permission from RSC, copyright 2020.

Table 4 Various rhizomes, peel, tube/bulb, whole plant, petals, latex, pod and callus extract used for the green synthesis of AgNPs and their antimicrobial activity

No.	Plants	Plant part	Shape and size	Test microorganisms	Ref.
1	*Bergenia ciliata*	Rhizome	Spherical; 35 nm	*M. luteus*, *S. aureus*, *E. aerogenes*, *B. bronchiseptica*, *A. niger*, *A. fumigatus*, *A. flavus*, *F. solani*	281
2	*Dryopteris crassirhizoma*	Rhizome	Spherical; 5–60 nm	*B. cereus* and *P. aeruginosa*	282
3	*Coptis chinensis*	Rhizome	Spherical; 15 nm	*E. coli*, *B. subtilis*	321
4	*Coptidis rhizome*	Rhizome	Spherical; 30 nm	*E. coli*, *S. aureus*	283
5	*Curcuma longa* (turmeric)	Rhizome	Spherical; 18 ± 0.5 nm	*E. coli*, *L. monocytogenes*	284
6	*Canna indica* L	Rhizome	Spherical; 20–70 nm	*S. aureus*, *K. pneumoniae*, *E. coli*	285
7	*Ferula foetida* (asafoetida gum)	Rhizome	Spherical; 5.6–8.6 nm	*E. coli*, *K. pneumoniae*, *C. albicans*	286
8	*Zingiber officinale* (ginger)	Rhizome	Polygonal; 20–80 nm	*V. anguillarum*, *V. alginolyticus*, *A. punctate*, *V. parahaemolyticus*, *V. splendidus*, *V. harveyi*	287
9	*Cavendish banana*	Peel	Spherical; 23–30 nm	*S. aureus*, *B. subtilis*, *K. pneumonia*, *E. coli*	45
10	Banana (*Musa paradisiaca*)	Peel	Spherical; 23.7 nm	*B. subtilis*, *S. aureus*, *P. aeruginosa*, *P. aeruginosa*, *E. coli*, *C. albicans*	288
11	*Carica papaya*	Peel	Spherical; 16–20 nm	*E. coli*, *S. aureus*	289
12	*Citrus sinensis*	Peel	Spherical; 48.1 ± 20.5 nm	*X. axonopodis pv. Citri* (Xac)	290
13	*Citrus maxima*	Peel	Spherical; 4–11 nm	*E. coli*, *S. aureus*, *F. oxysporum*, *V. dahliae*	291
14	*Punica granatum*	Peel	Spherical; 6–45 nm	*E. coli*, *S. aureus*	292
15	*Citrus* × *clementina*	Peel	Spherical; 15–20 nm	*E. coli*, *B. cereus*, *S. aureus*	293
16	*Solanum melongena*	Peel	Spherical; 92.4 nm	*P. fluorescens*, *B. amyloliquefaciens*	294
17	*Citrus limetta*	Peel	Spherical; 18 nm	*C. albicans*, *C. glabrata*, *C. parapsilosis*, *C tropicalis*, *M. luteus*, *S. mutans*, *S. epidermidis*, *S. aureus*, *E. coli*	295
18	*Allium cepa*	Tube/bulb	Spherical; 10 nm	*E. coli*, *P. aeruginosa*, *B. subtilis*, *F. oxysporium*, *F. oxysporum*	296
19	Sunroot tuber (*Helianthus tuberosus*)	Tube/bulb	Spherical; 10–70 nm	*R. solanacearum*, *X. axonopodis*	297
20	*Dioscorea alata*	Tube/bulb	Spherical; 10–25 nm	*E. coli*, *S. auricularis*	298
21	*Crocus hausknechtii Bois*	Tube/bulb	Spherical;; 10–25 nm	*S. aureus*, *P. aeruginosa*	299
22	*Allium sativum* (garlic)	Tube/bulb	Spherical; 50–70 nm	*P. aeruginosa*, *B. licheniformis*	300
23	*Sargassum muticum*	Whole plant	Spherical; 43–79 nm	*B. subtilis*, *K. pneumoniae*, *S. typhi*	301
24	*Brassica oleracea* L. (Broccoli)	Whole plant	Spherical; 30–45 nm	*E. coli*, *B. subtilis* and *S. aureus*, *Aspergillus* sp., *Pneumocystis* sp.	302
25	*Vernonia cinerea* L.	Whole plant	Spherical; 40–75 nm	*C. albicans*, *Penicillium* spp	303
26	*Artemisia marschalliana*	Whole plant	Spherical; 5–50 nm	*S. aureus*, *B. cereus*, *A. baumannii*, *P. aeruginosa*	304
27	*Linum usitatissimum* L.	Whole plant	Spherical; 49–54 nm, 19–24 nm respectively	*E. coli*, *K. pneumoniae*, *S. aureus*	305
28	*Elaeagnus umbellata*	Whole plant	Spherical; 20–100 nm	*E. coli*, *S. aureus*	306
29	*Sida cordifolia*	Whole plant	Spherical; 3–8 nm	*B. subtilis*, *S. aureus*, *E. coli*, *K. pneumonia*, *A. hydrophila*, *P. fluorescence*, *F. branchiophilum*, *E. tarda*, *Y. ruckeri*	307
30	*Sida acuta*	Whole plant	Spherical; 14.9 nm	*E. coli*, *S. aureus*, *S. faecalis*	308
31	*Rheum ribes*	Whole plant	Spherical; 3.32 ± 0.58 nm	*S. pyogenes*, *S. aureus*, *S. typhimurium*, *E. coli*	309
32	*Blumea eriantha*	Whole plant	Spherical; 50 nm	*B. cereus*, *B. subtilis*, *S. aureus*, *E. coli*	310
33	*Arnicae anthodium*	Whole plant	Irregular; 90–118 nm	*S. aureus*, *E. coli*, *P. aeruginosa*, *C. albicans*	311
34	*Salacia chinensis*	Whole plant	Irregular; 20–80 nm	*S. aureus*, *P. aeruginosa*, *E. coli*, *S. typhi*	312
35	*Ferocactus echidne*	Whole plant	Elliptical; 20–60 nm	*E. coli*, *S. aureus*, *C. Albicans*	313
36	*Rosa indica*	Petals	Spherical; 23.52–60.83 nm	*S. mutans*, *E. coli*, *K. pneumoniae*, *E. faecalis*	43
37	*Hibiscus rosa-sinensis*	Petals	Cube; 76.25 ± 0.17 nm	*V. cholerae*, *E. coli*, *K. pneumoniae*, *S. aureus*	314
38	*Clitoria ternatea* L.	Petals	Spherical and flat plate; 35–80 nm	*S. aureus*, *Shigella* sp.	39
39	*Euphorbia antiquorum* L.	Latex	Spherical; 10–50 nm	*E. coli*, *K. pneumoniae*, *P. mirabilis*, *V. cholerae*, *E. faecalis*	315
40	*Calotropis gigantea* L.	Latex	Spherical; 5–30 nm	*Bacillus*, *Enterococci*, *Shigella*, *P. aeruginosa*, *K. pneumonia*, *Staphylococcus*, *E. coli*	316
41	Cocoa	Pod	Spherical; 4–32 nm	*E. coli*, *K. pneumoniae*, *S. pyogenes*, *S. aureus P. aeruginosa*, *A. flavus*, *A. fumigatus* and *A. niger*	317

Table 4 (*Contd.*)

No.	Plants	Plant part	Shape and size	Test microorganisms	Ref.
42	*Cola nitida*	Pod	Spherical; 12–80 nm	*K. granulomatis*, *P. aeruginosa*, *E. coli*, *S. aureus*, *A. niger*, *A. flavus*, *A. fumigatus*	318
43	*Taxus yunnanensis*	Callus	Spherical; 6.4–27.2 nm	*E. coli*, *S. aureus*, *S. paratyphi*, *B. subtilis*	319
44	*Chlorophytum borivilianum* L.	Callus	Spherical; 52.0 nm	*P. aeruginosa*, *B. subtilis*, *Methicillin-resistant Escherichia coli*, *S. aureus*, *C. albicans*	320

incubation time. The authors reported that the synthesized AgNPs displayed synergistic effects with the antibiotic levofloxacin.[288] *Citrus maxima* peel extract was utilized as both reducing and capping agent for the green synthesis of AgNPs with size ranging from 4–11 nm. Bactericidal activity of the synthesized AgNPs was tested against *E. coli* and *S. aureus* and found that the *Citrus maxima* peel extract mediated AgNPs showed great inhibitory action against both the bacterial strain. Furthermore, bactericidal activity was also examined against plant pathogens such as *F. oxysporum* and *V. dahlia*, showed excellent inhibitory action against both the pathogens.[291] Besides, *Punica granatum*,[292] *Citrus* × *clementine*,[293] and *Solanum melongena* L.[294] peel extracts were exploited for the green synthesis of AgNPs and tested its bactericidal activity against various bacterial strains. The results revealed that the synthesized AgNPs displayed great cell wall damage of both Gram-positive and Gram-negative bacteria. Interestingly, AgNPs derived from *Punica granatum* peel extract showed high ZOI against *S. aureus* (16.5 mm) compared to *E. coli* (15.5 mm).[292] Microwave irradiation technique has been utilized for the green synthesis of AgNPs from *Solanum melongena* L. peel extract to increase the rate of bioreduction process of $AgNO_3$. Moreover, the size and the shape of the nanoparticles generated *via* this process is 92.4 nm and spherical.[294] In another work, Dutta *et al.*[295] have reported the green synthesis of AgNPs using *Citrus limetta* peel extract as both reducing and capping agent. Investigation of bactericidal activity of the synthesized AgNPs against various pathogens such as *C. albicans*, *C. glabrata*, *C. parapsilosis*, *C tropicalis*, *M. luteus*, *S. mutans*, *S. epidermidis*, *S. aureus*, *E. coli* revealed that the *Citrus limetta* peel extract mediated AgNPs have cell disruption potential and hence can be used in pharmaceutical industries. Furthermore, the antifungal activity test of the synthesized AgNPs against *Candida* species revealed that the nanoparticle has the ability of cell membrane distortion. The effect of AgNPs on micromorphological changes of *C. albicans* was clearly visible and found that AgNPs induces the cell blebs and a thick exudate deposition around the cell that demonstrate the leakage of intercellular components. From the results, the authors reported that *Citrus limetta* peel extract mediated AgNPs have excellent antifungal activity.

3.11 From tube/bulb

A diverse tube/bulb extract of plants are reported for the green synthesis of AgNPs (Table 4, entries 18–22). Recently, onion (*Allium cepa*) extract was employed as a reducing as well as a capping agent for the biosynthesis of spherical AgNPs with size ranging from 10–23 nm. The authors reported that the synthesized AgNPs have excellent antimicrobial activity against *B. subtilis*, *B. cereus*, *B. licheniformis*, *S. aureus*, *S. mutans*, *E. coli*, *K. pneumoniae*, *S. typhimurium*, *P. aeruginosa*, *P. vulgaris*, *S. marcescens*, *C. albicans.*[296] A wide variety of tube/bulb extract such as *Sunroot tuber*,[297] *Dioscorea alata*[298] and *Crocus haussknechtii Bois*[299] were utilized for the green synthesis of AgNPs and examined the bactericidal activity of the synthesized nanoparticles against both Gram-positive and Gram-negative bacterial strains. It is reported that, spherical AgNPs with size range 10–25 nm was obtained using 20 mM $AgNO_3$, 0.5 mL *Crocus haussknechtii Bois* extract at pH 7 and temperature of 75 °C.[299] An obvious result was obtained in case of *Dioscorea alata* mediated AgNPs, where it is observed that the ZOI for *E. coli* is greater than *S. aureus.*[298] In another work, aqueous extract of *Allium sativum* was employed as both reducing and capping agent for the synthesis of AgNPs. To investigate the antimicrobial activity, the authors have applied the synthesized NPs to the pathogenic bacteria such as *P. aeruginosa* and *B. licheniformis* and found that the nanoparticle has the cell permeable ability and hence can be used in biomedical applications to make antimicrobial drug.[300]

3.12 From the whole plant

The exploitation of plant extract in the biosynthesis of AgNPs is an important field in nanobiotechnology. To date, numerous literatures are available for the green synthesis of AgNPs using plant extract (Table 4, entries 23–35). *Sargassum muticum*,[301] *Brassica oleracea* L. (*Broccoli*),[302] *Vernonia cinerea* L.,[303] *Artemisia marschalliana*[304] and *Linum usitatissimum* L.[305] plant extracts were exploited for the green synthesis of AgNPs. The resulted nanoparticles were utilized against both Gram-negative and Gram-positive bacterial strains to investigate its bactericidal activity, and it is observed that the plant extract mediated AgNPs are capable of bacterial cell damage at a very low concentration. Different concentration of AgNPs derived from *Artemisia marschalliana* plant extract was used against *S. aureus*, *B. cereus*, *A. baumannii*, and *P. aeruginosa* and found that the ZOI is highest for *S. aureus* unlike other plant extract mediated AgNPs. Therefore, the authors claimed that the photosynthesized AgNPs from *Artemisia marschalliana* plant extract can compete with the commercial antibiotics.[304] In comparison of the bactericidal activity of AgNPs derived from callus extract and

whole plant extract revealed that callus extract mediated AgNPs are smaller in size and thus displayed high bactericidal activity.[305] Ali *et al.*[306] have reported shape/size-selective green synthesis of AgNPs using *Elaeagnus umbellate* extract and treated against various bacterial pathogens such as *E. coli* and *S. aureus* to examine its bactericidal activity. The results showed that the *Elaeagnus umbellate* extract mediated AgNPs can effectively damage the cell membranes as well as releases cellular matrix and hence can be used in pharmaceutics. To further investigate the morphological changes of the bacteria *S. aureus* and *E. coli*, SEM analysis was performed, where the images displayed that before AgNPs treatment the cell membranes of the two bacteria remain intake and have a regular morphology. However, after the treatment of AgNPs, no definite cell wall was observed, and membrane disruption occurs. Besides, antimicrobial activity of AgNPs derived from plant extract of *Sida cordifolia*,[307] *Sida acut*,[308] *Rheum ribes*,[309] *Blumea eriantha*[310] and *Arnicae anthodium*[311] were examined against various bacterial strains. The small size of AgNPs (50 nm) derived from *Blumea eriantha* plant extract displayed excellent growth inhibition of bacterial cell as it provides a high surface area to the pathogens and thus effects more compared to the larger AgNPs.[310] Similarly, *Salacia chinensis* extract was employed for the green synthesis of AgNPs and examine their antimicrobial activity against *S. aureus*, *P. aeruginosa*, *E. coli*, *S. typhi.* The antimicrobial activity testing results revealed that the *Salacia chinensis* extract mediated AgNPs showed high inhibition activity against *S. aureus* and *P. aeruginosa.* However, it showed minimum inhibition activity against *E. coli* and *S. typhi.*[312] Plant extract of *Ferocactus echidne* was utilized for the green synthesis of AgNPs. The synthesized nanoparticles were utilized against various human pathogens and found that the nanoparticle is active against both Gram-positive and Gram-negative bacteria.[313]

3.13 From petals, latex, pod and callus

Different parts of plants such as petals (Table 4, entries 36–38), latex (entries 39 and 40), pod (entries 41 and 42) and callus (entries 43 and 44) in the form of their aqueous/alcoholic extract have been utilized for the green synthesis of AgNPs. It is reported that *Rosa indica*[43] and *Hibiscus rosa-sinensis*[314] petal extract were utilized for the green synthesis of spherical AgNPs. Both the petal extract mediated AgNPs displayed good bactericidal activity against Gram-negative bacteria compared to Gram-positive bacteria.[43,314] The size of the synthesized nanoparticle plays a vital role in the bactericidal activity test. Smaller the size of the nanoparticle greater is the surface available to adhere to the microorganisms, which led to the change in the Physico-chemical properties of the bacterial cell and finally led to bacterial cell damage.[314] Vanaraj *et al.*[39] reported the green synthesis of AgNPs by using *Clitoria ternatea* L. extract as a bioreducing agent and examined their antimicrobial activity against *S. aureus* and *Shigella* sp. and found that the synthesized AgNPs can effectively disrupt the cell membranes of both the bacterial pathogens.

Latex extract of *Euphorbia antiquorum* L. was employed for the green synthesis of AgNPs with size ranging from 10–50 nm. Antimicrobial activity of the synthesized AgNPs was tested against various human pathogens such as *E. coli*, *K. pneumoniae*, *P. mirabilis*, *V. cholera* and *E. faecalis* and showed mild inhibition activity against all mentioned pathogens.[315] Similarly, antimicrobial activity of spherical AgNPs derived from *Calotropis gigantea* L. against various human pathogens has been investigated and displayed remarkable activity against both Gram-positive and Gram-negative bacteria.[316] Pod extract of Cocoa was utilized for the biosynthesis of AgNPs. The synthesized nanoparticles showed great inhibition against *E. coli* and *K. pneumonia*. Moreover, the nanoparticle improves the activity of cefuroxime and ampicillin synergistically.[317] In addition, Lateef *et al.*[318] have reported the green synthesis of AgNPs using pod extract of *Cola nitida* as a reducing as well as capping and stabilizing agent. Antimicrobial activity of the synthesized AgNPs revealed that at different AgNPs concentration ranging from 50–150 μg mL^{-1} showed great inhibition activity against *K. granulomatis*, *P. aeruginosa*, and *E. coli*. Besides, incorporation of 5 μg mL^{-1} of pod extract of *Cola nitida* mediated AgNPs into the paint completely inhibits the growth of bacteria such as *S. aureus*, *E. coli*, *P. aeruginosa*, *A. niger*, *A. flavus* and *A. fumigatus* and hence can be utilized in paint manufacture industries and biomedical.

Recently, callus extract of *Taxus yunnanensis* has been employed as a reducing and stabilizing agent for the green synthesis of AgNPs and examined their bactericidal activity against both Gram-positive and Gram-negative bacteria. The bactericidal activity test of the synthesized AgNPs revealed that the inhibition effect is more pronounced in case of Gram-positive compared to Gram-negative bacteria. Therefore, callus extract of *Taxus yunnanensis* mediated AgNPs can be used in antibiotic therapeutics, an alternative to the antibacterial drug.[319] Spherical and well-dispersed AgNPs were also prepared from callus extract of *Chlorophytum borivilianum* L. It is reported that the synthesized nanoparticle can effectively inhibit almost all kinds of human pathogens.[320]

4. Mechanism of antibacterial inhibition by bioinspired AgNPs

The actual mode and reactive species, whether AgNPs[321–323] or the released Ag^+,[80] in the bactericidal activity of AgNPs is not well established to date and is still a topic of hot debate. However, most of the recent studies revealed that released Ag^+, not the actual AgNPs, is possible the antimicrobial agent that causes cell damage and consequent death.[11,324,325] Several pathways have been that proposed for the bactericidal activity of AgNPs which include the generation of reactive oxygen species,[326] free radicals derived from the surface of AgNPs,[327] silver ion stress,[328] coating agents,[329] interactions with the bacterial cell that leads to depletion of intracellular ATP level[322] and damage in respiratory enzymes.[330]

The possible mechanism for the antibiotic activity of AgNPs is displayed in Fig. 9. It is reported that the smaller the size of AgNPs greater is the bactericidal activity as it provides a greater surface to the bacterial membrane. The interaction between the

positively charged Ag ion with the negatively charged cell membranes led to the disruption of the cell morphology and hence cell leakage occurred, resulting in cell death. Besides, AgNPs bind strongly with phosphorus and sulfur of the extracellular and intracellular membrane proteins, thus affects the cell replication, respiration and finally, the lifetime of the cell. Apart from that, AgNPs can also bind with the thiol and amino groups of membrane protein and led to the formation of reactive oxygen species (ROS), which inhibits the cell respiration. The excellent bactericidal activity of AgNPs can be attributed to the interaction with the plasma membrane and peptidoglycan cell wall of the bacterial strain.[331] It has also been suggested that the interaction of AgNPs with cell wall increases the membrane permeability by forming pores or pits and thereby causing the death of bacteria.[332,333]

5. Conclusion and future outlook

Taking into account the many benefits of green synthesis of AgNPs using plant extracts and their excellent antimicrobial activities as bare or in conjugation with antibiotic drugs, there is no doubt that this research field will continue to attract much interest in recent years. Here different biogenic methods for the synthesis of AgNPs using phytochemicals, nontoxic, inexpensive, and eco-friendly route has been comprehensively reviewed. The antimicrobial susceptibility of the produced AgNPs against several pathogenic microbes has also been highlighted. Although the rapid and green synthetic methods using plant extracts have shown great potential in AgNPs, understanding the mechanism by which phytochemicals of these plants are involved in the synthesis and the mode of antimicrobial inhibition are still not fully understood. In addition, controlling the shape of biosynthesized AgNPs, which have many positive effects on its activities, remained largely unanswered till today although chemical methods are already well-known for shape-controlled synthesis. This problem is potentially due to the large number of different phytochemicals present in the plant extract, making it difficult for a systematic control of the interaction with the produced AgNPs. Hence, better understanding of each phytochemical, quantities and their interaction will pave the way for shape-selective synthesis of biogenic NPs. In general, the smaller the NPs better its antimicrobial activities due to the increase in surface are that are in contact with the microbial cell.[118,141] Of the same size range, antimicrobial activities of AgNPs are in the order; triangular > pentagonal, hexagonal, cubic, nano-rod > spherical. Triangular one showed the highest activity mainly due to better edge fitting due to sharp edge and predominant stable (1 1 1) facet.[109,112,113] Hexagonal, cubic, nano-rod have bend edge, which might have reduce their efficacy towards microbes as compared to triangular shape NPs.[334] whereas spherical shape NPs with no sharp edge and predominantly (1 0 0) facets showed least antimicrobial effects.[113]

Several authors revealed that Gram-positive bacteria (*e.g. S. aureus*), due to their thick cell wall of peptidoglycan layer (~20–80 nm thick), are less susceptible to AgNPs than Gram-negative bacteria (*e.g. E. coli*) with cell wall consisting of lipopolysaccharides at the exterior, followed underneath by layer of peptidoglycan (~7–8 nm).[75,102,103,107,108,118,130,166,236] However, this is not the case everywhere.[108,154,194,228,230,280] In the light of this, one must look into the role of lipopolysaccharides in Gram-negative that might have acted as a shield against some AgNPs and also the synergetic effect of AgNPs and biomolecules that act as a capping that might have alter the mode of interaction of NPs with the cell wall. Hence understanding the underlying mechanism of the interaction is still a challenge.

The antimicrobial efficacy of AgNPs can be greatly enhance by its synergistic interaction with many well-known antibiotic drugs.[10,11,77,80,104,127,183,261,288,317] This opens a new and exciting opportunity in combating numerous newly evolved highly infectious multi drug-resistant microbes. Hence, this research field has become a 'hot' topic in recent years although it is in its infancy. To have a better insight, understanding the mechanism of interaction of the AgNPs with drugs and the alteration in the mode of attack due to the synergetic interaction towards the microbes needs to be well understood and validated experimentally.

The successful green synthesis of AgNPs and evaluation, understanding the antimicrobial activities is a complex process till today although this research field has been explored several decades. However, looking at the literature we can draw several assumptions which potentially provide us AgNPs with high antimicrobial activities. Hence, knowing the complexity of the research on the green synthesis and antimicrobial activity of AgNPs, the below points are worth considered during AgNPs synthesis:

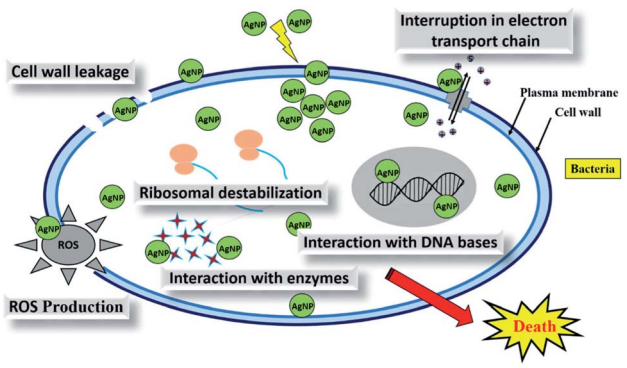

Fig. 9 Possible mechanism for the bactericidal activity of AgNPs. This figure has been reproduced from ref. [331] with permission from Elsevier, copyright 2004.

(1) Chemical composition of the plant extract

It is believed that the oxidation of different biomolecules such as flavonoids, ketones, aldehydes, tannins, carboxylic acids, phenolic and the protein of the plant are mainly responsible for the reduction of Ag^{+} to Ag^{0}. In addition, the stability and size of the produced AgNPs depends on the biomolecules acting as a capping agent.[138] Hence, one must first investigate the biomolecules present in the plant extract and its capping efficacy for successful synthesis of AgNPs. In general, greater the

capping activity greater the stability and lesser is the average particle size of NPs.[335,336] However, this is not true in some case.[337,338] Hence, specific interaction of the biomolecules and the formed NPs also need attention on case to case basis.

(2) Concentration of the plant extract

The shape and size of the synthesized AgNPs depend on the concentration of the plant extract used. At dilute concentration, formation of the NPs may not even take places; hence one need to investigate carefully. Formation of AgNPs is usually accompanied by colour change and prominent UV-Vis absorption at around 430 cm^{-1}. Increase in extract concentration leads to formation a large number of NPs to a certain level.[76] However, while desired concentration of extract can afford a highly disperse AgNPs with high antimicrobial activity, high concentration of extract often leads to agglomeration and large NPs, as excess reducing agents potential caused secondary reduction process on the surface of the preformed nuclei.[339]

(3) Concentration of $AgNO_3$

The number of AgNPs increased with the increase in $AgNO_3$ concentration up to the level where all the $AgNO_3$ salt are consumed *i.e.* all Ag^+ are reduced to Ag^0, which can be easily monitored by increasing intensities in UV-Vis spectroscopy. Once all the $AgNO_3$ are consumed, an equilibrium will be reach. Hence one need to see the balance between the $AgNO_3$ and the amount of reducing agent present in the extract.[76,235,261]

(4) Extraction solvent

Different biochemicals in the plant has different level of solubility in solvents; hence the successful extraction of the desired biochemicals for synthesis of AgNPs largely depends on the extraction solvent used. Phenolic compounds are known to be highly soluble in ethanol, methanol as well as their mixture with water (ethanol–water or methanol–water).[43,185,199,200,204] Hence, these are a solvent of choice for extraction along with pure water which is most used.

(5) Extraction time and temperature

Another important factor to consider for the successful synthesis of biogenic AgNPs is the extraction temperature. It is well known that solubility of biochemicals increased with increase in extraction temperature and time. Hence, more chemical will be extracted at a higher temperature which will make it a strong reducing agent. But there is a possibility of extracting a non-reactive biochemicals or decomposition of biochemicals at a long time at higher temperature.[185,187]

(6) pH

pH can change the electrical charges of biomolecules in the plant extract that might have affect the nature of their capping and stabilizing affinity and subsequently the growth of NPs. Increased in pH usually resulted in the increase rate of formation as well as promotes homogeneous distribution of size of NPs.[149,340] However, under acidic condition slow formation and agglomeration took place resulting in larger NPs.[151,152,341] At the same time, high pH can lead to precipitation of AgOH which is undesirable.[150] Hence, neutral pH (7) is highly recommended if an external buffer is used.

(7) Reaction time

The size of the NPs are reported to increases with time[74,111,163] as indicated by a red-shift in UV-Vis. Spectrometer data. Hence vigilant monitoring of the reaction to get a stable small size NPs is critical.

(8) Reaction temperature

High temperature is usually required to achieve complete reduction of $AgNO_3$ to AgNPs using chemical route,[337,342] although from economic and green chemistry prospective, RT reaction is the best choice. However, when it comes to green NPs synthesis, RT process, despite there are some exceptions, usually afford spherical shape NPs which are less susceptible to microbes as mentioned earlier. In the meantime, synthesis of different shapes of NPs for specific purpose is highly desirable. Literature review revealed that formation of cubic,[334,343] pentagonal, hexagonal,[111] triangular, rod-shape nanowire[343] AgNPs happen usually above RT, although some other parameters such as capping agents and stabilizers concentration needs to be taken care. Hence, in addition to increasing the speed of reaction and decreasing the size of NPs with temperature, one must consider the reaction temperature to produce NPs with different shape for a specific purpose, particularly as a potent antimicrobial.

Conflicts of interest

None to declare.

References

1 M. Ayelén Vélez, M. Cristina Perotti, L. Santiago, A. María Gennaro and E. Hynes, *Bioactive compounds delivery using nanotechnology: design and applications in dairy food*, Elsevier Inc., 2017.
2 A. Bera and H. Belhaj, *J. Nat. Gas Sci. Eng.*, 2016, **34**, 1284–1309.
3 L. J. Frewer, N. Gupta, S. George, A. R. H. Fischer, E. L. Giles and D. Coles, *Trends Food Sci. Technol.*, 2014, **40**, 211–225.
4 V. J. Mohanraj and Y. Chen, *Trop. J. Pharm. Res.*, 2007, **5**, 561–573.
5 L. Stadler, M. Homafar, A. Hartl, S. Najafishirtari, R. Zbo, M. Petr, M. B. Gawande, J. Zhi and O. Reiser, *ACS Sustainable Chem. Eng.*, 2019, **7**, 2388–2399.
6 M. D. Purkayastha and A. K. Manhar, *Nanosci. Food Agri.*, 2016, **2**, 59–128.
7 S. Chatterjee, Dhanurdhar and L. Rokhum, *Renewable Sustainable Energy Rev.*, 2017, **72**, 560–564.
8 S. Bagheri and N. M. Julkapli, *J. Magn. Magn. Mater.*, 2016, **416**, 117–133.

9 A. P. Ingle, A. Biswas, C. Vanlalveni, R. Lalfakzuala, I. Gupta, P. Ingle, L. Rokhum and M. Rai, *Microb. Bionanotechnol.*, 2020, 135–161.
10 C. Medina, M. J. Santos-Martinez, A. Radomski, O. I. Corrigan and M. W. Radomski, *Br. J. Pharmacol.*, 2007, **150**, 552–558.
11 H. Deng, D. McShan, Y. Zhang, S. S. Sinha, Z. Arslan, P. C. Ray and H. Yu, *Environ. Sci. Technol.*, 2016, **50**, 8840–8848.
12 C. Xu, O. U. Akakuru, J. Zheng and A. Wu, *Front. Bioeng. Biotechnol.*, 2019, **7**, 141.
13 S. Bagheri, M. Yasemi, E. Safaie-Qamsari, J. Rashidiani, M. Abkar, M. Hassani, S. A. Mirhosseini and H. Kooshki, *Artif. Cells, Nanomed., Biotechnol.*, 2018, **46**, 462–471.
14 A. Muthuraman, N. Rishitha and S. Mehdi, in *Design of Nanostructures for Theranostics Applications*, 2018, pp. 529–562.
15 S. Tortorella and T. C. Karagiannis, in *Molecular Mechanisms and Physiology of Disease: Implications for Epigenetics and Health*, 2014.
16 S. Ahmed, M. Ahmad, B. L. Swami and S. Ikram, *J. Adv. Res.*, 2016, **7**, 17–28.
17 S. R. Vijayan, P. Santhiyagu, R. Ramasamy, P. Arivalagan, G. Kumar, K. Ethiraj and B. R. Ramaswamy, *Enzyme Microb. Technol.*, 2016, **95**, 45–57.
18 S. Ahmed, Annu, S. Ikram and S. Yudha, *J. Photochem. Photobiol., B*, 2016, **161**, 141–153.
19 P. Mohanpuria, N. K. Rana and S. K. Yadav, *J. Nanopart. Res.*, 2008, **10**, 507–517.
20 G. Pathak, K. Rajkumari and L. Rokhum, *Nanoscale Adv.*, 2019, **1**, 1013–1020.
21 S. A. Saiqa Ikram, *J. Nanomed. Nanotechnol.*, 2015, **6**, 1000309.
22 S. Ahmed and S. Ikram, *Nano Res. Appl.*, 2015, **1**, 1–6.
23 K. Rajkumari, D. Das, G. Pathak and L. Rokhum, *New J. Chem.*, 2019, **43**, 2134–2140.
24 B. Changmai, I. B. Laskar and L. Rokhum, *J. Taiwan Inst. Chem. Eng.*, 2019, **102**, 276–282.
25 B. Changmai, P. Sudarsanam and L. Rokhum, *Ind. Crops Prod.*, 2020, **145**, 111911.
26 B. Nath, B. Das, P. Kalita and S. Basumatary, *J. Cleaner Prod.*, 2019, **239**, 118112.
27 S. Nour, N. Baheiraei, R. Imani, M. Khodaei, A. Alizadeh, N. Rabiee and S. M. Moazzeni, *J. Mater. Sci.: Mater. Med.*, 2019, **30**, 120.
28 O. Bondarenko, K. Juganson, A. Ivask, K. Kasemets, M. Mortimer and A. Kahru, *Arch. Toxicol.*, 2013, **87**, 1181–1200.
29 A. Pal, S. Shah and S. Devi, *Mater. Chem. Phys.*, 2009, **114**, 530–532.
30 T. Wu, H. Shen, L. Sun, B. Cheng, B. Liu and J. Shen, *ACS Appl. Mater. Interfaces*, 2012, **4**, 2041–2047.
31 X. Zhang, H. Sun, S. Tan, J. Gao, Y. Fu and Z. Liu, *Inorg. Chem. Commun.*, 2019, **100**, 44–50.
32 V. R. Remya, V. K. Abitha, P. S. Rajput, A. V. Rane and A. Dutta, *Chem. Int.*, 2019, **3**, 165–171.
33 M. Rafique, I. Sadaf, M. S. Rafique and M. B. Tahir, *Artif. Cells, Nanomed., Biotechnol.*, 2017, **45**, 1272–1291.
34 C. Vanlalveni, K. Rajkumari, A. Biswas, P. P. Adhikari, R. Lalfakzuala and L. Rokhum, *Bionanoscience*, 2018, **8**, 624–631.
35 N. Durán, P. D. Marcato, G. I. H. De Souza, O. L. Alves and E. Esposito, *J. Biomed. Nanotechnol.*, 2007, **3**, 203–208.
36 A. J. Kora, R. B. Sashidhar and J. Arunachalam, *Carbohydr. Polym.*, 2010, **82**, 670–679.
37 A. Ahmad, Y. Wei, F. Syed, K. Tahir, A. U. Rehman, A. Khan, S. Ullah and Q. Yuan, *Microb. Pathog.*, 2017, **102**, 133–142.
38 S. Sumitha, S. Vasanthi, S. Shalini, S. V. Chinni, S. C. B. Gopinath, P. Anbu, M. B. Bahari, R. Harish, S. Kathiresan and V. Ravichandran, *Molecules*, 2018, **23**, 3311.
39 S. Vanaraj, B. B. Keerthana and K. Preethi, *J. Inorg. Organomet. Polym. Mater.*, 2017, **27**, 1412–1422.
40 S. M. Ali, N. M. H. Yousef and N. A. Nafady, *J. Nanomater.*, 2015, 1–10.
41 V. Dhand, L. Soumya, S. Bharadwaj, S. Chakra, D. Bhatt and B. Sreedhar, *Mater. Sci. Eng., C*, 2016, **58**, 36–43.
42 B. Ajitha, Y. Ashok Kumar Reddy, S. Shameer, K. M. Rajesh, Y. Suneetha and P. Sreedhara Reddy, *J. Photochem. Photobiol., B*, 2015, **194**, 84–92.
43 R. Manikandan, B. Manikandan, T. Raman, K. Arunagirinathan, N. M. Prabhu, M. Jothi Basu, M. Perumal, S. Palanisamy and A. Munusamy, *Spectrochim. Acta, Part A*, 2015, **138**, 120–129.
44 A. Biswas, C. Vanlalveni, P. P. Adhikari, R. Lalfakzuala and L. Rokhum, *IET Nanobiotechnol.*, 2018, **12**, 933–938.
45 T. Kokila, P. S. Ramesh and D. Geetha, *Appl. Nanosci.*, 2015, **5**, 911–920.
46 V. Kathiravan, S. Ravi, S. Ashokkumar, S. Velmurugan, K. Elumalai and C. P. Khatiwada, *Spectrochim. Acta, Part A*, 2015, **139**, 200–205.
47 A. K. Jha, K. Prasad and A. R. Kulkarni, *Colloids Surf., B*, 2009, **71**, 226–229.
48 N. Vigneshwaran, N. M. Ashtaputre, P. V. Varadarajan, R. P. Nachane, K. M. Paralikar and R. H. Balasubramanya, *Mater. Lett.*, 2007, **61**, 1413–1418.
49 S. Shivaji, S. Madhu and S. Singh, *Process Biochem.*, 2011, **46**, 1800–1807.
50 M. J. Ahmed, G. Murtaza, A. Mehmood and T. M. Bhatti, *Mater. Lett.*, 2015, **153**, 10–13.
51 A. Miri, M. Sarani, M. Rezazade Bazaz and M. Darroudi, *Spectrochim. Acta, Part A*, 2015, **141**, 287–291.
52 S. Medda, A. Hajra, U. Dey, P. Bose and N. K. Mondal, *Appl. Nanosci.*, 2014, **5**, 875–880.
53 P. Premasudha, M. Venkataramana, M. Abirami, P. Vanathi, K. Krishna and R. Rajendran, *Bull. Mater. Sci.*, 2015, **38**, 965–973.
54 B. Ajitha, Y. A. K. Reddy and P. S. Reddy, *J. Photochem. Photobiol., B*, 2015, **146**, 1–9.
55 M. Kumara Swamy, K. M. Sudipta, K. Jayanta and S. Balasubramanya, *Appl. Nanosci.*, 2014, **5**, 73–81.
56 S. R. Goswami, T. Sahareen, M. Singh and S. Kumar, *J. Ind. Eng. Chem.*, 2015, **26**, 73–80.

57 M. Harshiny, M. Matheswaran, G. Arthanareeswaran, S. Kumaran and S. Rajasree, *Ecotoxicol. Environ. Saf.*, 2015, **121**, 135–141.
58 N. Krithiga, A. Rajalakshmi and A. Jayachitra, *J. Nanosci.*, 2015, **1**, 128204.
59 S. S. Sana, V. R. Badineni, S. K. Arla and V. K. Naidu Boya, *Mater. Lett.*, 2015, **145**, 347–350.
60 P. Velmurugan, M. Cho, S. S. Lim, S. K. Seo, H. Myung, K. S. Bang, S. Sivakumar, K. M. Cho and B. T. Oh, *Mater. Lett.*, 2015, **138**, 272–275.
61 D. Bose and S. Chatterjee, *Indian J. Microbiol.*, 2015, **55**, 163–167.
62 G. Marslin, R. K. Selvakesavan, G. Franklin, B. Sarmento and A. C. P. Dias, *Int. J. Nanomed.*, 2015, **10**, 5955–5963.
63 B. Sadeghi, A. Rostami and S. S. Momeni, *Spectrochim. Acta, Part A*, 2015, **134**, 326–332.
64 A. Devadiga, K. V. Shetty and M. B. Saidutta, *Int. Nano Lett.*, 2015, **5**, 205–214.
65 R. K. Salar, P. Sharma and N. Kumar, *Resour.-Effic. Technol.*, 2015, **1**, 106–115.
66 A. Verma and M. S. Mehata, *J. Radiat. Res. Appl. Sci.*, 2016, **9**, 109–115.
67 V. Ravichandran, S. Vasanthi, S. Shalini, S. Adnan and A. Shah, *Mater. Lett.*, 2016, **180**, 264–267.
68 S. Ahmed, A. K. Manzoor and S. Ikram, *J. Bionanosci.*, 2016, **10**, 282–287.
69 B. Sundararajan, G. Mahendran, R. Thamaraiselvi and B. D. Ranjitha Kumari, *Bull. Mater. Sci.*, 2016, **39**, 423–431.
70 D. Bose and S. Chatterjee, *Appl. Nanosci.*, 2016, **6**, 895–901.
71 Y. K. Mohanta, S. K. Panda, K. Biswas, A. Tamang, J. Bandyopadhyay, D. De, D. Mohanta and A. K. Bastia, *IET Nanobiotechnol.*, 2016, **10**, 438–444.
72 C. S. Espenti, K. S. V. K. Rao and K. M. Rao, *Mater. Lett.*, 2016, **147**, 129–133.
73 K. Anandalakshmi, J. Venugobal and V. Ramasamy, *Appl. Nanosci.*, 2016, **6**, 399–408.
74 S. Ahmed, Saifullah, M. Ahmad, B. L. Swami and S. Ikram, *J. Radiat. Res. Appl. Sci.*, 2016, **9**, 1–7.
75 K. Khanra, S. Panja, I. Choudhuri, A. Chakraborty and N. Bhattacharyya, *Nanomed. J.*, 2015, **7**, 128–133.
76 J. L. López-Miranda, M. Vázquez, N. Fletes, R. Esparza and G. Rosas, *Mater. Lett.*, 2016, **176**, 285–289.
77 K. Jyoti, M. Baunthiyal and A. Singh, *J. Radiat. Res. Appl. Sci.*, 2016, **9**, 217–227.
78 S. Soman and J. G. Ray, *J. Photochem. Photobiol., B*, 2016, **163**, 391–402.
79 B. Ajitha, Y. A. K. Reddy, P. S. Reddy, Y. Suneetha, H. J. Jeon and C. W. Ahn, *J. Mol. Liq.*, 2016, **219**, 474–481.
80 D. McShan, Y. Zhang, H. Deng, P. C. Ray and H. Yu, *J. Environ. Sci. Health, Part C: Environ. Carcinog. Ecotoxicol. Rev.*, 2015, **33**, 369–384.
81 V. P. Manjamadha and K. Muthukumar, *Bioprocess Biosyst. Eng.*, 2016, **39**, 401–411.
82 N. Chauhan, A. K. Tyagi, P. Kumar and A. Malik, *Front. Microbiol.*, 2016, **7**, 1748.
83 D. K. Verma, S. H. Hasan and R. M. Banik, *J. Photochem. Photobiol., B*, 2016, **155**, 51–59.
84 B. Ajitha, Y. Ashok Kumar Reddy, K. M. Rajesh and P. Sreedhara Reddy, *Mater. Today: Proc.*, 2016, **3**, 1977–1984.
85 G. Kuppurangan, B. Karuppasamy, K. Nagarajan, R. Krishnasamy Sekar, N. Viswaprakash and T. Ramasamy, *Appl. Nanosci.*, 2015, **6**, 973–982.
86 A. R. Allafchian, S. Z. Mirahmadi-Zare, S. A. H. Jalali, S. S. Hashemi and M. R. Vahabi, *J. Nanostruct. Chem.*, 2016, **6**, 129–135.
87 R. Kumari, G. Brahma, S. Rajak, M. Singh and S. Kumar, *Orient. Pharm. Exp. Med.*, 2016, **16**, 195–201.
88 O. Azizian-Shermeh, A. Einali and A. Ghasemi, *Adv. Powder Technol.*, 2017, **28**, 3167–3171.
89 B. Bhuyan, A. Paul, B. Paul, S. S. Dhar and P. Dutta, *J. Photochem. Photobiol., B*, 2017, **173**, 210–215.
90 S. Mahadevan, S. Vijayakumar and P. Arulmozhi, *Microb. Pathog.*, 2017, **113**, 445–450.
91 E. E. Elemike, D. C. Onwudiwe, O. E. Fayemi, A. C. Ekennia, E. E. Ebenso and L. R. Tiedt, *J. Cluster Sci.*, 2016, **28**, 309–330.
92 N. Soni and R. C. Dhiman, *Chin. Herb. Med.*, 2017, **9**, 289–294.
93 Y. K. Mohanta, S. K. Panda, R. Jayabalan, N. Sharma, A. K. Bastia and T. K. Mohanta, *Front. Mol. Biosci.*, 2017, **4**, 14.
94 E. E. Elemike, D. C. Onwudiwe, A. C. Ekennia, R. C. Ehiri and N. J. Nnaji, *Mater. Sci. Eng., C*, 2017, **75**, 980–989.
95 I. Ocsoy, A. Demirbas, E. S. McLamore, B. Altinsoy, N. Ildiz and A. Baldemir, *J. Mol. Liq.*, 2017, **238**, 263–269.
96 H. S. A. Al-Shmgani, W. H. Mohammed, G. M. Sulaiman and A. H. Saadoon, *Artif. Cells, Nanomed., Biotechnol.*, 2016, **45**, 1234–1240, DOI: 10.1080/21691401.2016.1220950.
97 K. Sahayaraj and S. Rajesh, *Sci. against Microb. Pathog. Communicating Current Research and Technological Advances*. 2011, vol. 23, pp. 228–244.
98 E. E. Elemike, D. C. Onwudiwe, A. C. Ekennia and L. Katata-Seru, *Res. Chem. Intermed.*, 2016, **43**, 1383–1394.
99 S. V. Otari, S. H. Pawar, S. K. S. Patel, R. K. Singh, S. Y. Kim, J. H. Lee, L. Zhang and J. K. Lee, *J. Microbiol. Biotechnol.*, 2017, **27**, 731–738.
100 T. Rasheed, M. Bilal, H. M. N. Iqbal and C. Li, *Colloids Surf., B*, 2017, **158**, 408–415.
101 P. Thatoi, R. G. Kerry, S. Gouda, G. Das, K. Pramanik, H. Thatoi and J. K. Patra, *J. Photochem. Photobiol., B*, 2016, **163**, 311–318.
102 L. Wang, Y. Wu, J. Xie, S. Wu and Z. Wu, *Mater. Sci. Eng., C*, 2018, **86**, 1–8.
103 R. Geethalakshmi and D. V. L. Sarada, *Ind. Crops Prod.*, 2013, **51**, 107–115.
104 R. G. Saratale, G. Benelli, G. Kumar, D. S. Kim and G. D. Saratale, *Environ. Sci. Pollut. Res.*, 2017, **25**, 10392–10406.
105 A. Lateef, B. I. Folarin, S. M. Oladejo, P. O. Akinola, L. S. Beukes and E. B. Gueguim-Kana, *Prep. Biochem. Biotechnol.*, 2018, **1–7**, 1479864.
106 R. Vijayan, S. Joseph and B. Mathew, *Part. Sci. Technol.*, 2018, **1–11**, 1450312.

107 D. Kavaz, H. Umar and S. Shehu, *Artif. Cells, Nanomed., Biotechnol.*, 2019, **1–11**, 1536060.
108 F. Erci, R. Cakir-Koc and I. Isildak, *Artif. Cells, Nanomed., Biotechnol.*, 2017, **1–9**, 1415917.
109 S. Pal, Y. K. Tak and J. M. Song, *Appl. Environ. Microbiol.*, 2007, **73**, 1712–1720.
110 R. Vijayan, S. Joseph and B. Mathew, *Artif. Cells, Nanomed., Biotechnol.*, 2017, **46**, 861–871.
111 M. Kumari, S. Pandey, V. P. Giri, A. Bhattacharya, R. Shukla, A. Mishra and C. S. Nautiyal, *Microb. Pathog.*, 2017, **105**, 346–355.
112 P. Kanmani and S. T. Lim, *Process Biochem.*, 2013, **48**, 1099–1106.
113 V. K. Sharma, R. A. Yngard and Y. Lin, *Adv. Colloid Interface Sci.*, 2009, **145**, 83–96.
114 A. Biswas and L. Rokhum, *Int. Conf. Syst. Process. Physics, Chem. Biol.*, 2018, pp. 1–7.
115 M. Baghayeri, B. Mahdavi, Z. Hosseinpor-Mohsen Abadi and S. Farhadi, *Appl. Organomet. Chem.*, 2017, **32**, e4057.
116 S. Ghotekar, A. Savale and S. Pansambal, *J. Water Environ. Nanotechnol.*, 2018, **3**, 95–105.
117 A. Biswas, L. Chawngthu, C. Vanlalveni, R. Hnamte, R. Lalfakzuala and L. Rokhum, *J. Bionanosci.*, 2018, **12**, 227–232.
118 N. Manosalva, G. Tortella, M. Cristina Diez, H. Schalchli, A. B. Seabra, N. Durán and O. Rubilar, *World J. Microbiol. Biotechnol.*, 2019, **35**, 1–9.
119 S. Onitsuka, T. Hamada and H. Okamura, *Colloids Surf., B*, 2019, **173**, 242–248.
120 E. Bernardo-Mazariegos, B. Valdez-Salas, D. González-Mendoza, A. Abdelmoteleb, O. Tzintzun Camacho, C. Ceceña Duran and F. Gutiérrez-Miceli, *Rev. Argent. Microbiol.*, 2019, **51**, 103–109.
121 K. Kanagamani, P. Muthukrishnan, K. Shankar, A. Kathiresan, H. Barabadi and M. Saravanan, *J. Cluster Sci.*, 2019, **30**, 1415–1424.
122 S. Paosen, S. Jindapol, R. Soontarach and S. P. Voravuthikunchai, *APMIS*, 2019, **127**, 764–778.
123 E. H. Ibrahim, M. Kilany, H. A. Ghramh, K. A. Khan and S. ul Islam, *Saudi J. Biol. Sci.*, 2019, **26**, 1689–1694.
124 M. Nilavukkarasi, S. Vijayakumar and S. Prathip Kumar, *Mater. Sci. Energy Technol.*, 2020, **3**, 371–376.
125 Z. Shunying, Y. Yang, Y. Huaidong, Y. Yue and Z. Guolin, *J. Ethnopharmacol.*, 2005, **96**, 151–158.
126 P. Moteriya and S. Chanda, *J. Inorg. Organomet. Polym. Mater.*, 2020, **30**, 3920–3932.
127 W. Huang, M. Yan, H. Duan, Y. Bi, X. Cheng and H. Yu, *J. Nanomater.*, 2020, **1–7**, 9535432.
128 F. Ö. Küp, S. Çoşkunçay and F. Duman, *Mater. Sci. Eng., C*, 2020, **107**, 110207.
129 M. A. Ramadan, A. E. Shawkey, M. A. Rabeh and A. O. Abdellatif, *J. Herb. Med.*, 2020, **20**, 100289.
130 S. Javan bakht Dalir, H. Djahaniani, F. Nabati and M. Hekmati, *Heliyon*, 2020, **6**, e03624.
131 R. K. Chahande, B. A. Mehere, P. K. Pantawane, P. B. Chouke and S. R. Murai, *Mater. Today: Proc.*, 2020, **29**, 923–928.
132 S. A. Khan, S. Shahid and C. S. Lee, *Biomolecules*, 2020, **10**, 835.
133 A. O. Nyabola, P. G. Kareru, E. S. Madivoli, S. I. Wanakai and E. G. Maina, *J. Inorg. Organomet. Polym. Mater.*, 2020, **30**, 3493–3501.
134 S. Jebril, R. Khanfir Ben Jenana and C. Dridi, *Mater. Chem. Phys.*, 2020, **248**, 122898.
135 R. Parvataneni, *Drug Chem. Toxicol.*, 2020, **43**, 307–321.
136 E. S. Madivoli, P. G. Kareru, A. N. Gachanja, S. M. Mugo, D. S. Makhanu, S. I. Wanakai and Y. Gavamukulya, *J. Inorg. Organomet. Polym. Mater.*, 2020, **30**, 2842–2850.
137 A. Biswas, C. Vanlalveni, P. P. Adhikari, R. Lalfakzuala and L. Rokhum, *Micro Nano Lett.*, 2019, **14**, 799–803.
138 C. Vijilvani, M. R. Bindhu, F. C. Frincy, M. S. AlSalhi, S. Sabitha, K. Saravanakumar, S. Devanesan, M. Umadevi, M. J. Aljaafreh and M. Atif, *J. Photochem. Photobiol., B*, 2020, **202**, 111713.
139 M. Maghimaa and S. Ali, *J. Photochem. Photobiol., B*, 2020, **204**, 111806.
140 M. A. Asghar, E. Zahir, M. A. Asghar, J. Iqbal and A. A. Rehman, *PLoS One*, 2020, **15**, e0234964.
141 B. Reidy, A. Haase, A. Luch, K. A. Dawson and I. Lynch, *Materials*, 2013, **6**, 2295–2350.
142 A. A. Lourthuraj, M. M. Selvam, M. S. Hussain, A. W. A. Abdel-Warith, E. M. I. Younis and N. A. Al-Asgah, *Saudi J. Biol. Sci.*, 2020, **27**, 1753–1759.
143 A. K. Keshari, R. Srivastava, P. Singh, V. B. Yadav and G. Nath, *J. Ayurveda Integr. Med.*, 2020, **11**, 37–44.
144 A. J. Kora, J. Mounika and R. Jagadeeshwar, *Fungal Biol.*, 2020, **124**, 671–681.
145 A. M. Elgorban, A. E. R. M. El-Samawaty, M. A. Yassin, S. R. Sayed, S. F. Adil, K. M. Elhindi, M. Bakri and M. Khan, *Biotechnol. Biotechnol. Equip.*, 2015, **30**, 56–62.
146 A. Nouri, M. Tavakkoli Yaraki, A. Lajevardi, Z. Rezaei, M. Ghorbanpour and M. Tanzifi, *Colloids Interface Sci. Commun.*, 2020, **35**, 100252, DOI: 10.1016/j.colcom.2020.100252.
147 M. Ghaedi, M. Yousefinejad, M. Safarpoor, H. Z. Khafri and M. K. Purkait, *J. Ind. Eng. Chem.*, 2015, **31**, 167–172.
148 S. Muthukrishnan, S. Bhakya, T. Senthil Kumar and M. V. Rao, *Ind. Crops Prod.*, 2015, **63**, 119–124.
149 N. L. Gavade, A. N. Kadam, M. B. Suwarnkar, V. P. Ghodake and K. M. Garadkar, *Spectrochim. Acta, Part A*, 2015, **136**, 953–960.
150 T. J. I. Edison and M. G. Sethuraman, *Process Biochem.*, 2012, **47**, 1351–1357.
151 R. Vivek, R. Thangam, K. Muthuchelian, P. Gunasekaran, K. Kaveri and S. Kannan, *Process Biochem.*, 2012, **47**, 2405–2410.
152 Y. Sun, Y. Yin, B. T. Mayers, T. Herricks and Y. Xia, *Chem. Mater.*, 2002, **14**, 4736–4745.
153 R. M. Gengan, K. Anand, A. Phulukdaree and A. Chuturgoon, *Colloids Surf., B*, 2013, **105**, 87–91.
154 P. Logeswari, S. Silambarasan and J. Abraham, *J. Saudi Chem. Soc.*, 2015, **19**, 311–317.
155 H. Kolya, P. Maiti, A. Pandey and T. Tripathy, *J. Anal. Sci. Technol.*, 2015, **6**, 33.

156 S. N. Sinha and D. Paul, *Spectrosc. Lett.*, 2015, **48**, 600–604.
157 X. Yao, M. Jericho, D. Pink and T. Beveridge, *J. Bacteriol.*, 1999, **181**, 6865–6875.
158 K. Elangovan, D. Elumalai, S. Anupriya, R. Shenbhagaraman, P. K. Kaleena and K. Murugesan, *J. Photochem. Photobiol., B*, 2015, **151**, 118–124.
159 S. B. Ulaeto, G. M. Mathew, J. K. Pancrecious, J. B. Nair, T. P. D. Rajan, K. K. Maiti and B. C. Pai, *ACS Biomater. Sci. Eng.*, 2020, **6**, 235–245.
160 B. Ajitha, Y. A. K. Reddy, H. J. Jeon and C. W. Ahn, *Adv. Powder Technol.*, 2018, **29**, 86–93.
161 M. Khatami, S. Pourseyedi, M. Khatami, H. Hamidi, M. Zaeifi and L. Soltani, *Bioresour. Bioprocess.*, 2015, **2**, 19.
162 H. Xu, L. Wang, H. Su, L. Gu, T. Han, F. Meng and C. Liu, *Food Biophys.*, 2014, **10**, 12–18.
163 M. S. Alsalhi, S. Devanesan, A. A. Alfuraydi, R. Vishnubalaji, M. A. Munusamy, K. Murugan, M. Nicoletti and G. Benelli, *Int. J. Nanomed.*, 2016, **11**, 4439–4449.
164 A. Lateef, M. A. Akande, M. A. Azeez, S. A. Ojo, B. I. Folarin, E. B. Gueguim-Kana and L. S. Beukes, *Nanotechnol. Rev.*, 2016, **5**, 507–520.
165 M. K. Choudhary, J. Kataria, S. S. Cameotra and J. Singh, *Appl. Nanosci.*, 2016, **6**, 105–111.
166 Z. H. Pak, H. Abbaspour, N. Karimi and A. Fattahi, *Appl. Sci.*, 2016, **6**, 69.
167 M. Khatami, M. S. Nejad, S. Salari and P. G. N. Almani, *IET Nanobiotechnol.*, 2016, **10**, 237–243.
168 M. Khatami, R. Mehnipor, M. H. S. Poor and G. S. Jouzani, *J. Cluster Sci.*, 2016, **27**, 1601–1612.
169 A. Chahardoli, N. Karimi and A. Fattahi, *Iran. J. Pharm. Res.*, 2017, **16**, 1167–1175.
170 M. T. Haseeb, M. A. Hussain, K. Abbas, B. G. M. Youssif, S. Bashir, S. H. Yuk and S. N. A. Bukhari, *Int. J. Nanomed.*, 2017, **12**, 2845–2855.
171 M. Dhayalan, M. I. J. Denison, L. Anitha Jegadeeshwari, K. Krishnan and N. Nagendra Gandhi, *Nat. Prod. Res.*, 2016, **31**, 465–468.
172 S. Pirtarighat, M. Ghannadnia and S. Baghshahi, *Nanomed. J.*, 2017, **4**, 184–190.
173 R. Kumar, P. Sharma, A. Bamal, S. Negi and S. Chaudhary, *Green Process. Synth.*, 2017, **6**, 0146.
174 Y. He, F. Wei, Z. Ma, H. Zhang, Q. Yang, B. Yao, Z. Huang, J. Li, C. Zeng and Q. Zhang, *RSC Adv.*, 2017, **7**, 39842–39851.
175 S. Balakrishnan, I. Sivaji, S. Kandasamy, S. Duraisamy, N. S. Kumar and G. Gurusubramanian, *Environ. Sci. Pollut. Res.*, 2017, **24**, 14758–14769.
176 A. Qidwai, R. Kumar and A. Dikshit, *Green Chem. Lett. Rev.*, 2018, **11**, 176–188.
177 M. A. Ansari and M. A. Alzohairy, *J. Evidence-Based Complementary Altern. Med.*, 2018, **1–9**, 1860280.
178 A. Rautela, J. Rani and M. Debnath, *J. Anal. Sci. Technol.*, 2019, **10**, 1–10.
179 N. G. Girón-Vázquez, C. M. Gómez-Gutiérrez, C. A. Soto-Robles, O. Nava, E. Lugo-Medina, V. H. Castrejón-Sánchez, A. R. Vilchis-Nestor and P. A. Luque, *Results Phys.*, 2019, **13**, 102142.
180 L. Hernández-Morales, H. Espinoza-Gómez, L. Z. Flores-López, E. L. Sotelo-Barrera, A. Núñez-Rivera, R. D. Cadena-Nava, G. Alonso-Núñez and K. A. Espinoza, *Appl. Surf. Sci.*, 2019, **489**, 952–961.
181 R. Varghese, M. A. Almalki, S. Ilavenil, J. Rebecca and K. C. Choi, *Saudi J. Biol. Sci.*, 2019, **26**, 148–154.
182 S. Arokiyaraj, S. H. Choi, Y. Lee, R. Bharanidharan, V. I. Hairul-Islam, B. Vijayakumar, Y. K. Oh, V. Dinesh-Kumar, S. Vincent and K. H. Kim, *Molecules*, 2015, **20**, 384–395.
183 M. Adnan, M. Obyedul Kalam Azad, A. Madhusudhan, K. Saravanakumar, X. Hu, M. H. Wang and C. D. Ha, *Nanotechnology*, 2020, **31**, 26.
184 F. A. Qais, A. Shafiq, I. Ahmad, F. M. Husain, R. A. Khan and I. Hassan, *Microb. Pathog.*, 2020, **144**, 104172.
185 M. F. Zayed, R. A. Mahfoze, S. M. El-kousy and E. A. Al-Ashkar, *Colloids Surf., A*, 2020, **585**, 124167.
186 J. H. Kim, *J. Chromatogr. B: Anal. Technol. Biomed. Life Sci.*, 2017, **1063**, 196–203.
187 T. Belwal, P. Dhyani, I. D. Bhatt, R. S. Rawal and V. Pande, *Food Chem.*, 2016, **207**, 115–124.
188 H. Padalia, P. Moteriya and S. Chanda, *Arabian J. Chem.*, 2015, **8**, 732–741.
189 N. Gogoi, P. J. Babu, C. Mahanta and U. Bora, *Mater. Sci. Eng., C*, 2015, **46**, 463–469.
190 P. Moteriya and S. Chanda, *Artif. Cells, Nanomed., Biotechnol.*, 2016, **45**, 1556–1567.
191 A. Ebrahiminezhad, Y. Barzegar, Y. Ghasemi and A. Berenjian, *Chem. Ind. Chem. Eng. Q.*, 2017, **232**, 31–37.
192 N. Chandrasekhar and S. P. Vinay, *Appl. Nanosci.*, 2017, **7**, 851–861.
193 M. Hariram, S. Vivekanandhan, V. Ganesan, S. Muthuramkumar, A. Rodriguez-uribe, A. K. Mohanty and M. Misra, *Bioresour. Technol. Rep.*, 2019, **7**, 100298.
194 M. R. Bindhu, M. Umadevi, G. A. Esmail, N. A. Al-Dhabi and M. V. Arasu, *J. Photochem. Photobiol., B*, 2020, **205**, 111836.
195 B. Ajitha, Y. A. K. Reddy, Y. Lee, M. J. Kim and C. W. Ahn, *Appl. Organomet. Chem.*, 2019, **33**, e4867.
196 A. K. Mittal, D. Tripathy, A. Choudhary, P. K. Aili, A. Chatterjee, I. P. Singh and U. C. Banerjee, *Mater. Sci. Eng., C*, 2015, **53**, 120–127.
197 S. Pugazhendhi, E. Kirubha, P. K. Palanisamy and R. Gopalakrishnan, *Appl. Surf. Sci.*, 2015, **357**, 1801–1808.
198 P. R. Rathi Sre, M. Reka, R. Poovazhagi, M. Arul Kumar and K. Murugesan, *Spectrochim. Acta, Part A*, 2015, **135**, 1137–1144.
199 N. H. Rao, N. Lakshmidevi, S. V. N. Pammi, P. Kollu, S. Ganapaty and P. Lakshmi, *Mater. Sci. Eng., C*, 2016, **62**, 553–557.
200 L. Pethakamsetty, K. Kothapenta, H. R. Nammi, L. K. Ruddaraju, P. Kollu, S. G. Yoon and S. V. N. Pammi, *J. Environ. Sci.*, 2017, **55**, 157–163.
201 K. M. Ezealisiji, X. S. Noundou and S. E. Ukwueze, *Appl. Nanosci.*, 2017, **7**, 905–911.
202 D. Wang, J. Markus, C. Wang, Y. J. Kim, R. Mathiyalagan, V. C. Aceituno, S. Ahn and D. C. Yang, *Artif. Cells, Nanomed., Biotechnol.*, 2016, **45**, 1548–1555.

203 S. Kantipudi, L. Pethakamsetty, S. M. Kollana, J. R. Sunkara, P. Kollu, N. R. Parine, M. Rallabhandi and S. V. N. Pammi, *IET Nanobiotechnol.*, 2018, **12**, 133–137.
204 G. Şeker Karatoprak, G. Aydin, B. Altinsoy, C. Altinkaynak, M. Koşar and I. Ocsoy, *Enzyme Microb. Technol.*, 2017, **97**, 21–26.
205 S. Arokiyaraj, S. Vincent, M. Saravanan, Y. Lee, Y. K. Oh and K. H. Kim, *Artif. Cells, Nanomed., Biotechnol.*, 2016, **45**, 372–379.
206 E. F. P. Henie, H. Zaiton and M. Suhaila, *Int. Food Res. J.*, 2009, **16**, 297–311.
207 F. Benakashani, A. Allafchian and S. A. H. Jalali, *Green Chem. Lett. Rev.*, 2017, **10**, 324–330.
208 J. Markus, D. Wang, Y. J. Kim, S. Ahn, R. Mathiyalagan, C. Wang and D. C. Yang, *Nanoscale Res. Lett.*, 2017, **12**, 46.
209 M. Oves, M. Aslam, M. A. Rauf, S. Qayyum, H. A. Qari, M. S. Khan, M. Z. Alam, S. Tabrez, A. Pugazhendhi and I. M. I. Ismail, *Mater. Sci. Eng., C*, 2018, **89**, 429–443.
210 T. T. N. Nguyen, T. T. Vo, B. N. H. Nguyen, D. T. Nguyen, V. S. Dang, C. H. Dang and T. D. Nguyen, *Environ. Sci. Pollut. Res.*, 2018, **25**, 34247–34261.
211 P. P. N. Vijay Kumar, R. L. Kalyani, S. C. Veerla, P. Kollu, U. Shameem and S. V. N. Pammi, *Mater. Res. Express*, 2019, **6**, 10.
212 D. Garibo, H. A. Borbón-Nuñez, J. N. D. de León, E. García Mendoza, I. Estrada, Y. Toledano-Magaña, H. Tiznado, M. Ovalle-Marroquin, A. G. Soto-Ramos, A. Blanco, J. A. Rodríguez, O. A. Romo, L. A. Chávez-Almazán and A. Susarrey-Arce, *Sci. Rep.*, 2020, **10**, 12805.
213 M. N. Khan, T. A. Khan, Z. Khan and S. A. AL-Thabaiti, *Bioprocess Biosyst. Eng.*, 2015, **38**, 2397–2416.
214 A. A. Alfuraydi, S. Devanesan, M. Al-Ansari, M. S. AlSalhi and A. J. Ranjitsingh, *J. Photochem. Photobiol., B*, 2019, **192**, 83–89.
215 P. S. Ramesh, T. Kokila and D. Geetha, *Spectrochim. Acta, Part A*, 2015, **142**, 339–343.
216 S. Lokina, A. Stephen, V. Kaviyarasan, C. Arulvasu and V. Narayanan, *Synth. React. Inorg., Met.-Org., Nano-Met. Chem.*, 2013, **45**, 37–41.
217 S. J. Mane Gavade, G. H. Nikam, R. S. Dhabbe, S. R. Sabale, B. V. Tamhankar and G. N. Mulik, *Adv. Nat. Sci.: Nanosci. Nanotechnol.*, 2015, **6**, 045015.
218 N. Mapara, M. Sharma, V. Shriram, R. Bharadwaj, K. C. Mohite and V. Kumar, *Appl. Microbiol. Biotechnol.*, 2015, **99**, 10655–10667.
219 M. Ramar, B. Manikandan, P. N. Marimuthu, T. Raman, A. Mahalingam, P. Subramanian, S. Karthick and A. Munusamy, *Spectrochim. Acta, Part A*, 2015, **140**, 223–228.
220 S. A. A. L. Rahisuddin, Z. Khan and N. Manzoor, *Bioprocess Biosyst. Eng.*, 2015, **38**, 1773–1781.
221 P. Yugandhar and N. Savithramma, *Appl. Nanosci.*, 2015, **6**, 223–233.
222 G. Mahendran and B. D. Ranjitha Kumari, *Food Sci. Hum. Well.*, 2016, **5**, 207–218.
223 P. Mosae Selvakumar, C. A. Antonyraj, R. Babu, A. Dakhsinamurthy, N. Manikandan and A. Palanivel, *Synth. React. Inorg., Met.-Org., Nano-Met. Chem.*, 2015, **46**, 291–294.
224 Z. A. Ali, R. Yahya, S. D. Sekaran and R. Puteh, *Adv. Mater. Sci. Eng.*, 2016, **2016**, 4102196.
225 C. M. K. Kumar, P. Yugandhar and N. Savithramma, *J. Intercult. Ethnopharmacol.*, 2017, **6**, 296–310.
226 M. M. O. Rashid, K. N. Akhter, J. A. Chowdhury, F. Hossen, M. S. Hussain and M. T. Hossain, *BMC Complementary Altern. Med.*, 2017, **17**, 336.
227 N. Jayaprakash, J. J. Vijaya, K. Kaviyarasu, K. Kombaiah, L. J. Kennedy, R. J. Ramalingam, M. A. Munusamy and H. A. Al-Lohedan, *J. Photochem. Photobiol., B*, 2017, **169**, 178–185.
228 S. Farhadi, B. Ajerloo and A. Mohammadi, *Acta Chim. Slov.*, 2017, **67**, 1.
229 S. A. Umoren, A. M. Nzila, S. Sankaran, M. M. Solomon and P. S. Umoren, *Pol. J. Chem. Technol.*, 2017, **19**, 128–136.
230 Z. E. Jiménez Pérez, R. Mathiyalagan, J. Markus, Y. J. Kim, H. M. Kang, R. Abbai, K. H. Seo, D. Wang, V. Soshnikova and D. C. Yang, *Int. J. Nanomed.*, 2017, **12**, 709–723.
231 B. A. Providence, A. A. Chinyere, A. A. Ayi, O. O. Charles, T. A. Elijah and H. L. Ayomide, *Int. J. Phys. Sci.*, 2018, **13**, 24–32.
232 K. H. Oh, V. Soshnikova, J. Markus, Y. J. Kim, S. C. Lee, P. Singh, V. Castro-Aceituno, S. Ahn, D. H. Kim, Y. J. Shim, Y. J. Kim and D. C. Yang, *Artif. Cells, Nanomed., Biotechnol.*, 2017, **46**, 599–606.
233 T. Sowmyya and G. Vijaya Lakshmi, *Bionanoscience*, 2017, **8**, 179–195.
234 R. Dobrucka, M. Kaczmarek and J. Dlugaszewska, *Adv. Nat. Sci.: Nanosci. Nanotechnol.*, 2018, **9**, 025015.
235 G. M. Sangaonkar and K. D. Pawar, *Colloids Surf., B*, 2018, **164**, 210–217.
236 N. Joshi, N. Jain, A. Pathak, J. Singh, R. Prasad and C. P. Upadhyaya, *J. Sol-Gel Sci. Technol.*, 2018, **86**, 682–689.
237 S. Batool, Z. Hussain, M. B. K. Niazi, U. Liaqat and M. Afzal, *J. Drug Delivery Sci. Technol.*, 2019, **52**, 403–414.
238 S. Andra, S. Balu, R. Ramoorthy, M. Muthalagu and V. S. Manisha, *Mater. Today: Proc.*, 2019, **9**, 639–644.
239 F. K. Saidu, A. Mathew, A. Parveen, V. Valiyathra and G. V. Thomas, *SN Appl. Sci.*, 2019, **1**, 1368.
240 M. I. Masum, M. M. Siddiqa, K. A. Ali, Y. Zhang, Y. Abdallah, E. Ibrahim, W. Qiu, C. Yan and B. Li, *Front. Microbiol.*, 2019, **10**, 820.
241 J. Du, Z. Hu, Z. Yu, H. Li, J. Pan, D. Zhao and Y. Bai, *Mater. Sci. Eng., C*, 2019, **102**, 247–253.
242 F. Gulbagca, S. Ozdemir, M. Gulcan and F. Sen, *Heliyon*, 2019, **5**, e02980.
243 C. Vishwasrao, B. Momin and L. Ananthanarayan, *Waste Biomass Valorization*, 2018, **10**, 8.
244 M. M. R. Mollick, D. Rana, S. K. Dash, S. Chattopadhyay, B. Bhowmick, D. Maity, D. Mondal, S. Pattanayak, S. Roy, M. Chakraborty and D. Chattopadhyay, *Arabian J. Chem.*, 2019, **12**, 2572–2584, DOI: 10.1016/j.arabjc.2015.04.033.
245 R. Renuka, K. R. Devi, M. Sivakami, T. Thilagavathi, R. Uthrakumar and K. Kaviyarasu, *Biocatal. Agric. Biotechnol.*, 2020, **24**, 101567.

246 M. Devi, S. Devi, V. Sharma, N. Rana, R. K. Bhatia and A. K. Bhatt, *J. Tradit. Complement. Med.*, 2020, **10**, 158–165.
247 M. A. Odeniyi, V. C. Okumah, B. C. Adebayo-Tayo and O. A. Odeniyi, *Sustainable Chem. Pharm.*, 2020, **15**, 100197.
248 D. Sasidharan, T. R. Namitha, S. P. Johnson, V. Jose and P. Mathew, *Sustainable Chem. Pharm.*, 2020, **16**, 100255.
249 T. Shankar, P. Karthiga, K. Swarnalatha and K. Rajkumar, *Resour.-Effic. Technol.*, 2017, **3**, 303–308.
250 S. P. Vinay and N. Chandrasekhar, *Mater. Today: Proc.*, 2019, **9**, 499–505.
251 P. Velusamy, J. Das, R. Pachaiappan, B. Vaseeharan and K. Pandian, *Ind. Crops Prod.*, 2015, **66**, 103–109.
252 I. Murali Krishna, G. Bhagavanth Reddy, G. Veerabhadram and A. Madhusudhan, *Appl. Nanosci.*, 2015, **6**, 681–689.
253 J. Du, H. Singh and T. H. Yi, *Bioprocess Biosyst. Eng.*, 2016, **39**, 1923–1931.
254 A. C. d. J. Oliveira, A. R. de Araújo, P. V. Quelemes, D. Nadvorny, J. L. Soares-Sobrinho, J. R. S. d. A. Leite, E. C. da Silva-Filho and D. A. da Silva, *Carbohydr. Polym.*, 2019, **213**, 176–183.
255 A. V. Samrot, J. L. A. Angalene, S. M. Roshini, P. Raji, S. M. Stefi, R. Preethi, A. J. Selvarani and A. Madankumar, *J. Cluster Sci.*, 2019, **30**, 1599–1610.
256 M. Z. Siddiqui, A. R. Chowdhury, B. R. Singh, S. Maurya and N. Prasad, *Natl. Acad. Sci. Lett.*, 2020, DOI: 10.1007/s40009-020-00982-4.
257 A. Mumtaz, H. Munir, M. T. Zubair and M. H. Arif, *Mater. Res. Express*, 2019, **6**, 105308.
258 C. A. Eric, V. Benjamín, C. Monica, A. C. Mario, D. M. Francisco, A. R. Rogelio, R. Navor and M. B. Jose, *Afr. J. Biotechnol.*, 2017, **16**, 400–407.
259 M. Khatami, I. Sharifi, M. A. L. Nobre, N. Zafarnia and M. R. Aflatoonian, *Green Chem. Lett. Rev.*, 2018, **11**, 125–134.
260 V. Ahluwalia, S. Elumalai, V. Kumar, S. Kumar and R. S. Sangwan, *Microb. Pathog.*, 2018, **114**, 402–408.
261 P. Moteriya and S. Chanda, *J. Genet. Eng. Biotechnol.*, 2018, **16**, 105–113.
262 P. Karthiga, *Biotechnol. Res. Innov.*, 2018, **2**, 30–36.
263 F. Zandpour, A. R. Allafchian, M. R. Vahabi and S. A. H. Jalali, *IET Nanobiotechnol.*, 2018, **12**, 491–495.
264 M. Cakić, S. Glišić, D. Cvetković, M. Cvetinov, L. Stanojević, B. Danilović and K. Cakić, *Colloid J.*, 2018, **80**, 803–813.
265 S. Dehghanizade, J. Arasteh and A. Mirzaie, *Artif. Cells, Nanomed., Biotechnol.*, 2017, **46**, 160–168.
266 M. Moyo, M. Gomba and T. Nharingo, *Int. J. Ind. Chem.*, 2015, **6**, 329–338.
267 P. Yugandhar, R. Haribabu and N. Savithramma, *3 Biotech*, 2015, **5**, 1031–1039.
268 A. Sasikala, M. Linga Rao, N. Savithramma and T. N. V. K. V. Prasad, *Appl. Nanosci.*, 2014, **5**, 827–835.
269 D. Nayak, S. Ashe, P. R. Rauta, M. Kumari and B. Nayak, *Mater. Sci. Eng., C*, 2016, **58**, 44–52.
270 S. Priya Velammal, T. A. Devi and T. P. Amaladhas, *J. Nanostruct. Chem.*, 2016, **6**, 247–260.
271 S. Bhakya, S. Muthukrishnan, M. Sukumaran, M. Grijalva, L. Cumbal, J. F. Benjamin and M. V. Rao, *RSC Adv.*, 2016, **6**, 81436–81446.
272 Q. Ahmed, N. Gupta, A. Kumar and S. Nimesh, *Artif. Cells, Nanomed., Biotechnol.*, 2016, **45**, 1192–1200.
273 S. Pattanayak, M. Rahaman, D. Maity, S. Chakraborty, S. Kumar and S. Chattopadhyay, *J. Saudi Chem. Soc.*, 2017, **21**, 673–684.
274 G. Arya, R. M. Kumari, N. Gupta, A. Kumar and S. Nimesh, *Artif. Cells, Nanomed., Biotechnol.*, 2017, 1–9.
275 P. Karthiga, S. Rajeshkumar and G. Annadurai, *J. Cluster Sci.*, 2018, **29**, 1233–1241.
276 S. Ramanathan, S. C. B. Gopinath, P. Anbu, T. Lakshmipriya, F. H. Kasim and C. G. Lee, *J. Mol. Struct.*, 2018, **1160**, 80–91.
277 M. Das and S. S. Smita, *Appl. Nanosci.*, 2018, **8**, 1059–1067.
278 E. C. Sekhar, K. S. V. K. Rao, K. M. S. Rao and S. B. Alisha, *J. Appl. Pharm. Sci.*, 2018, **8**, 1.
279 D. Bharathi, M. Diviya Josebin, S. Vasantharaj and V. Bhuvaneshwari, *J. Nanostruct. Chem.*, 2018, **8**, 83–92.
280 R. P. Illanes Tormena, E. V. Rosa, B. d. F. Oliveira Mota, J. A. Chaker, C. W. Fagg, D. O. Freire, P. M. Martins, I. C. Rodrigues da Silva and M. H. Sousa, *RSC Adv.*, 2020, **10**, 20676–20681.
281 A.-R. Phull, Q. Abbas, A. Ali, H. Raza, S. J. kim, M. Zia and I. Haq, *Future J. Pharm. Sci.*, 2016, **2**, 31–36.
282 J. H. Lee, J. M. Lim, P. Velmurugan, Y. J. Park, Y. J. Park, K. S. Bang and B. T. Oh, *J. Photochem. Photobiol., B*, 2016, **162**, 93–99.
283 G. Sharma, J. S. Nam, A. R. Sharma and S. S. Lee, *Molecules*, 2018, **23**, 2268.
284 F. K. Alsammarraie, W. Wang, P. Zhou, A. Mustapha and M. Lin, *Colloids Surf., B*, 2018, **171**, 398–405.
285 N. T. Selvi, R. Navamathavan, H. Y. Kim and R. Nirmala, *Macromol. Res.*, 2019, **27**, 1155–1160.
286 S. Devanesan, K. Ponmurugan, M. S. AlSalhi and N. A. Al-Dhabi, *Int. J. Nanomed.*, 2020, **15**, 4351–4362.
287 Y. Nan, L. I. Fuyan, J. Tiancai, L. I. U. Chongchong, S. U. N. Hushan, W. Lei and X. U. Hui, *Acta Oceanol. Sin.*, 2017, **36**, 95–100.
288 H. M. M. Ibrahim, *J. Radiat. Res. Appl. Sci.*, 2015, **8**, 265–275.
289 J. Balavijayalakshmi and V. Ramalakshmi, *J. Appl. Res. Technol.*, 2017, **15**, 413–422.
290 C. H. N. de Barros, G. C. F. Cruz, W. Mayrink and L. Tasic, *Nanotechnol., Sci. Appl.*, 2018, **11**, 1–14.
291 C. Huo, M. Khoshnamvand, P. Liu, C. G. Yuan and W. Cao, *Mater. Res. Express*, 2018, **6**, 1.
292 M. Annu, S. Ahmed, G. Kaur, P. Sharma, S. Singh and S. Ikram, *Toxicol. Res.*, 2018, **7**, 923–930.
293 R. G. Saratale, H. S. Shin, G. Kumar, G. Benelli, G. S. Ghodake, Y. Y. Jiang, D. S. Kim and G. D. Saratale, *Environ. Sci. Pollut. Res.*, 2017, **25**, 10250–10263.
294 R. K. Das and D. Bhuyan, *Nanotechnol. Environ. Eng.*, 2019, **4**, 1.
295 T. Dutta, N. N. Ghosh, M. Das, R. Adhikary, V. Mandal and A. P. Chattopadhyay, *J. Environ. Chem. Eng.*, 2020, **8**, 104019.
296 E. Z. Gomaa, *J. Genet. Eng. Biotechnol.*, 2017, **15**, 49–57.
297 A. Aravinthan, M. Govarthanan, K. Selvam, L. Praburaman, T. Selvankumar, R. Balamurugan, S. Kamala-Kannan and J. H. Kim, *Int. J. Nanomed.*, 2015, **10**, 1977–1983.

298 S. Pugazhendhi, P. Sathya, P. K. Palanisamy and R. Gopalakrishnan, *J. Photochem. Photobiol., B*, 2016, **159**, 155–160.
299 M. Mosaviniya, T. Kikhavani, M. Tanzifi, M. Tavakkoli Yaraki, P. Tajbakhsh and A. Lajevardi, *Colloids Interface Sci. Commun.*, 2019, **33**, 100211.
300 M. Saha and P. K. Bandyopadhyay, *Proc. Zool. Soc.*, 2019, **72**, 180–186.
301 S. Rajesh, V. Dharanishanthi and A. V. Kanna, *J. Exp. Nanosci.*, 2014, **10**, 1143–1152.
302 P. Kuppusamy, S. J. A. Ichwan, N. R. Parine, M. M. Yusoff, G. P. Maniam and N. Govindan, *J. Environ. Sci.*, 2015, **29**, 151–157.
303 U. Ramaswamy, D. Mukundan, A. Sreekumar and V. Mani, *Mater. Today: Proc.*, 2015, **2**, 4600–4608.
304 S. Salehi, S. A. S. Shandiz, F. Ghanbar, M. R. Darvish, M. S. Ardestani, A. Mirzaie and M. Jafari, *Int. J. Nanomed.*, 2016, **11**, 1835–1846.
305 S. Anjum and B. H. Abbasi, *Int. J. Nanomed.*, 2016, **11**, 715–728.
306 S. Ali, S. Perveen, M. Ali, T. Jiao, A. S. Sharma, H. Hassan, S. Devaraj, H. Li and Q. Chen, *Mater. Sci. Eng., C*, 2020, **108**, 110421.
307 P. N. V. K. Pallela, S. Ummey, L. K. Ruddaraju, S. V. N. Pammi and S. G. Yoon, *Microb. Pathog.*, 2018, **124**, 63–69.
308 M. Idrees, S. Batool, T. Kalsoom, S. Raina, H. M. A. Sharif and S. Yasmeen, *Environ. Technol.*, 2019, **40**, 1071–1078.
309 A. Aygün, F. Gülbağça, M. S. Nas, M. H. Alma, M. H. Çalımlı, B. Ustaoglu, Y. C. Altunoglu, M. C. Baloğlu, K. Cellat and F. Şen, *J. Pharm. Biomed. Anal.*, 2020, **179**, 113012.
310 R. R. Chavan, S. D. Bhinge, M. A. Bhutkar, D. S. Randive, G. H. Wadkar, S. S. Todkar and M. N. Urade, *Mater. Today Commun.*, 2020, **24**, 101320.
311 R. Dobrucka and J. Długaszewska, *Indian J. Microbiol.*, 2015, **55**, 168–174.
312 K. Jadhav, D. Dhamecha, B. Dalvi and M. Patil, *Part. Sci. Technol.*, 2015, **33**, 445–455.
313 A. T. Shah, M. I. Din, S. Bashir, M. A. Qadir and F. Rashid, *Anal. Lett.*, 2015, **48**, 1180–1189.
314 D. Nayak, S. Ashe, P. R. Rauta and B. Nayak, *IET Nanobiotechnol.*, 2015, **9**, 288–293.
315 C. Rajkuberan, S. Prabukumar, G. Sathishkumar, A. Wilson, K. Ravindran and S. Sivaramakrishnan, *J. Saudi Chem. Soc.*, 2017, **21**, 911–919.
316 C. Rajkuberan, K. Sudha, G. Sathishkumar and S. Sivaramakrishnan, *Spectrochim. Acta, Part A*, 2015, **136**, 924–930.
317 A. Lateef, M. A. Azeez, T. B. Asafa, T. A. Yekeen, A. Akinboro, I. C. Oladipo, L. Azeez, S. A. Ojo, E. B. Gueguim-Kana and L. S. Beukes, *J. Nanostruct. Chem.*, 2016, **6**, 159–169.
318 A. Lateef, M. A. Azeez, T. B. Asafa, T. A. Yekeen, A. Akinboro, I. C. Oladipo, L. Azeez, S. E. Ajibade, S. A. Ojo, E. B. Gueguim-kana and L. S. Beukes, *J. Taibah Univ. Sci.*, 2015, **10**, 551–562.
319 Q. H. Xia, Y. J. Ma and J. W. Wang, *Nanomaterials*, 2016, **6**, 160.
320 F. Huang, Y. Long, Q. Liang, B. Purushotham, M. K. Swamy and Y. Duan, *J. Nanomater.*, 2019, **2019**, 2418785.
321 C. N. Lok, C. M. Ho, R. Chen, Q. Y. He, W. Y. Yu, H. Sun, P. K. H. Tam, J. F. Chiu and C. M. Che, *J. Proteome Res.*, 2006, **5**, 916–924.
322 M. Rai, A. Yadav and A. Gade, *Biotechnol. Adv.*, 2009, **27**, 76–83.
323 L. S. Dorobantu, C. Fallone, A. J. Noble, J. Veinot, G. Ma, G. G. Goss and R. E. Burrell, *J. Nanopart. Res.*, 2015, **17**, 172.
324 F. Kang, P. J. Alvarez and D. Zhu, *Environ. Sci. Technol.*, 2013, **48**, 316–322.
325 H. Xu, F. Qu, H. Xu, W. Lai, Y. A. Wang, Z. P. Aguilar and H. Wei, *BioMetals*, 2011, **25**, 45–53.
326 J. S. Kim, E. Kuk, K. N. Yu, J. H. Kim, S. J. Park, H. J. Lee, S. H. Kim, Y. K. Park, Y. H. Park, C. Y. Hwang, Y. K. Kim, Y. S. Lee, D. H. Jeong and M. H. Cho, *Nanomedicine*, 2007, **3**, 91–101.
327 J. S. McQuillan, H. Groenaga Infante, E. Stokes and A. M. Shaw, *Nanotoxicology*, 2011, **6**, 857–866.
328 C. M. Zhao and W. X. Wang, *Nanotoxicology*, 2011, **6**, 361–370.
329 W. R. Li, X. B. Xie, Q. S. Shi, H. Y. Zeng, Y. S. Ou-Yang and Y. Ben Chen, *Appl. Microbiol. Biotechnol.*, 2009, **85**, 1115–1122.
330 M. P. Patil and G. Kim, *Appl. Microbiol. Biotechnol.*, 2017, **101**, 79–92.
331 I. Sondi and B. Salopek-Sondi, *J. Colloid Interface Sci.*, 2004, **275**, 177–182.
332 J. R. Morones, J. L. Elechiguerra, A. Camacho, K. Holt, J. B. Kouri, J. T. Ramírez and M. J. Yacaman, *Nanotechnology*, 2005, **16**, 2346–2353.
333 D. Yu and V. W. W. Yam, *J. Am. Chem. Soc.*, 2004, **126**, 13200–13201.
334 M. G. Bawendi, P. J. Carroll, W. L. Wilson and L. E. Brus, *J. Chem. Phys.*, 1992, **96**, 946–954.
335 N. Herron, Y. Wang and H. Eckert, *J. Am. Chem. Soc.*, 1990, **112**, 1322–1326.
336 Z. S. Pillai and P. V. Kamat, *J. Phys. Chem. B*, 2004, **108**, 945–951.
337 A. Henglein and M. Giersig, *J. Phys. Chem. B*, 1999, **103**, 9533–9539.
338 J. Y. Song and B. S. Kim, *Bioprocess Biosyst. Eng.*, 2008, **32**, 79–84.
339 M. M. H. Khalil, E. H. Ismail, K. Z. El-Baghdady and D. Mohamed, *Arabian J. Chem.*, 2014, **7**, 1131–1139.
340 K. Chitra and G. Annadurai, *BioMed Res. Int.*, 2014, 1–6.
341 S. S. Sana and L. K. Dogiparthi, *Mater. Lett.*, 2018, **226**, 47–51.
342 A. Khan, U. Farooq, T. Ahmad, R. Sarwar, J. Shafiq, Y. Raza, A. Ahmed, S. Ullah, N. Ur Rehman and A. Al-Harrasi, *Int. J. Nanomed.*, 2019, **14**, 3983–3993.
343 Y. Sun and Y. Xia, *Science*, 2002, **298**, 5176–5179.